MARIA ROHM

DISSERTATION

DISSERTATION

submitted to the

Combined Faculties for the Natural Sciences and for Mathematics

of the Ruperto-Carola University of Heidelberg, Germany

for the degree of

Doctor of Natural Sciences

Presented by

Dipl. biol. **Maria Rohm**

Born in Berlin, Germany

Heidelberg 2012

Transcriptional co-factor TBLR1 controls lipid mobilization in white adipose tissue

Referees:

PD Dr. Renate Voit

Prof. Dr. Stephan Herzig

Abstract

Obesity as a cause of diseases like metabolic syndrome, type 2 diabetes and cardiovascular disease is increasingly becoming a worldwide health problem. Dysfunctional lipid metabolism is a key catalyst for the development of obesity, as impaired triglyceride storage and mobilization (lipolysis) lead to lipotoxicity and cellular stress in white adipose tissue (WAT) and other metabolically active organs. WAT is central to systemic energy metabolism as it has the potential to adapt to external and internal signals by tightly regulated lipid uptake and removal as well as adipocytokine release. Although it is widely accepted that lipolysis in adipose tissue critically determines lipid turnover and obesity, the molecular mechanisms of WAT lipid handling are largely unknown.

In this context, the transcriptional co-factors transducin beta like (TBL) 1 and TBL related (TBLR) 1, that have previously been described as regulators of lipid handling in liver, were investigated to establish co-factor function in adipose tissue triglyceride metabolism. Genetic inactivation of TBLR1, but not TBL1, in adipocytes increases triglyceride content of these cells by inhibiting lipolysis at the level of gene transcription. Gene expression profiling revealed an involvement of adipocyte TBLR1 in peroxisome proliferator-activated receptor (PPAR) and adipocytokine signaling and fatty acid metabolism pathways. Indeed, TBLR1 interacts with PPARγ and RXR, and treatment with the PPARγ agonist rosiglitazone partly reverses the effects of TBLR1 knockdown on triglyceride hydrolysis. Consistent with its role as a transcriptional co-factor TBLR1 regulates gene expression of the key lipases involved in lipolysis, hormone sensitive lipase (HSL) and adipocyte triglyceride lipase (ATGL). Apart from that, TBLR1 also influences hormone-stimulated activation of lipid breakdown by interfering with the activating adrenoceptor-cAMP-PKA axis at the level of receptor expression.

Adipocyte specific deletion of TBLR1 in mice leads to increased body weight and adiposity, adipocyte hypertrophy, as well as impaired lipid mobilization in fasting. Consistent with the finding that impaired lipolysis favors the development of obesity, body weight and adiposity increase in the adipocyte specific TBLR1 knockout (ATKO) mice with proceeding age. When fed a high fat diet, ATKO mice gain more weight and body fat than their wild type littermates, are less glucose tolerant and insulin sensitive and show increased signs of adiposity, namely adipocyte hypertrophy and increased adipocytokine release.

Importantly, TBLR1 levels in white adipose tissue increase in states with high lipolytic activity like fasting and obesity in both mice and human patients and correlate with serum parameters and adrenoceptor expression. In summary, TBLR1 expression is activated in situations with augmented lipid mobilization and required for efficient triglyceride breakdown in adipocytes. Thus, manipulating TBLR1 levels in adipocytes may represent a future perspective to treat metabolic diseases like obesity or metabolic syndrome.

Zusammenfassung

Ein häufiger Grund für die Entstehung von Krankheiten wie Typ 2 Diabetes, Herz-Kreislauf-Erkrankungen oder Metabolischem Syndrom ist Übergewicht. Dadurch wird es zunehmend zu einem weltweiten Gesundheitsproblem. Eine Schlüsselrolle in der Entstehung von Übergewicht spielt der Fettstoffwechsel: Ein gestörtes Gleichgewicht aus Triglyzerid-Speicherung und -Bereitstellung (Lipolyse) kann zu erhöhten Lipidmengen im Blutkreislauf führen, die gewebespezifische oder systemische Toxizität und damit Organschäden oder Zellstress hervorrufen. Weißes Fettgewebe beeinflusst den systemischen Energiehaushalt durch Ausschüttung von Adipozytokinen oder Anpassung des Fettstoffwechsels an externe und interne Signale. Es ist bekannt, dass dysfunktionale Lipolyse im weißen Fettgewebe zu gestörtem Lipidstoffwechsel und Übergewicht führen kann. Die molekularen Grundlagen dieses Mechanismus sind jedoch noch weitgehend unklar.

Die transkriptionellen Kofaktoren *Transducin beta like (TBL) 1* und *TBL related (TBLR) 1* regulieren den Lipidstoffwechsel in der Leber. In der vorliegenden Arbeit wird deren Funktion in Adipozyten untersucht. Genetische Inaktivierung von TBLR1 in Adipozyten hemmt die Lipolyse und erhöht so den zellulären Triglyzeridspiegel. Die Regulation erfolgt auf transkriptioneller Ebene. Im Gegensatz dazu wirkt sich die Inaktivierung von TBL1 nicht auf den Lipidhaushalt der Zellen aus. Mithilfe eines Genexpressionsprofils in Adipozyten mit verringerter TBLR1 Menge konnte gezeigt werden, dass PPAR (*peroxisome proliferator-activated receptor*)- und Adipozytokin-Signalwege sowie Fettsäure-Metabolismus zu den meistregulierten zellulären Vorgängen zählen. TBLR1 interagiert mit PPARγ und RXR in Adipozyten. Zudem führt die Stimulation mit dem PPARγ Agonisten Rosiglitazon zur Umkehrung der durch Abwesenheit von TBLR1 hervorgerufenen Effekte auf den Lipidstoffwechsel. TBLR1 reguliert die Genexpression der Lipolyse-Schlüsselenzyme *Hormone Sensitive Lipase* (HSL) und *Adipocyte Triglyceride Lipase* (ATGL) auf transkriptioneller Ebene. Außerdem beeinflusst TBLR1 deren Aktivierung durch hormonabhängige Signalwege über die Rezeptor-cAMP-PKA Achse durch Regulation der adrenergen Rezeptorexpression.

Adipozyten-spezifische Deletion von TBLR1 in Mäusen führt zu erhöhtem Körpergewicht und Adipositas, Hypertrophie von Adipozyten sowie verminderter Hunger-induzierter Lipidmobilisierung. Verringerte Lipolyse beim Menschen führt über einen längeren Zeitraum hinweg zur Entstehung von Übergewicht. Das gleiche gilt für die ATKO (Adipozyten-spezifische TBLR1 Knockout) Mäuse, die ebenfalls eine Verstärkung der Adipositas mit fortschreitendem Alter zeigen. Füttert man diese Mäuse mit einer Hochfettdiät, nehmen sie stärker an Körpergewicht und Körperfett zu und zeigen typische Anzeichen von Übergewicht, wie erhöhte Leptin- und Resistinmengen im Blut, Hypertrophie von Adipozyten, verminderte Glukosetoleranz und Insulinsensitivität sowie erhöhte Produktion von Entzündungsmediatoren im Fettgewebe.

Die Expression von TBLR1 in humanem und murinem Fettgewebe wird durch Hungern oder Übergewicht induziert. Zudem korreliert die TBLR1 Menge in humanem weißem Fettgewebe mit der Menge an freien Fettsäuren und Adiponektin im Blut sowie der Expression der beta-adrenergen Rezeptoren. Die TBLR1 Expression wird also bei erhöhtem Bedarf an Lipolyse induziert und für eine effiziente Lipidmobilisierung benötigt. Daher könnte die fettspezifische Manipulation von TBLR1 zukünftig eine therapeutische Option zur Bekämpfung von Übergewicht und assoziierten Erkrankungen darstellen.

Acknowledgements

Many people have contributed to the completion of this thesis, and I would like to take this precious opportunity to express my gratitude to those who have in many ways supported, challenged or enlightened me during this time.

First of all I would like to thank Stephan Herzig for his constant multifaceted support, starting from the inspiration for the project and the opportunity to be part of the A170 lab, for uncounted discussions, biochemical pathway coaching, great conferences, and not to forget for his indestructible (and often unbelievable) optimism.

Also, I wish to thank all former and current A170 lab members for an inspiring environment and a great time. It's been fantastic to work with you all! I am very grateful to Anke, who was not only an excellent diploma thesis supervisor but stayed interested in the project at all times and contributed greatly by invaluable discussions and sharing knowledge. I also very much appreciated the scientific discussions with Adam, Alex, Inka and Mauricio, who would always be supportive with new, inspiring ideas. I'd like to thank Annika, Oksana, Yvonne and our Hiwis for all the excellent work they've put into my project. Tjeerd has been a great and irreplaceable help for many experiments. Especially, I have to thank Dany for just amazing and invaluable practical support during all the time and in particular in the last couple of months - and for brilliant cookies and cupcakes. Without you I'd probably still be isolating RNAs, and I would have definitely missed so much fun! Speaking of it, a special 'thank you' goes to the BB boy and all the BB girls, Anja, Anke, Dany, Julia, Michaela, Yvonne, Tjeerd, who have sweetened my life in many different ways - just think of the 'Frustlade', but also of all the little things in the everyday lab routine and many truly unscientific conversations. Many thanks also to Allan for a great time at conferences, seminars, coffee breaks and countless scientific and nonscientific discussions.

I am very grateful to our collaborators in Mannheim, Wien and Zürich, Carsten Sticht, Maria Saile, Max Zeyda, Thomas Stulnig and Christian Wolfrum, whose work directly contributed to this project.

I want to express my gratitude to the members of my thesis advisory committee, Renate Voit and Angelika Bierhaus, for very good discussions and suggestions throughout the whole project and to Renate Voit, Karin Müller-Decker, who also shared many hours at the microscope with me, and Suat Özbek for reading and evaluating my thesis.

A large credit goes to my parents for always encouraging me and supporting me in so many ways that it is impossible to list them. Thank you for everything! Many thanks also to the rest of my great family for the constant courage and encouragement in the last years. Finally, I am truly grateful to Dennis who more than once had to endure science lessons and is still willing to ask for progress at work, for matchless support during the whole time and for always being able to cheer me up.

Wenn die Neugier sich auf ernsthafte Dinge richtet,
dann nennt man sie Wissensdrang.

Marie von Ebner-Eschenbach
Österreichische Schriftstellerin (1830-1916)

INDEX

1 INTRODUCTION

1.1 Obesity and the metabolic syndrome

1.1.1 Obesity as a worldwide pandemic

In the past years, obesity has developed as a major health threat all over the world and numbers are increasing. According to the World Health Organization (WHO), the worldwide prevalence of obesity has doubled since 1980 and obesity, overweight and their associated diseases now kill more people than underweight (WHO fact sheet No 311, 2011). Thus, obesity may be considered as a pandemic being defined as something (for example a disease) prevalent throughout an entire country, continent, or the whole world (Fig. 1).
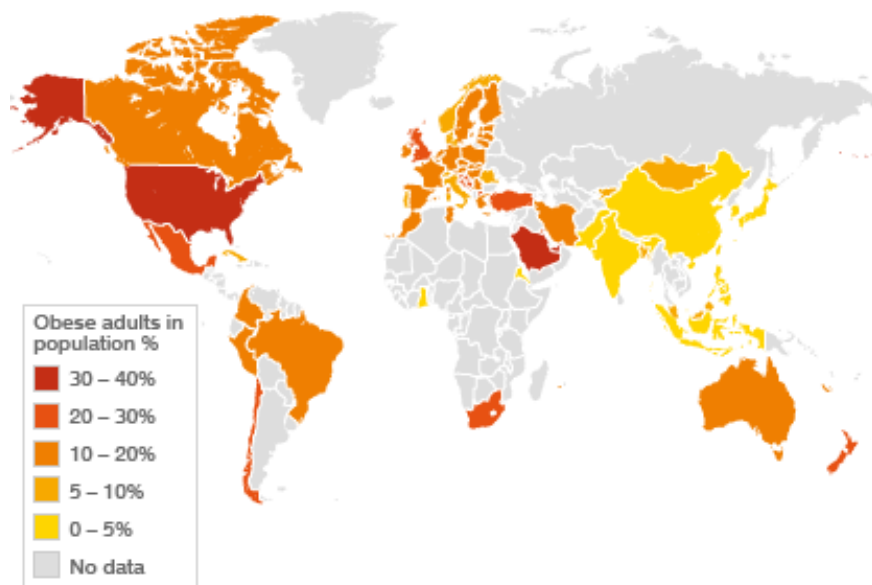
Fig. 1: Obesity as a pandemic. *Global distribution of obesity as defined by a BMI ≥ 30 kg/m². From: Global database on Body Mass Index, WHO, 2011.*

The reason for the current obesity pandemic is complex, as it cannot be attributed to one single reason but rather is a combination of many factors including genetic predisposition, reduced physical activity, malnutrition and a global nutrition transition towards more processed food and higher fat and sugar contents (Popkin, B.M., 2012). Once thought to be a problem of the Western world, obesity has now started to become a major health threat in the developing or newly industrializing countries, too, and in many cases overweight and underweight occur as a double burden of diseases within the same country or community (WHO fact sheet No 311, 2011).

The consequences of obesity are even more adverse than the causes. Overweight and obesity, as defined by a body mass index (BMI) ≥ 25 kg/m² and ≥ 30 kg/m², respectively, increase the risk for non-communicable diseases such as cardiovascular diseases (hypertension, heart disease, stroke), type 2 diabetes mellitus, musculoskeletal disorders like osteoarthritis (Kopelman, P.G., 2000), and some types of cancer such as endometrial, breast, and colon (Wolin, K.Y., 2010), and are the fifth leading cause of death worldwide (WHO fact sheet No 311, 2011). Thus, studying obesity and associated diseases is essential for future generations and prevention or treatment of this disease a worthwhile aim for increasing health.

1.1.2 Obesity is a risk factor for the development of the metabolic syndrome

Obesity is one of the major risk factors for the development of the metabolic syndrome, a multifactorial disease with many causes and faces that - due to its diversity - is very difficult to diagnose. Other risk factors for the metabolic syndrome include lifestyle (insufficient activity, unbalanced diet) and a certain genetic predisposition (Fig. 2). While the first description of the syndrome dates back to the 1920s, where it was described as a 'syndrome involving hypertension, hyperglycaemia and hyperuricaemia' (Kylin, E., 1923), it was only until 1998 that it was officially defined by certain criteria by the World Health Organization (Alberti, K.G. and Zimmet, P.Z., 1998). Ever since, there has been much controversy about the formal definition, and the development of a consensus definition continues to be a work in progress, further complicating a standardized diagnosis (Cornier, M.A., 2008).
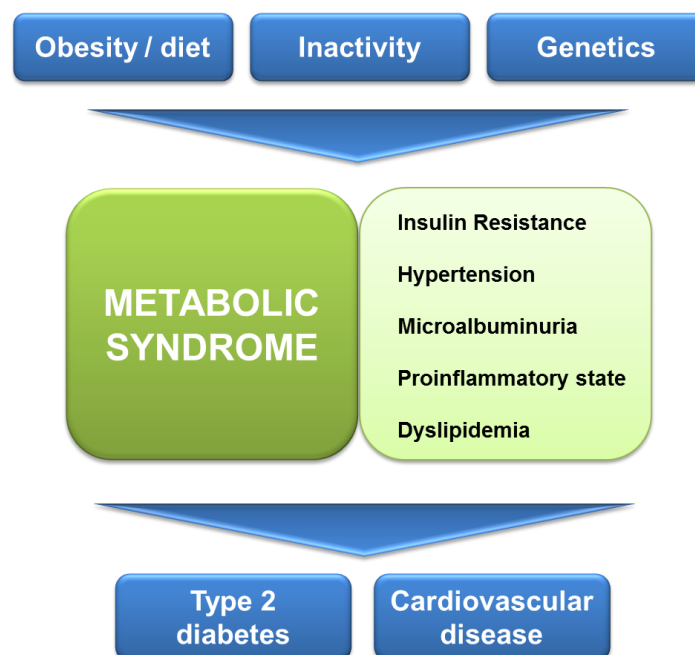
Fig. 2: Typical features of the metabolic syndrome. *Causes (top), characteristics (middle) and typical consequences of the metabolic syndrome as defined by the WHO 1998.*

Nowadays it is generally accepted that the core components of the metabolic syndrome include obesity (waist circumference), insulin resistance or impaired glucose tolerance, dyslipidemia (high serum triglycerides or HDL-cholesterol), low-grade proinflammatory state and hypertension (Alberti, K.G., 2006). The WHO additionally adds microalbuminuria (high albumin secretion or albumin: creatinine ratio) to the list of risk factors. Altogether the combination of these anomalies increases the cardiovascular risk and the risk to develop type 2 diabetes, which are the major consequences of the metabolic syndrome, and is associated with other comorbidities including the prothrombotic state, proinflammatory state, nonalcoholic fatty liver disease, and reproductive disorders (Cornier, M.A., 2008).

Both diagnosis and also therapy have proven to be difficult due to the complexity of the syndrome. A unifying definition of the syndrome may help with earlier diagnosis in order to intervene earlier in the course of disease and eventually prevent the progression into life-threatening conditions (Fulop, T., 2006). Apart from alterations in life style, which strongly reduce the risk of developing type 2 diabetes or cardiovascular disease (Costa, B., 2012), pharmacological treatments so far mostly target

the individual components of the syndrome, e.g. controlling blood sugar, cholesterol, lipids, and high blood pressure (Fulop, T., 2006). Although many of these symptoms are connected, the pharmacological therapies so far failed to treat the metabolic syndrome as a whole (Fulop, T., 2006).

1.2 Adipose tissue and its role in metabolism

1.2.1 Lipolysis is a major function of the adipose tissue

Storage and release of triglycerides and fatty acids in adipose tissue are regulated in a way that during postprandial periods lipids are stored, and during periods of fasting fatty acids are released in order to supply sink organs like liver or muscle with energy (Yu, Y. H. and Ginsberg, H. N., 2005). These mechanisms taking place in adipose tissue are critical to whole body energy homeostasis, and as such they are under tight hormonal control by catecholamines (promoting release) and insulin (promoting storage) (Bhathena, S.J., 2006).

Lipolysis, the mechanism by which triglycerides are stepwise hydrolyzed to fatty acids and glycerol, precedes fatty acid release and is activated by catecholamines like norepinephrine binding to beta-adrenergic receptors, thereby starting a signaling cascade ultimately leading to activation of a number of key lipases (schematic representation of the pathway shown in Fig. 3). In mice, there are three beta-adrenergic receptors responsible for induction of lipolysis, the $\beta1$, $\beta2$ and $\beta3$ adrenergic receptor. In humans, only two adrenoceptors mediate lipolysis ($\beta1$, $\beta2$), while the $\beta3$ adrenergic receptor is hardly expressed in WAT (Zechner, R., 2009 and own observations).

Catecholamine binding to beta-adrenergic receptors activates adenylate cyclase to produce the second messenger cAMP (Zechner, R., 2009). cAMP then binds to the regulatory subunits of the cAMP-dependent kinase protein kinase A (PKA) heterotetramer and thereby liberates the PKA catalytic subunits (Moorthy, B.S., 2011). Dissociated catalytic subunits ultimately phosphorylate target genes like hormone sensitive lipase (HSL), directly activating lipolysis, or translocate to the nucleus and activate transcription factors like the cAMP response element binding protein (CREB) (Sands, W.A. and, Palmer, T.M., 2008). In addition, PKA phosphorylates the lipid droplet protein perilipin A. Without stimulation, perilipin binds to the adipocyte triglyceride lipase (ATGL) co-activator comparative gene identification 58 (CGI-58) at the lipid droplet surface. Upon phosphorylation of perilipin, CGI-58 is released and binds to ATGL, thereby increasing its activity by 20-fold (Lass, A. et al. 2006).

ATGL and HSL catalyze the first two steps of lipolysis, the hydrolysis of trigacylglycerol and the subsequent hydrolysis of diacylglycerol. The last step of the reaction is catalyzed by the enzyme monoacylglycerol lipase (MGL) (Zechner, R., 2009). MGL is constitutively active and has not been found to be regulated by beta-adrenergic signaling, indicating that ATGL and HSL are the rate limiting enzymes of the lipolytic cascade (Lampidonis, A.D., 2011). The products of the reactions, three molecules of free fatty acids and one molecule of glycerol, are then exported out of the cell by transporters like fatty acid transport protein (FATP, Schaffer, J.E. and Lodish, H.F. 1994) or aquaporin 7 (Maeda N., 2008) or recycled inside the cell (Festuccia, W.T., 2006).

The pathway is negatively regulated by insulin to prevent triglyceride breakdown during times of high external energy supply. Insulin binds to the insulin receptor and signals to activate

phosphodiesterase 3B (PDE3B) and protein phosphatases (PP), which rapidly degrade cAMP and de-phosphorylate target proteins, respectively. This negative signaling pathway efficiently blocks the lipolytic cascade (Lampidonis, A.D., 2011).
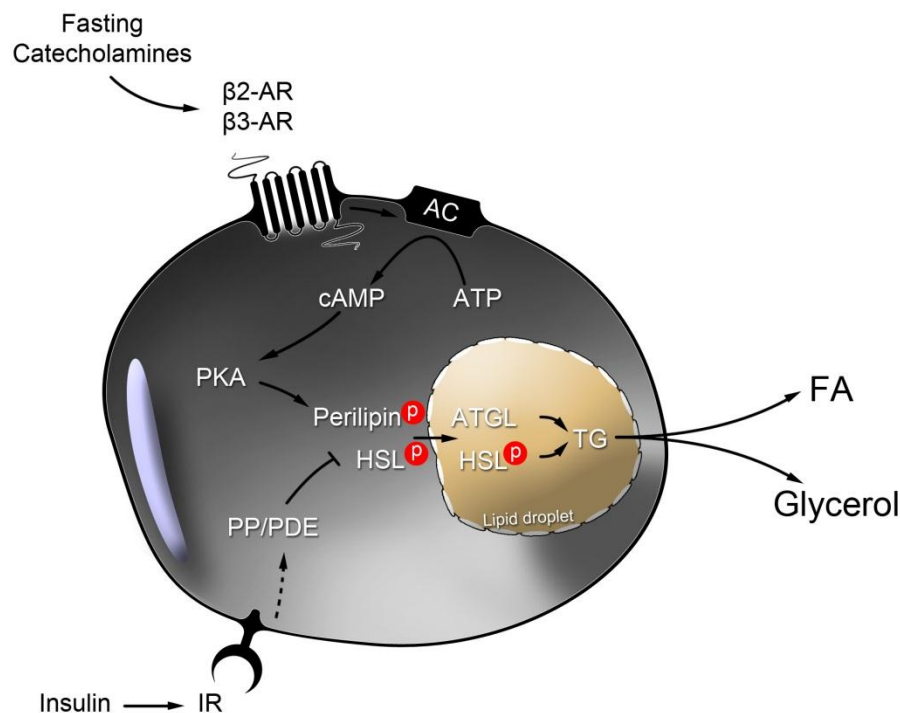
Fig. 3: Schematic representation of adipocyte lipolysis. *Fasting or the hormonal catecholamine signals activate β-adrenergic signaling via β2- or β3-adrenergic receptors (β2-, β3-AR). They in turn activate adenylate cyclase (AC) to produce cyclic AMP out of ATP. cAMP activates protein kinase A (PKA), which then phosphorylates target genes like hormone sensitive lipase (HSL) or the lipid droplet coating protein perilipin. Phosphorylated HSL in concert with activated adipocyte triglyceride lipase (ATGL) mediate triglyceride (TG) hydrolysis into fatty acids (FA) and glycerol. The cascade is negatively regulated by insulin, which activates insulin receptor (IR) and over several steps leads to activation of protein phosphatases (PP) or phosphodiesterases (PDE) to negatively influence PKA action.*

In obesity, the lipolytic cascade is dysregulated in that basal lipolysis is increased while beta-adrenergic signaling is almost blunted (Gaidhu, M.P., 2010). The increase in basal lipolysis rates are attributed to reduced sensitivity to the lipolysis-lowering actions of insulin and increased function of repressive adrenergic receptors like the α2-adrenoceptor (Gaidhu, M.P., 2010). Also, the pro-inflammatory cytokine TNFα, which is present at higher levels in obese adipose tissue, has potential to activate lipolysis (Guilherme, A., 2008). The decreased expression of the α2-adrenoceptor as well as decreased expression and activation of HSL and ATGL, accompanied by low cAMP levels, additionally decrease the capacity of catecholamine-stimulated lipolysis characteristic in obesity (Arner, P., 1999).

1.2.2 Adipose tissue is central to whole body lipid metabolism

White adipose tissue is the organ where dietary fatty acids are stored until needed, and are incorporated into triglycerides depending on energy demand of the body. Triglyceride storage is favorable over glucose storage, providing fuel at a high energy density because of its hydrophobic nature and high caloric value compared with carbohydrates (39.1 kJ/g vs. 15.4–17.5 kJ/g) (Trayhurn,

P., 2007). The balance between fatty acid storage and release determines body fat mass, and a disruption or dysfunction in this system may be causal for the development of obesity and associated disorders (Arner, P., 2011).

Under normal conditions, lipid storage and release are well-balanced, favoring one or the other depending on the actual energy demand. In obesity, lipid storage is higher than lipid removal, leading to adipose tissue expansion by adipocyte hyperplasia and hypertrophy (Jo, J., 2009). While basal adipocyte numbers are established early in life, the adipose tissue remains capable of expanding throughout life by increased proliferation and differentiation of preadipocytes (Kirkland, J., 1990). Adipocyte differentiation is a process that requires an ordered progression of well defined transcriptional events ultimately leading to a phenotypic switch from fibroblast-like precursor cells to triglyceride-rich adipocytes, which is accompanied by an increase in expression of lipid-metabolizing enzymes and adipocyte proteins such as FAPB4 (adipocyte fatty acid binding protein) and adiponectin. Key regulators of this process are the transcription factors peroxisome proliferator-activated receptor-gamma (PPARγ) and CCAAT/enhancer binding protein (C/EBP) (reviewed in Henry, S.L., 2012). In obesity, adipocyte hyperplasia is often secondary to hypertrophy due to paracrine actions of growth factors or cytokines released from hypertrophied adipocytes (Avram, M.M., 2007).

An increased number of enlarged adipocytes does not necessarily mean harm – in contrast, a good triglyceride storage capacity has proven to be beneficial for glucose tolerance and insulin sensitivity since it prevents lipotoxicity in other organs (Samocha-Bonet, D., 2012). High lipid load, however, may lead to lipid spillover into the blood flow, where hyperlipidemia can cause lipotoxicity and ectopic fat accumulation for example in liver, muscle or heart and clot arteries. This in turn can promote the development of serious complications like hepatic steatosis or cardiomyopathy (Feldstein, A.E., 2004; Maisch, B., 2011).

Of note, not only the quantity of adipose tissue accounts for obesity-related disorders, but rather the quality of it. Adipose tissue is source of adipocytokines like adiponectin, leptin, or resistin, which signal metabolic status throughout the whole body, regulating multiple metabolic and inflammatory processes (Wozniak, S.E., 2009). Altered adipocyte function for example in obesity leads to a shift in adipocytokine release from these cells: while leptin, resistin and cytokines like interleukin 6 (IL6) are produced to a larger extent, adiponectin release is reduced, all together leading to worsened insulin sensitivity and the development of metabolic syndrome (Fig. 4) (Iyer, A., Brown, L., 2010; Rasouli, N., Kern, P.A. 2008). In obesity, increased production of pro-inflammatory cytokines like macrophage chemoattractant protein (MCP) 1 or IL6 by the enlarged adipocytes activates macrophages and recruits them to the adipose tissue (Wellen, K.E., 2003). These adipose tissue residing macrophages (ATM) in turn produce inflammatory cytokines, especially tumor necrosis factor (TNF) α, eventually leading to a potentiation of the low-grade systemic inflammation that is typical for chronic pathologies associated with the metabolic syndrome, like atherosclerosis (Nishimura, S. et al., 2009), and is correlated with insulin resistance (Hotamisligil, G.S., 2006). Thus, proper adipose tissue function is fundamental to maintain a balanced whole body energy metabolism through a wide array of metabolic and endocrine functions, and adipose tissue dysfunction in obesity may cause the development of diseases like the metabolic syndrome or type 2 diabetes.
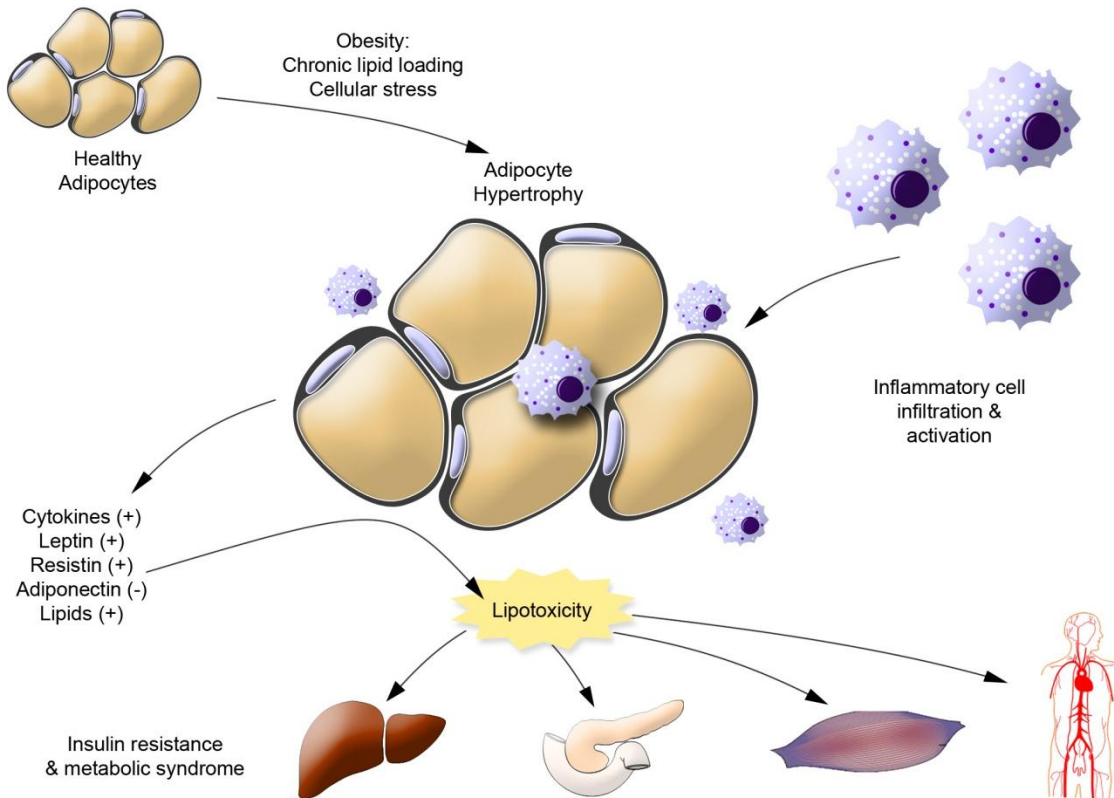
Fig. 4: Adipocyte dysfunction and local inflammation induce lipotoxicity and insulin resistance and increase the risk for developing metabolic syndrome. Adipocyte overload induces cellular stress leading to chronic low-grade inflammation and macrophage recruitment, thereby changing adipocyte function. The altered release of lipids and adipocytokines leads to lipotoxicity, ectopic lipid accumulation and insulin resistance in non-adipose tissues, favoring the development of the metabolic syndrome. Adapted from Iyer, A., Brown, L. (2010).

1.2.3 Manipulating adipose tissue function may help fighting the pandemic of obesity and the metabolic syndrome

The most obvious means of fighting the obesity and metabolic syndrome pandemic is the transition towards a healthier lifestyle with more exercise and a balanced diet. Indeed, recent studies have confirmed long term benefits of moderate weight loss and improved glucose homeostasis (Perreault, L., 2012; Costa, B., 2012). Lifestyle changes, however, require extensive educational programs and present the long-term goal in diabetes prevention.

In the meantime, it is important to intervene in other elements of the metabolic syndrome (Fig. 5). For example, treatment with thiazolidinediones like pioglitazone can improve insulin sensitivity by mechanisms including partitioning of lipid stores and the regulation of adipocytokines by activating PPARγ transcriptional activity, leading amongst other things to enhanced adipocyte proliferation, reducing adipose tissue lipid spill over into other organs (Tontonoz, P. and Spiegelman, B.M., 2008). A second means of adipocyte manipulation is activating adipocyte lipolysis. In order to avoid lipotoxicity, however, activators of lipolysis are only beneficial if the same molecule also stimulates fatty acid oxidation and energy expenditure, like beta3-adrenergic receptor agonists in rodents (Langin, D., 2006). Activating beta-adrenergic signaling in rodents activates not only lipolysis but also leads to production or activation of brown or brite adipocytes (brown-like adipocytes appearing in

white adipose tissue), which burn fat rather than storing it. In brown and brite adipocytes, triglycerides are used as fuel for thermogenesis by uncoupled mitochondrial respiration (Mottillo, E.P. and Granneman, J.G., 2011). This strategy and others aiming at manipulating adipocyte lipolysis, including inhibition of key lipases, have not yet been successful in humans (Langin, D., 2006) due to severe side effects like increased heart rate or blood pressure, favoring cardiovascular disease (Hom, G.J., 2001).

Many adverse effects of obesity are caused by the low-grade inflammation accompanying adipocyte stress. Thus, anti-inflammatory treatment may be beneficial, for example with statins or even aspirin (Fulop, T., 2006). TZDs also have anti-inflammatory functions. Lowering the systemic inflammation may ameliorate many of the adverse effects caused by the metabolic syndrome, like atherosclerosis or liver damage. Both anti-inflammatory drugs as well as TZDs improve adipocytokine profiles towards a healthier state and improve the 'quality' of the fat (Langin, D., 2006).
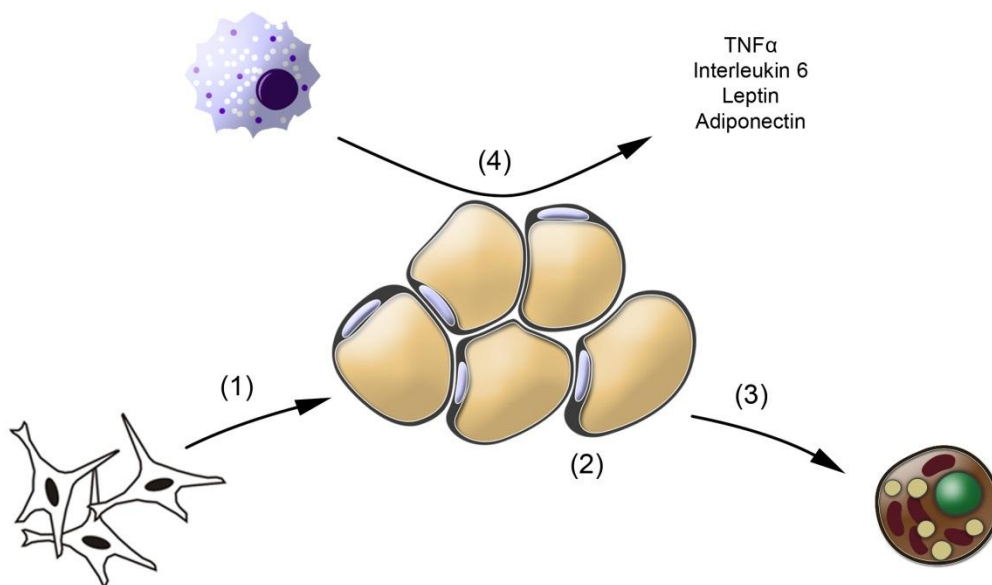
Fig. 5: Stages in adipocyte biology where pharmacological intervention may provide strategies against obesity and diabetes. (1) Activation of adipocyte differentiation for improved triglyceride storage and reduced lipotoxicity. (2) Activation of lipolysis and fatty acid oxidation to reduce adiposity and serum triglyceride levels. (3) Production or activation of brown or brite adipocytes to increase fatty acid oxidation. (4) Improvement of adipocytokine profile to improve insulin sensitivity in non-adipose tissues.

1.3 The transcriptional co-factors transducin beta like (TBL) 1 and transducin beta like related (TBLR) 1

1.3.1 TBL1 and TBLR1 are transcriptional co-factors

All metabolic and cellular functions have to be coordinated and regulated in a robust system, starting from cell division to maintaining organ homeostasis. Indeed, while the number of genes does not necessarily increase with complexity of an organism, the number of regulatory mechanisms raises dramatically the more complex an organism is (Barrett, L.W., 2012). Internal or external messages have to congregate in a coordinated relay of events, the signal transduction chains. These allow for

well-coordinated and fine-tuned responses to all kinds of signals through mechanisms like protein complex formation, conformational changes or subcellular localization as well as transcriptional activation or repression of target genes (Scott, J.D. and Pawson, T., 2009).

A well-defined example of proteins converting external signals to cellular responses are nuclear receptors. Nuclear receptors are transcription factors that are involved in a wide array of physiological processes including homeostasis, reproduction, development, and metabolism (Anbalagan, M., 2011). The family of nuclear receptors encompasses more than 40 members in humans and includes receptors for steroid hormones, thyroid hormone, various lipids and oxysterols (Burris, T.P., 2012). Nuclear receptors can bind directly to DNA and recruit co-activator or co-repressor complexes to mediate transcription of target genes (Anbalagan, M., 2011). A central regulator of lipid and glucose homeostasis is the peroxisome proliferator-activated receptor (PPAR) family of nuclear receptors, representing important molecular targets for drugs to treat hyperlipidaemia and type 2 diabetes. In adipose tissue, PPARγ is the master regulator of differentiation and metabolic function (Christodoulides C., Vidal-Puig, A., 2010).

There are three classes of nuclear receptors that are distinguished by the ligands they bind: a) the group of endocrine receptors, binding high affinity ligands synthesized exclusively from endogenous endocrine sources and present in nanomolar concentrations, b) the group of adopted orphan receptors, binding ligands from external sources present in the micromolar range, like lipids or xenobiotics, and c) the group of orphan receptors, where no physiologic ligands have been identified yet (Fig. 6). While primary and tertiary structures are common to all nuclear receptors, they further differ in their choice of dimerization partners: endocrine receptors form homodimers, adopted orphan receptors form heterodimers with retinoic x receptor (RXR), and orphan receptors can also act as monomers (Fig. 6) (Chawla, A., 2001; Glass, C.K. and Ogawa, S., 2006).
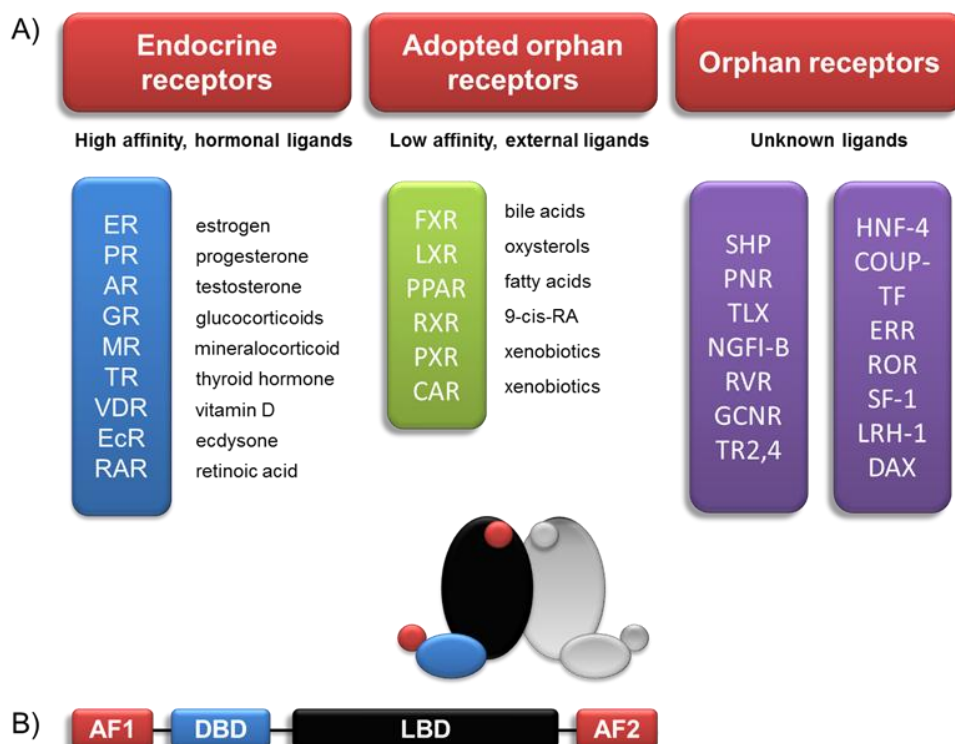
Fig. 6: The family of nuclear receptors. A) The nuclear receptor family consists of three subgroups, the endocrine receptors, adopted orphan receptors, and the orphan receptors. Receptors (white writing) are grouped to one or the other subfamily depending on their ligand (black writing). B) Primary and tertiary structure of nuclear receptor or nuclear receptor dimer (grey). AF1,2-transactivation domains, DBD-DNA binding domain, LBD-ligand binding domain. Adapted from Chawla, A., 2001.

Depending on ligand binding and post-translational modifications, nuclear receptors can mediate both repression and activation of transcription. Thus, it is perspicuous that, as most transcription factors, nuclear receptors rely on binding of further regulatory units to mediate their full range of transcriptional events (Anbalagan, M., 2011).

Transcriptional co-factors are important regulators of transcriptional events mediated by nuclear receptors and other transcription factors. While not binding directly to DNA, co-factors recruit other regulatory units by protein interactions, thereby mediating either repression or activation of transcription through methods like post-translational modification (phosphorylation, acetylation, ubiquitination, SUMOylation) (Anbalagan, M., 2011). Two of the best studied repressors involved in transcriptional repression by unliganded nuclear receptors are nuclear receptor co-repressor (NCoR) and silencing mediator of retinoic acid and thyroid hormone receptor (SMRT) (Watson, P.J., 2012), which mediate repression by the recruitment of histone deacetylases (HDACs). Transcriptional activators include the CBP/p300 family of co-activators, which mediate transcriptional activation by their histone acetyl transferase activity (Liu, X., 2008).

Binding of co-repressors or co-activators happens in a tightly regulated manner involving large protein complexes whose composition differs depending on cell-type, function and ligand availability. The core components of these regulatory complexes have been shown to consist of the histone deacetylase HDAC3, G-protein pathway suppressor-2 (GPS2), and transducin beta like 1/ transducin beta like 1 related 1 (TBL1/TBLR1) (Guenther, M.G., 2000; Li, J., 2000; Zhang, J., 2002). TBL1 and TBLR1 share a high (~90%) similarity in protein sequence and structure (Fig. 7A) and can form homo- and heterodimers (Yoon, H.G., 2003). Both are required for repression mediated by unliganded nuclear receptors like TR (thyroid hormone receptor) (Yoon, H.G., 2003).

Interestingly, TBL1/TBLR1 are also implicated in transcriptional activation. They were shown to activate transcription mediated by the nuclear receptors estrogen receptor (ER), retinoic acid receptor (RAR), TR, and PPAR and by other transcription factors like nuclear factor kappa B (NFκB) or activator protein 1 (AP-1) (Perissi, V., 2004). The term 'nuclear exchange factors' was established by the same group, meaning that TBL1/TBLR1 can function in both repression and activation of transcription by exchanging co-repressors for co-activators. The co-factors recruit ubiquitin/19S proteasome units to the transcriptional complex, resulting in dismissal of SMRT-NCoR-HDAC3 complex and binding of co-activators (Fig. 7B, Perissi, V., 2004). TBL1 and TBLR1 have similar but non-identical functions in this setting, differing mostly in CK1/GSK3- or PKCδ-mediated phosphorylation at five distinct sites (Perissi, V., 2008).
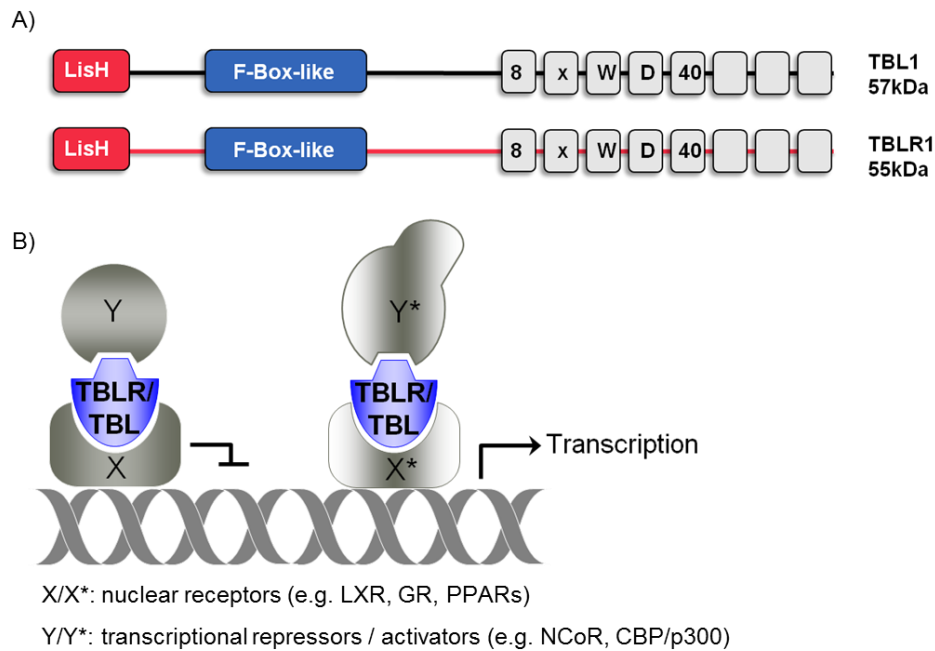
Fig. 7: TBL1 and TBLR1 share a high similarity in protein structure and act as part of transcriptional activator or repressor complexes. *A) TBL1 and TBLR1 consist of three major protein domains. The N-terminal LisH domain is essential for dimerization. The F-Box-like domain is necessary for protein interaction with ubiquitin ligases. The WD40 or transducin beta repeats are protein interaction domains giving the protein a propeller like tertiary structure and can act as platforms for the assembly of multi-protein complexes. B) TBL1 and TBLR1 can act in repressive as well as activating transcriptional complexes by interacting with a wide range of transcription factors like nuclear receptors (X, X*) and recruiting transcriptional repressors or activators (Y, Y*).*

Apart from acting as nuclear exchange factors, TBL1/TBLR1 have also been shown to be involved in wnt/β-catenin signaling in a SUMOylation dependent manner: Recruitment of β-catenin to the wnt target gene promoter leads to activation of wnt-β-catenin-induced gene expression and oncogenic growth, which can be inhibited by TBL1/TBLR1 depletion (Li, J. and Wang, C.Y., 2008; Choi, H.K., 2011).

1.3.2 TBL1 and TBLR1 are implicated in liver lipid metabolism

The regulation of wnt-β-catenin signaling as well as the activation of NFκB transcriptional activity leading to increased invasiveness of adenocarcinoma (Ramadoss, S., 2011) are suggestive of the implication of TBL1/TBLR1 in important signaling cascades. However, there is not much known about the function of TBL1/TBLR1 in metabolism or homeostasis. Whole body TBL1 or TBLR1 knockout mice are embryonically lethal (Perissi, V., 2010), further complicating TBL1/TBLR1 research.

Our group recently identified a novel role for TBL1/TBLR1 in liver lipid metabolism (Kulozik, P., 2011). TBL1 levels in the liver negatively correlate with liver triglyceride content in humans, and TBL1 levels are decreased in liver of mouse models of obesity and steatosis. Accordingly, adenovirus- or adeno-associated virus-mediated knock down of TBL1 in mouse livers promotes hepatic steatosis and hypertriglyceridemia in both low and high fat diet feeding. The increase in liver and VLDL triglycerides is explained by reduced mitochondrial and peroxisomal fatty acid oxidation pathways and increased lipogenesis. Consistent with the described role as transcriptional co-factors of nuclear receptors, TBL1/TBLR1 mediate their function in hepatic lipid homeostasis through interaction with and activation of PPARα. Thus, TBL1/TBLR1 as regulators of liver lipid metabolism provide a first hint of a

critical role of these co-factors in energy homeostasis and diseases like obesity or the metabolic syndrome, and further investigation will lead towards a better understanding of TBL1/TBLR1-regulated pathways and tissue-specific functions in health and disease.

1.4 Aim of the project

The transcriptional co-factors TBL1/TBLR1 have been shown to play a critical role in differentiation, oncogenesis and liver lipid metabolism by regulating important signaling networks such as the wnt-β-catenin, NFκB and PPAR pathways. The aim of this study was to elucidate the role of the transcriptional co-factors TBL1 and TBLR1 in adipose tissue biology with a focus on adipocyte endocrine function and lipid metabolism. This was to be achieved by comprehensive i*n vitro* experiments in 3T3-L1 and primary adipocytes, illuminating cellular functions of TBL1/TBLR1 in adipocytes. Knowledge gained in the *in vitro* system was applied to an *in vivo* model. To this end, adipocyte specific knockout mice were created in order to investigate tissue-specific and systemic consequences of co-factor deficiencies in basal and challenged conditions. Knowledge gained during *in vitro* and *in vivo* experiments was to be used for conductive analysis of patient data in order to shed light on co-factor function in humans, ultimately aiming at identifying a novel therapeutic approach for the treatment of metabolic diseases.

2 RESULTS

2.1 Analysis of TBL1 and TBLR1 expression in white adipose tissue of mouse disease models

Mouse models have a high potential for studying human diseases. Mice and humans share 99% of their genes, and in many cases mouse models mimic the situation in men. Thus, investigating models of metabolic disorders, such as obesity, systemic inflammation, or altered lipid metabolism, and genetic models improves our understanding of the underlying biology of human disease and may thus represent a potent tool to identify genes contributing to the onset of the disease (Rosenthal, N. and Brown, S., 2007).

2.1.1 TBL1 and TBLR1 are ubiquitously expressed in various mouse tissues

In order to investigate the expression of TBL1 and TBLR1 throughout the body, protein levels of the co-factors were analyzed in various mouse tissues by immunoblotting.

Both TBL1 and TBLR1 could be detected by western blot in the different organs using specific antibodies, and while in some tissues both proteins were mutually expressed, in others only one of the co-factors could be detected (Fig. 8): In accordance with a role for TBL1 in regulating hepatic lipid metabolism (Kulozik, P., 2011), TBL1 protein expression was high in liver. Concerning other metabolically important organs, TBL1 was also present in intestine, pancreas and brown adipose tissue (BAT), but could not be detected in white adipose tissue (WAT). In contrast, TBLR1 protein was readily detectable in inguinal white adipose tissue, but also in spleen, intestine, brain, and stomach. The organ-specific protein expression of the highly related co-factors therefore indicates that the two genes are not functionally redundant but have tissue specific functions.
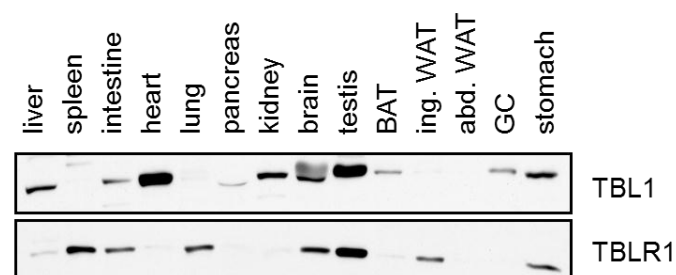
Fig. 8: TBL1 and TBLR1 protein expression in different mouse organs. Protein lysates from mouse liver, spleen, intestine, heart, lung, pancreas, kidney, brain, testis, brown adipose tissue (BAT), inguinal white adipose tissue, abdominal white adipose tissue, gastrocnemius muscle (GC) and stomach were assessed in regard to TBL1 and TBLR1 expression using specific antibodies in immunoblotting.

2.1.2 TBL1 and TBLR1 expression in mouse models of obesity

To investigate adipose tissue TBL1 and TBLR1 regulation in adiposity, mRNA expression of the co-factors was assessed in abdominal WAT of various mouse models of obesity. Mice fed a high fat diet develop obesity and associated disorders and represent a potent model for the human situation (Buettner, R., 2007). Here, we used mice fed a high fat diet containing 45% calories from fat (HFD) for 20 weeks (S. Kersten lab). Mice homozygous for lacking the leptin gene (*ob/ob*) or the leptin receptor

gene (*db/db*) representing monogenic models of obesity and obesity-associated complications and the metabolic syndrome become obese and develop type-2-diabetes mellitus like symptoms like hyperinsulinemia or hypertriglyceridemia (Kobayashi, K., 2000; Lindstrom, P., 2007). Lastly, New Zealand Obese (NZO) mice represent a polygenic model of obesity (Jürgens, H.S., 2006). The background strain of these mice is the New Zealand Black (NZB) strain.

In the polygenic obesity model, the NZO mice, TBL1 levels were decreased while TBLR1 levels were unchanged in the obese state (Fig. 9 G, H). In contrast, in all other investigated obesity models, TBL1 levels in WAT were unchanged in the obese state (Fig. 9 A, C, E), while TBLR1 mRNA expression was significantly increased (Fig. 9 B, D, F), pointing towards a specific role of WAT TBLR1 but not TBL1 in hyperphagia or energy imbalance associated obesity.
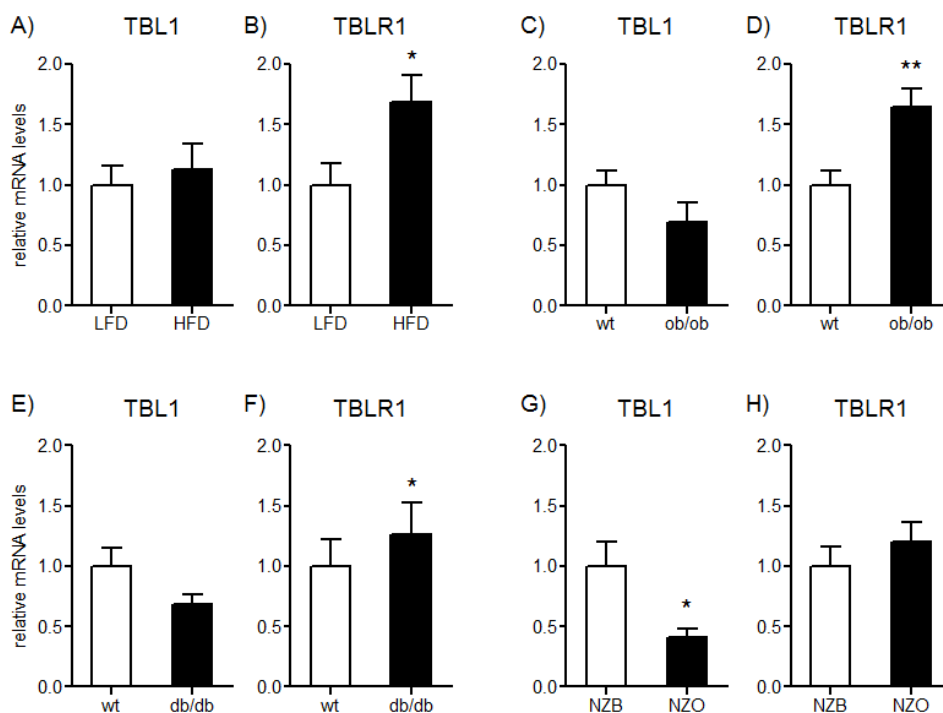
*Fig. 9: Abdominal adipose tissue TBL1 and TBLR1 mRNA expression in mouse models of obesity. (A), (B), Mice were fed a low fed control diet (LFD) or a high fat diet containing 45% calories from fat for 20 weeks starting from 11 weeks of age. TBL1 and TBLR1 mRNA levels were analyzed by qPCR from abdominal WAT. (C), (D), TBL1 and TBLR1 mRNA levels in abdominal WAT of 12 week old random fed ob/ob and control mice. (E), (F), TBL1 and TBLR1 mRNA levels in abdominal WAT of 9 week old random fed db/db and control mice. (G), (H), TBL1 and TBLR1 mRNA levels in abdominal WAT of New Zealand Black (NZB) or New Zealand Obese (NZO) mice. n=4-7, means ±SEM, *indicates significance.*

2.1.3 TBLR1 but not TBL1 levels are increased in LPS-induced sepsis

Injection of bacterial lipopolysaccharides (LPS) into mice stimulates an acute septic shock and leads to systemic inflammation and increased lipolysis (Zu, L., 2009). Here, mice were starved over night and subsequently injected intraperitoneally with LPS at a dose of 20 mg/kg body weight or with PBS as a control. LPS injected mice are anorexic, so PBS control animals were fasted for the course of the experiment. After 8 hours, mice were sacrificed, RNA and protein extracts were isolated from the abdominal fat pads and gene expression was analyzed by qPCR or immunoblotting, respectively. As

seen in Fig. 10, TBL1 levels were unchanged in LPS injected animals compared to the PBS controls, while TBLR1 levels were increased in septic mice both on mRNA and protein levels.

To investigate which cell type within the adipose tissue was responsible for the increase in TBLR1 expression upon LPS stimulation, abdominal adipose tissue of LPS injected mice was collagenase digested and separated into mature adipocytes (mAd), the stromal vascular fraction (SVF) containing precursor cells, fibroblasts and immune cells, and the SVF subfraction of CD11 positive macrophages (CD11+). TBLR1 expression in these fractions was analyzed by qPCR. As shown in Fig. 10 C, LPS increased TBLR1 expression in the adipose tissue as well as in the mature adipocytes, but not in the SVF or CD11 positive macrophages, indicating that adipocyte TBLR1 is responsible for the LPS-induced increase in WAT gene expression.
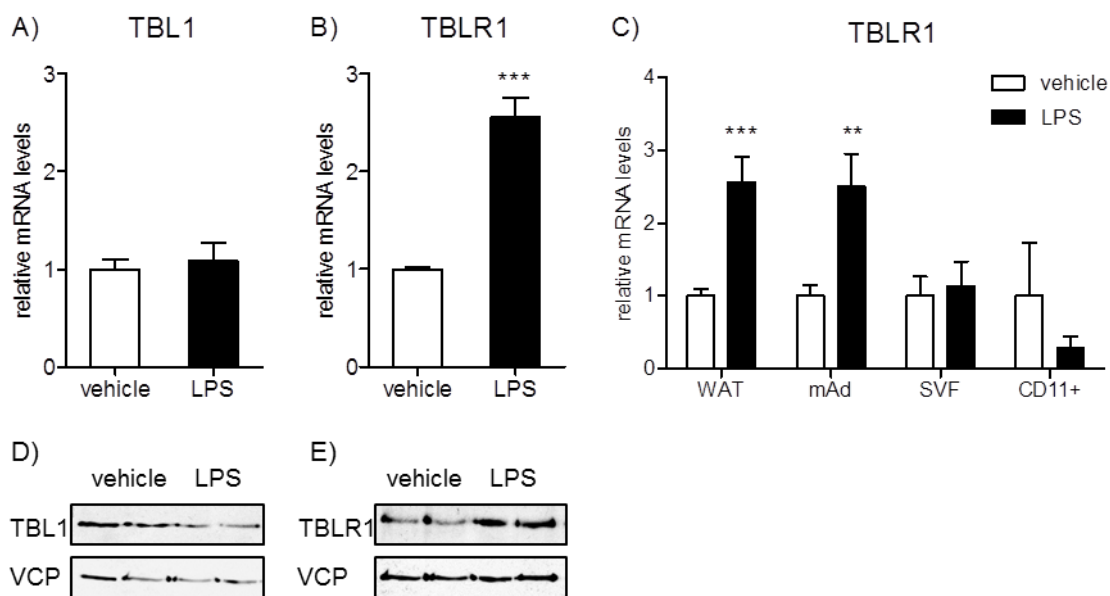
*Fig. 10: TBLR1 but not TBL1 mRNA expression is increased in adipose tissue of septic mice. Mice were fasted over night before they were injected i.p. with 20 mg/kg BW LPS or PBS for 8 hours. mRNA from abdominal WAT was analyzed by qPCR. A) TBL1 mRNA expression, B) TBLR1 mRNA expression in abdominal WAT. C) TBLR1 expression in WAT, mature adipocytes, stromal vascular fraction and CD11 positive cells of LPS treated mice. n=5, means ±SEM, *indicates significance. D), E) Immunoblot of protein extracts isolated from abdominal WAT of the same mice. TBL1, TBLR1 and VCP were detected by specific antibodies.*

2.1.4 TBLR1 but not TBL1 levels are regulated by fasting and restricted feeding

To determine if fasting influences TBL1 or TBLR1 mRNA levels, gene expression of the co-factors was analyzed in abdominal WAT of 8, 24, or 48 hrs fasted mice or mice that were fasted for the respective times and subsequently refed for 24 hrs. As shown in Fig. 11 A, B, WAT TBL1 expression was unchanged upon fasting, while TBLR1 levels were significantly increased after 8 hrs fasting and decreased after 48 hrs fasting, representing a time-dependent expression curve of the co-factor TBLR1 in fasting.

The Colon26 mouse model shows the typical phenotype of cancer cachexia, with symptoms like loss of weight mainly through wasting of adipose and muscle tissue, muscle atrophy and loss of appetite (Tanaka Y., 1990). Balb/C mice were injected subcutaneously with Colon26 adenocarcinoma cells and as a consequence developed tumors and the cachectic phenotype as measured by body weight loss

since tumor implantation. Three groups of mice were tested: a) a control group that was fed ad libitum, b) a control group on a restricted diet, getting exactly the amount of food that the Colon26 animals received (pair fed), and c) the Colon26 cachectic mice. The mice were sacrificed 16 days after injection of the Colon26 cells. As seen in Fig. 11 C-D, TBL1 mRNA levels were unchanged in the Colon26 cachectic mice and the pair-fed control animals, while TBLR1 levels tended to be higher in the Colon26 cachectic animals and were significantly increased in pair-fed mice. This indicates that TBLR1 levels in WAT may be influenced by the feeding behavior or nutritional status of the mice rather than by tumor development.
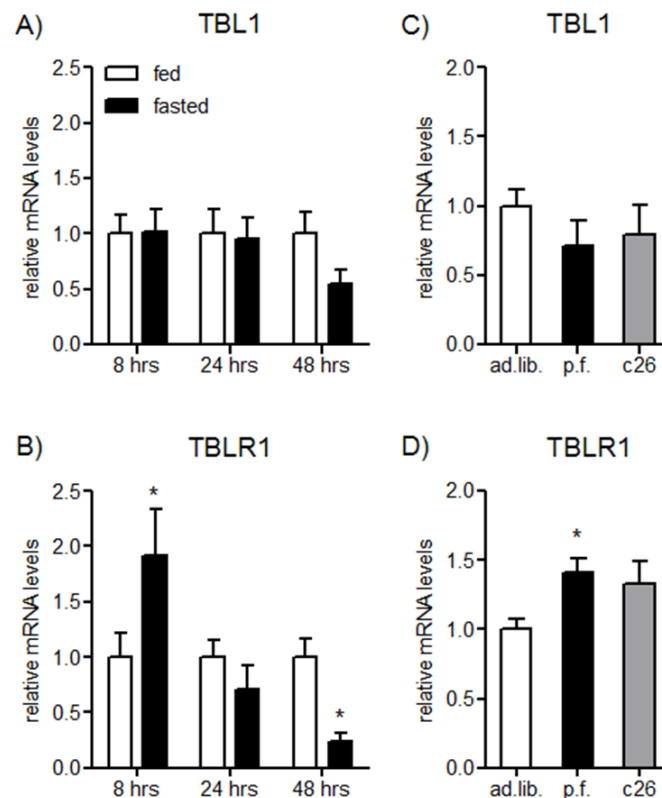
Fig. 11: TBLR1 but not TBL1 mRNA expression is changed in a time-dependent manner upon fasting or restricted feeding. (A), (B) TBL1 and TBLR1 qPCR from mRNA isolated from abdominal WAT of 8, 24, or 48 hrs fasted mice or 24 hrs refed control mice. n=4, means ±SEM, 2-way ANOVA, Bonferroni post test, *p < 0.05. (C), (D) Mice were injected with Colon26 adenocarcinoma cells and developed cancer cachexia. From the point on when they lost weight, pair-fed (p.f.) control mice received equal amounts of food as the cachectic animals for 3 days (approximately 70% less than ad libitum fed mice). TBL1 and TBLR1 mRNA levels in abdominal WAT of cachectic colon26 or ad libitum or pair-fed control mice were analyzed by qPCR. n=5, means ±SEM, *indicates significance.

2.1.5 TBLR1, but not TBL1 levels are increased by β-adrenergic signaling

Based on the gene expression data of obese, septic and fasted mice and animals on a restricted diet, we hypothesized that especially TBLR1 may be regulated in situations with increased lipolysis in WAT, which is at least in part dependent on β-adrenergic signaling (Zechner, R. et al., 2009). To test if β-adrenergic signaling had direct effects on TBLR1 expression, random fed mice were injected intraperitoneally with a β3-adrenergic receptor agonist (1 mg/kg BW CL316,243 in 0.9% saline) or vehicle for 3 or 8 hours and mRNA was extracted from abdominal WAT to analyze gene expression by qPCR.

As shown in Fig. 12 A, B, treatment of the mice with CL for 3 or 8 hours did not change TBL1 mRNA levels in abdominal WAT, while TBLR1 levels were significantly increased by 2.5- and 4.5- fold, respectively. The same was true for injecting mice with a β1/2/3-adrenergic receptor agonist (norepinephrine, NE) (Fig. 12 C, D). Thus, TBLR1 levels seem to be acutely regulated in WAT in response to β-adrenergic signaling.
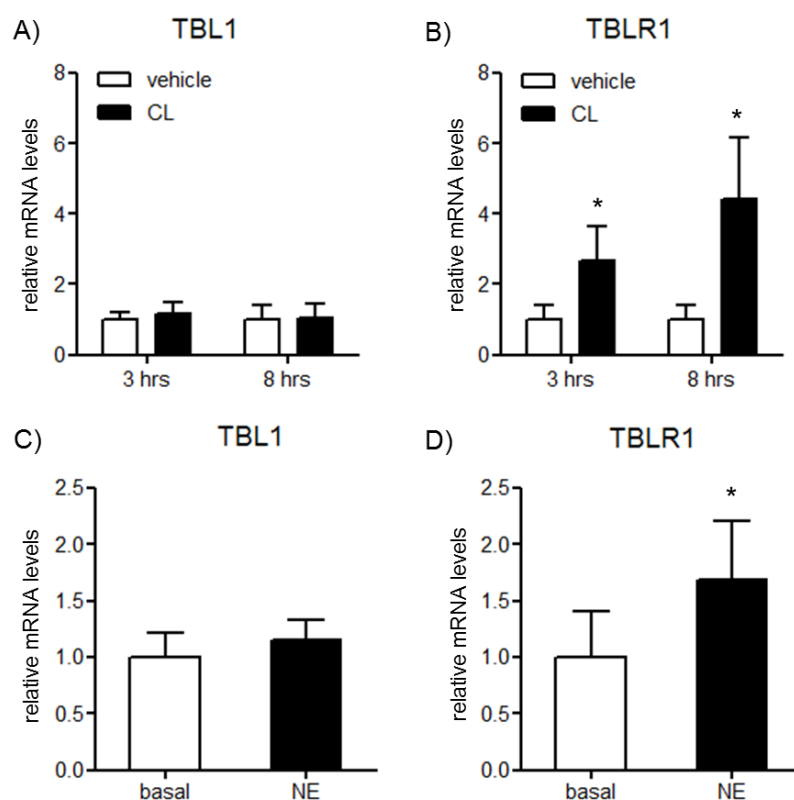
*Fig. 12: TBLR1, but not TBL1 levels in WAT are increased by treatment of mice with β-adrenergic receptor agonists. Mice were injected intraperitoneally with 1 mg/kg BW CL in 0.9% saline or vehicle for 3 or 8 hours (A, B) or 1 mg/kg norepinephrine for 3 hrs (C, D). mRNA levels in abdominal WAT were measured by qPCR. A, C) TBL1 and B, D) TBLR1 mRNA expression in CL or NE injected animals. n=5, means ±SEM, *indicates significance.*

Long term exposure to β-adrenergic receptor signaling leads to constantly increased lipolysis and browning of white adipose tissues (Collins, S., 2010). To investigate whether TBLR1 is regulated only by short-term adrenergic stimulation or is also involved in long-term signaling events, mice were injected intraperitoneally with CL for 2 or 10 consecutive days and TBLR1 mRNA expression was measured. As observed upon short-term stimulation, long term CL led to an increase in TBLR1 mRNA expression (Fig. 13 A).

PPARs represent potent regulators of metabolism and are implicated in β-adrenergic signaling (Rodriguez-Cuenca, S., 2012a). To investigate whether PPAR signaling was also implicated in the regulation of TBLR1 expression, WAT TBLR1 mRNA levels were analyzed in PPARα, PPARβ/δ and PPARγ knockout mice injected with CL for 10 consecutive days. As shown in Fig. 13 B-D, the increase in TBLR1 expression upon β-adrenergic receptor activation was dependent on PPARα, as it could not be observed in PPARα KO mice.
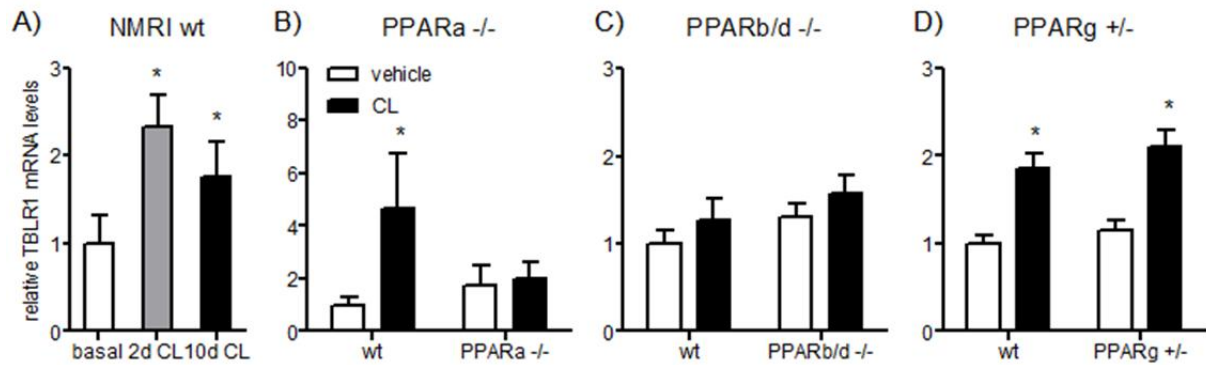
Fig. 13: TBLR1 levels are increased by long-term β-adrenergic stimulation, which is dependent on PPARα. *Female NMRI mice or male PPARα-/-, PPARβ/δ-/- and PPARγ+/- mice and their corresponding wt littermates were injected with 1 mg/kg BW CL316,243 in 0.9% saline or vehicle for (A) 2 or 10 consecutive days or (B-D) 10 consecutive days and TBLR1 mRNA levels were determined by qPCR. n=4, means ±SEM, *indicates significance.*

2.2 Impact of TBL1 and TBLR1 on adipocyte differentiation

2.2.1 TBL1 and TBLR1 levels are increased during the course of adipocyte differentiation

Adipocytes are differentiated from precursor cells (3T3-L1 or primary preadipocytes) by the addition of a differentiation cocktail consisting of high (4.5 g/l) glucose DMEM, insulin, 3-isobutyl-1-methylxanthine (IBMX), dexamethasone and ABP (L-ascorbate, d-biotin, pantothenic acid). For this, confluent cells are stimulated with the differentiation cocktail for 4 days, followed by a 2-days phase of insulin treatment as described in 'Methods '.

To analyze the TBL1 and TBLR1 expression profile during the differentiation process, 3T3-L1 or primary preadipocytes (PA) isolated from the SVF of inguinal, abdominal or brown adipose tissue depots were differentiated and RNA samples were taken every two days for 14 days. cDNA was synthesized from mRNA and qPCRs were performed to measure TBL1 and TBLR1 transcript levels in these cells.
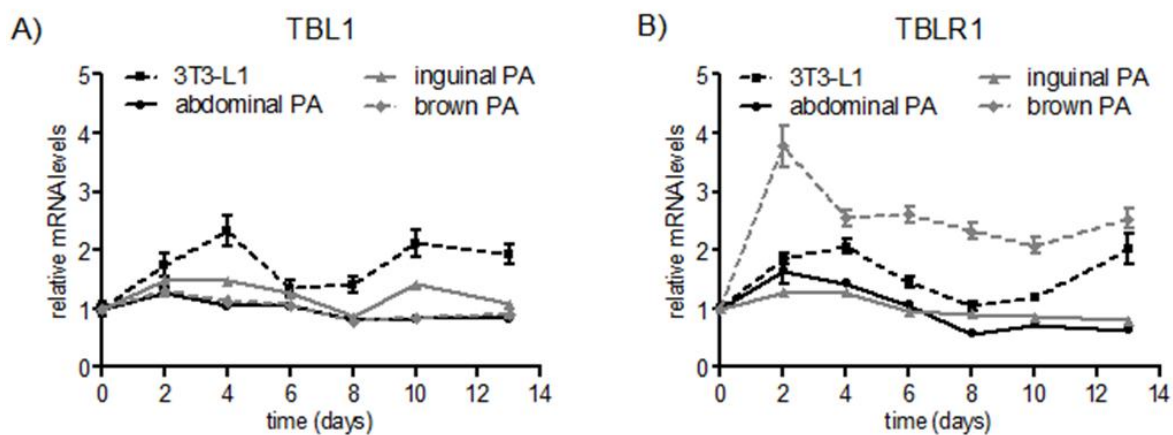
Fig. 14: TBL1 and TBLR1 mRNA expression are regulated during the course of adipocyte differentiation. *Adipocytes were differentiated as described in 'Methods' and mRNA levels were measured by qPCR. A) TBL1 and B) TBLR1 levels during 3T3-L1 adipocyte differentiation or during differentiation of preadipocytes (PA) isolated from SVF of abdominal and inguinal WAT and interscapular BAT depots. n=3, means ±SEM.*

As seen in Fig. 14, TBL1 and TBLR1 levels were increased 2.5-fold during early phases of 3T3-L1 adipocyte differentiation and decreased when adding only insulin to the cells. After insulin removal TBL1/TBLR1 expression increased again to a final 2-fold higher expression in mature adipocytes compared to the 3T3-L1 precursor cells (squares). As in 3T3-L1 cells, TBL1 and TBLR1 expression in primary cells was increased after initiation of differentiation but decreased with the addition of insulin. The attenuated induction of TBL1 and TBLR1 expression in primary cells (except for BAT) compared to 3T3-L1 cells may reflect a reduced differentiation capacity of the primary cells (40-60% differentiated primary adipocytes vs. 95% differentiated 3T3-L1 adipocytes), indicating that co-factor expression is rather indirectly regulated by events taking place during the differentiation process than the direct effects of the stimuli. This notion is further supported by the fact that the differentiation stimuli alone did not increase TBL1 or TBLR1 expression in 3T3-L1 adipocytes (Fig. 15). Overall, the induction of co-factor expression during adipocyte differentiation points towards a role of the co-factors in adipocyte biology.
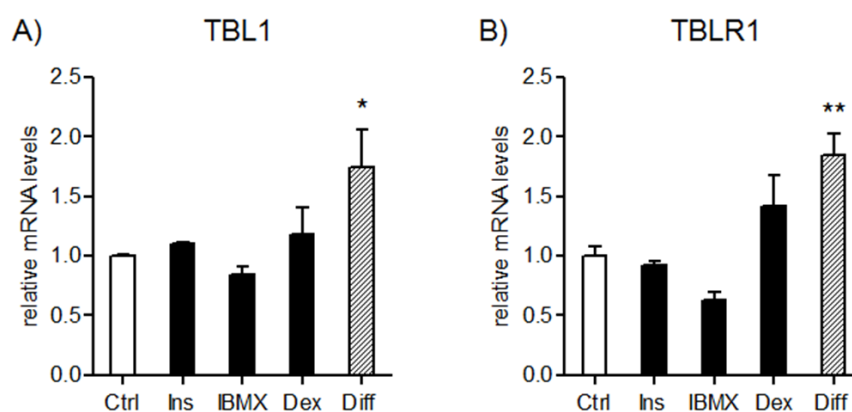
*Fig. 15: TBL1 and TBLR1 mRNA expression is unchanged in 3T3-L1 preadipocytes stimulated with insulin, IBMX or dexamethasone. 3T3-L1 cells were treated with 1 µg/ml insulin, 500 µM IBMX or 250 nM dexamethasone or a mixture of all three (differentiation cocktail) for 48 hrs, and mRNA levels were measured by qPCR. TBL1 (A) and TBLR1 (B) mRNA levels were analyzed by qPCR. n=3, means ±SEM, *indicates significance.*

2.2.2 TBL1 and TBLR1 are not required for adipocyte differentiation

Both TBL1 and TBLR1 levels are increased during the course of adipocyte differentiation, so it is tempting to speculate that they are required for proper function of this process. To investigate this, TBL1 and TBLR1 were knocked down in 3T3-L1 preadipocytes using adenovirus-mediated shRNA delivery, which resulted in an efficient reduction in TBL1 and TBLR1 mRNA expression during the course of adipocyte differentiation (Fig. 17 A, B). Ten days after induction of differentiation, cells were fixed with formaldehyde and lipids were stained using OilRedO-staining.

As seen in Fig. 16, 3T3-L1 cells could be differentiated into adipocytes with high triglyceride content within the lipid droplet. Comparing cells that were infected with adenoviruses carrying shRNA against TBL1, TBLR1, or both, with the negative control, no difference in differentiation capacity or lipid droplet number or size could be observed between the groups.

Control   TBL1 shRNA   TBLR1 shRNA   double k.d.
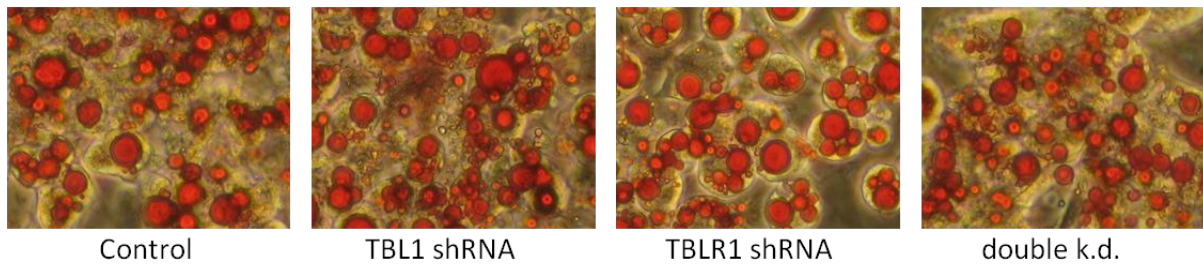
Fig. 16: TBL1 or TBLR1 knock down does not influence capacity of 3T3-L1 cells to differentiate into adipocytes. *3T3-L1 cells were transduced with adenoviruses carrying shRNAs against TBL1, TBLR1, or both, and differentiated into adipocytes as described in 'Methods'. Lipids were stained with OilRedO, and pictures were taken with 20-fold magnification.*

As shown in Fig. 17 C-F, TBL1, TBLR1, or double knock down did not lead to altered gene expression levels of PPARγ, FABP4, adiponectin, or lipoprotein lipase (LPL), again pointing towards a normal differentiation capacity of the 3T3-L1 adipocytes despite their lack of TBL1 or TBLR1.
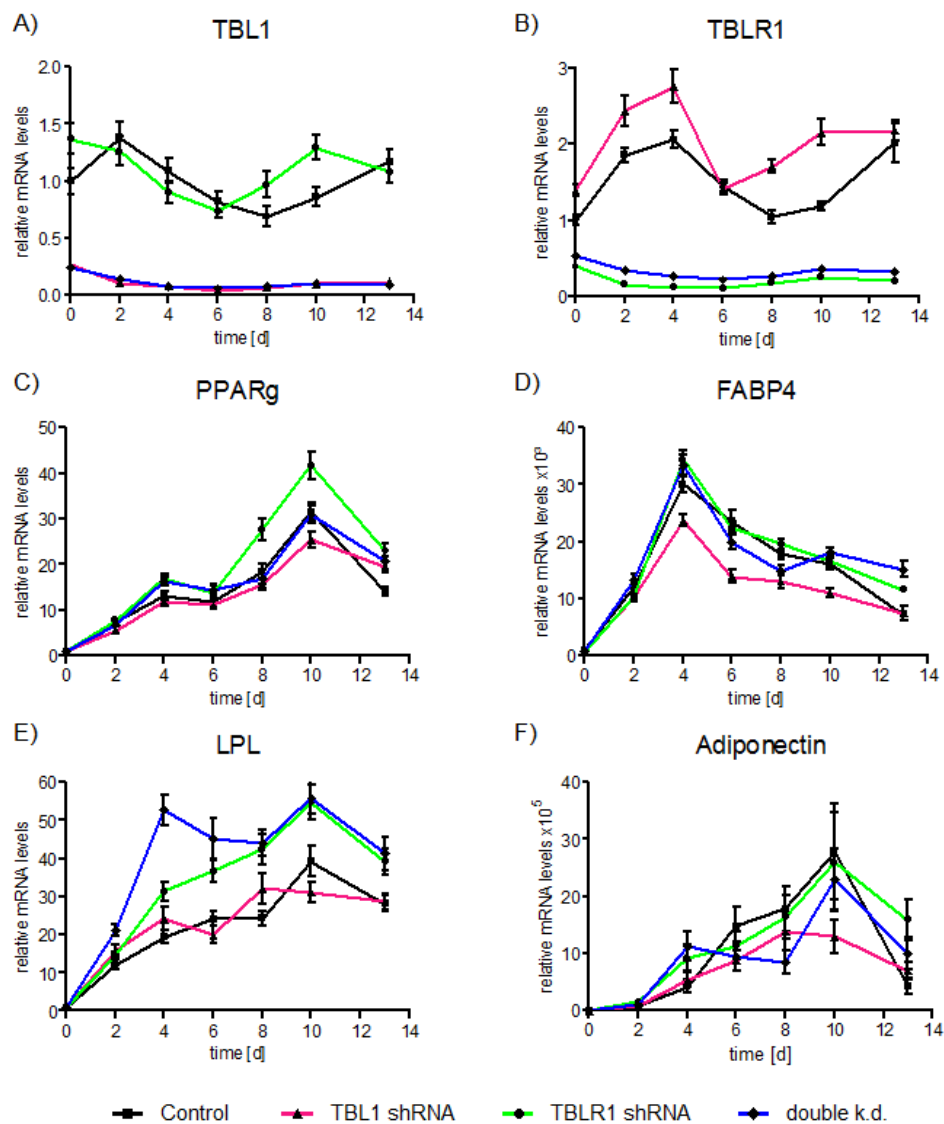
Fig. 17: mRNA expression levels of adipocyte marker genes during 3T3-L1 differentiation are unchanged upon TBL1 or TBLR1 knock down. *TBL1 (A) and TBLR1 (B) are efficiently knocked down during 3T3-L1 differentiation. Peroxisome proliferator-activated receptor γ (C), fatty acid binding protein 4 (D), lipoprotein lipase (E) and adiponectin (F) mRNA levels are shown. n=3, means ±SEM.*

2.3 TBL1 and TBLR1 play a role in adipocyte inflammation

2.3.1 TBL1 and TBLR1 are regulated by LPS and conditioned macrophage medium (CM) in 3T3-L1 adipocytes

It was shown before that TBLR1 levels were increased in WAT of LPS-injected mice. Here it was analyzed if the same was true for cultured adipocytes. For this, 3T3-L1 adipocytes were treated with either 100 ng/ml LPS or with medium containing macrophage-secreted cytokines (conditioned macrophage medium, CM) for 3 hours. To produce CM, confluent RAW264.7 macrophages were treated with normal culture medium with or without 100 ng/ml LPS for 9 hours and medium was collected and filtered through a 0.45 µm filter before adding it to the 3T3-L1 adipocytes. mRNA expression of TBL1 and TBLR1 was measured by qPCR.
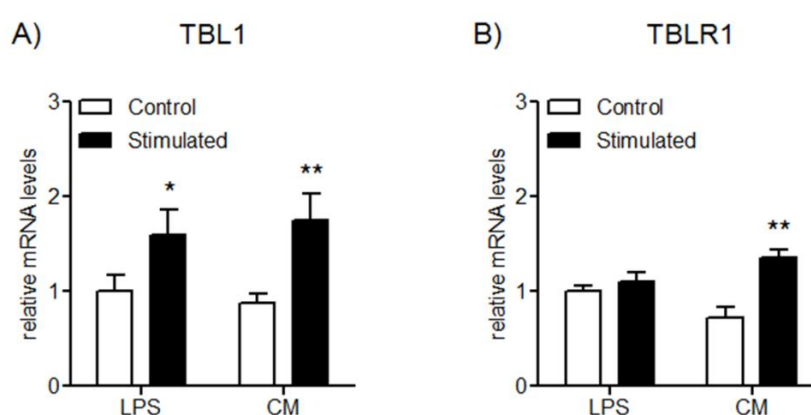
Fig. 18: TBL1 and TBLR1 expression is increased in 3T3-L1 adipocytes treated with LPS or CM. Cells were stimulated with 100 ng/ml LPS or conditioned macrophage medium for 3 hrs. mRNA levels were analyzed by qPCR. A) TBL1 mRNA expression, B) TBLR1 mRNA expression in control and stimulated states. n=4, means ±SEM, *indicates significance.

As shown in Fig. 18, TBL1 levels were induced by inflammatory stimuli like LPS or conditioned macrophage medium, while TBLR1 levels only increased with CM treatment, indicating that macrophage secreted factors are required to mediate the inflammation-dependent upregulation of this co-factor in adipocytes.

2.3.2 TBL1 and TBLR1 are efficiently knocked down in cultured adipocytes using adenovirus-mediated shRNA

To study the influence of TBL1 and TBLR1 on mature adipocytes, differentiated 3T3-L1 cells or primary adipocytes were infected with adenoviruses carrying shRNAs against TBL1, TBLR1, or a scrambled control sequence. For this, the differentiated cells were infected with the viruses (MOI 500 for 3T3-L1 and MOI 1000 for primary cells) for 3 days to allow for an efficient knock down of the co-factors. As seen in Fig. 19, TBL1 and TBLR1 were efficiently knocked down in 3T3-L1 and primary adipocytes both on mRNA and on protein levels.
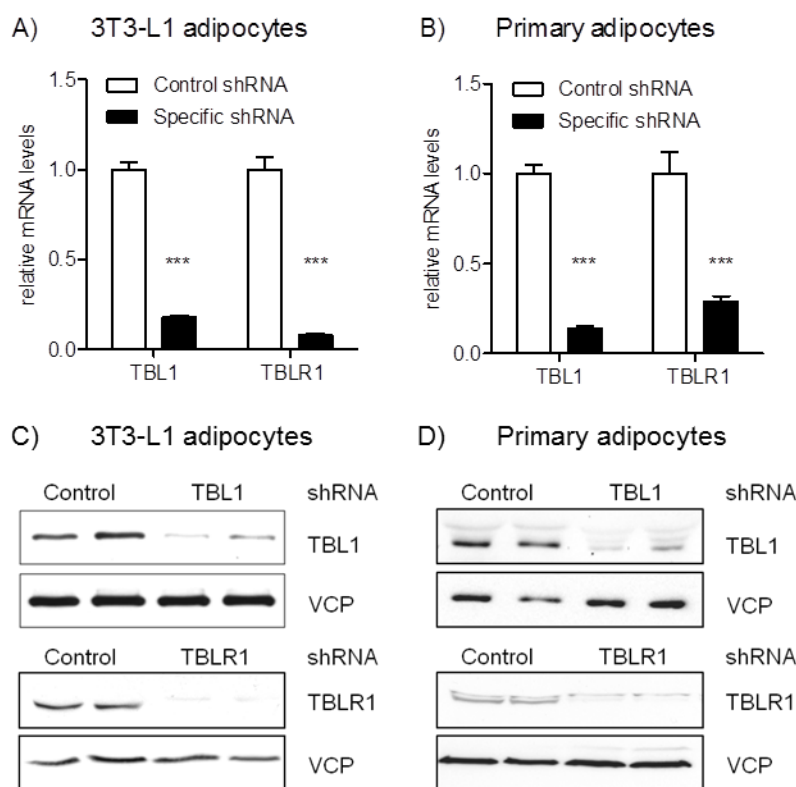
Fig. 19: TBL1 and TBLR1 are efficiently knocked down in 3T3-L1 and primary adipocytes. *3T3-L1 (A, C) or primary (B, D) adipocytes were infected with adenoviruses carrying shRNAs against TBL1, TBLR1, or a scrambled control sequence and harvested after 3 days. mRNA levels were analyzed by qPCR (A, B), protein levels were analyzed by immunoblotting using specific antibodies (C, D). n=2-6, means ±SEM, *indicates significance.*

2.3.3 Knock down of TBLR1 in adipocytes leads to blunted inflammatory response to LPS or CM

As TBL1 and TBLR1 are upregulated in inflamed adipocytes, it is tempting to speculate that they may play a role in mediating inflammatory responses of these cells. To test this, 3T3-L1 or primary inguinal adipocytes were treated with 100 ng/ml LPS or CM for 3 hrs and inflammatory gene expression was monitored upon adenovirus-mediated TBL1/TBLR1 knock down.

Fig. 20 shows that both LPS and CM treatment strongly induced gene expression of the inflammatory cytokines IL6 (by 15- and 1000-fold, respectively) and TNFα (by 8- and 150-fold). This was true for the control group as well as for cells lacking TBL1. Upon TBLR1 knock down, however, the inflammatory response was strongly inhibited by 90% (LPS) or 60% (CM) in case of IL6 or even blunted in case of TNFα, suggesting that TBLR1 but not TBL1 is a positive regulator of cytokine expression in adipocytes. Double knock down of TBL1 and TBLR1 did not further add to the effect of TBLR1 knock down alone, further supporting the notion that TBLR1 is sufficient to regulate inflammatory gene expression in these cells.
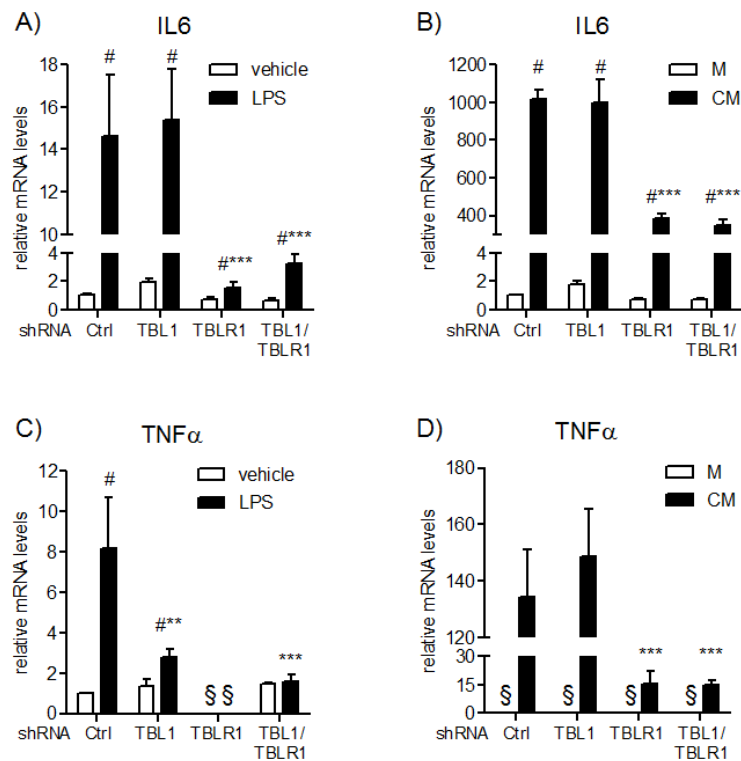
Fig. 20: IL6 and TNFα mRNA expression in 3T3L1 adipocytes treated with LPS or conditioned macrophage medium is decreased in cells lacking TBLR1. *3T3-L1 adipocytes with or without TBL1, TBLR1 or control shRNA were treated with 100 ng/ml LPS (A, C) or 9 hrs CM for 3 hrs and mRNA expression of cytokines was measured by qPCR. A) IL6 expression in 3T3-L1 treated with or without LPS, B) IL6 expression in 3T3-L1 treated with conditioned macrophage medium (CM) or control macrophage medium (M). C) TNFα expression in 3T3-L1 treated with LPS, D) TNFα expression in 3T3-L1 treated with CM or M. § indicates that mRNA levels are below detection limits. n=4, means ±SEM, # indicates significance between basal and stimulated, *indicates significance between Ctrl and specific shRNA.*

As observed in the 3T3-L1 adipocytes, TBLR1 knock down in primary adipocytes also led to a reduced induction of IL6 and TNFα stimulated by 3 hrs of LPS or CM treatment (Fig. 21).
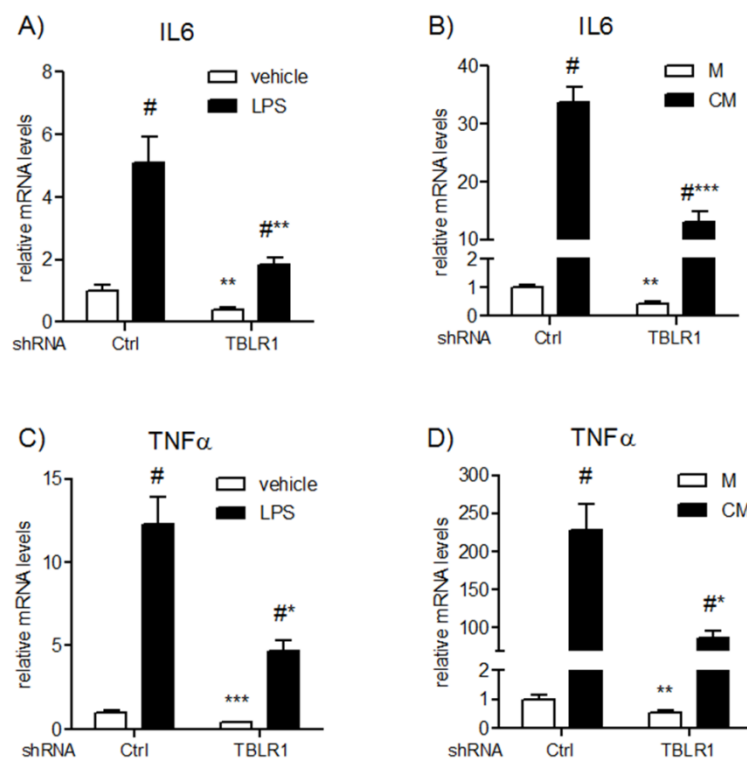
*Fig. 21: LPS or conditioned macrophage medium-stimulated expression of IL6 and TNFα in primary adipocytes is decreased in cells lacking TBLR1. Primary adipocytes with or without TBLR1 or control shRNA were treated with 100 ng/ml LPS (A, C) or 9 hrs CM for 3 hrs and mRNA expression of cytokines was measured by qPCR. A) IL6 expression in primary adipocytes treated with or without LPS, B) IL6 expression in primary adipocytes treated with conditioned macrophage medium (CM) or control macrophage medium (M). C) TNFα expression in primary adipocytes treated with LPS, D) TNFα expression in primary adipocytes treated with CM or M. n=4, means ±SEM. # indicates significance between basal and stimulated, *indicates significance between Ctrl and specific shRNA.*

2.3.4 TBLR1 is an NFκB dependent regulator of interleukin 6 expression

TBLR1 knock down in adipocytes led to reduced inflammatory response in these cells, so TBLR1 may act as an activator of inflammatory gene expression. To test this hypothesis, luciferase assays with the interleukin 6 promoter were performed. 3T3-L1 adipocytes were transfected with plasmids containing the IL6 promoter or deletion constructs of this promoter lacking the C/EBP, NFκB or AP1 binding sites in frame with the luciferase coding sequence. A second construct expressing either flag peptide as a control or flag-TBLR1 was co-transfected, and a third vector encoding β-galactosidase was used to normalize results.
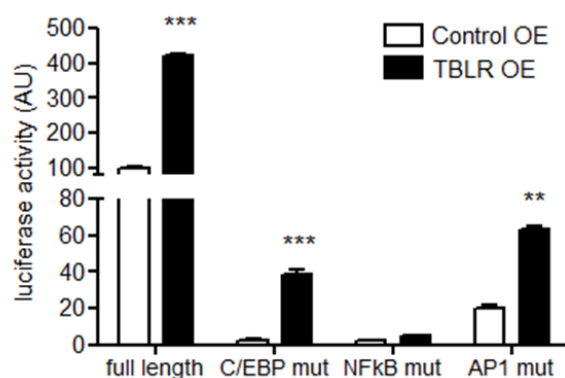
*Fig. 22: TBLR1 activates interleukin 6 promoter activity dependent on NFκB. 3T3-L1 adipocytes were transfected with plasmids containing the IL6 promoter or deletion constructs of this promoter lacking the C/EBP, NFκB or AP1 binding sites in frame with the luciferase coding sequence (C/EBP mut, NFκB mut, AP1 mut) and co-transfected with plasmids mediating TBLR1 or flag over expression (OE). Luciferase activity is normalized to β-galactosidase and plotted relative to control OE, full length IL6 and expressed in arbitrary units (AU). n=3, means ±SEM. *indicates significance.*

As expected from the reduced activation of interleukin 6 levels upon TBLR1 knock down, TBLR1 over expression activated IL6 expression as measured by a higher IL6 promoter activity in the luciferase assay. TBLR1 over expression also led to an increase in IL6 promoter activity when the C/EBP or AP1 transcription factor binding sites were mutated. In contrast, IL6 promoter activity was not activated by TBLR1 over expression when the NFκB binding site was mutated. Thus, TBLR1 seems to be an NFκB dependent activator of IL6 expression.

2.4 The role of TBLR1 in adipocyte lipid metabolism *in vitro*

2.4.1 TBLR1 expression influences adipocyte triglyceride levels

TBL1 and TBLR1 have been previously shown to influence liver lipid metabolism (Kulozik, P., 2011). Since lipid storage and hydrolysis is the main function of the adipose tissue apart from its endocrine functions, here we investigated whether TBL1 and TBLR1 also influenced triglyceride levels in the

adipocytes. 3T3-L1 adipocytes were transduced with adenoviruses carrying shRNA against TBL1, TBLR1 or a scrambled control sequence, and triglyceride levels were measured three days after transduction.

As seen in Fig. 23, 3T3-L1 adipocytes contained approximately 0.22 mg triglycerides per mg protein, and virus transduction did not influence triglyceride levels. TBL1 knock down did not have an effect on adipocyte TG levels. In contrast, TBLR1 knock down slightly but significantly increased triglyceride content of the cells.
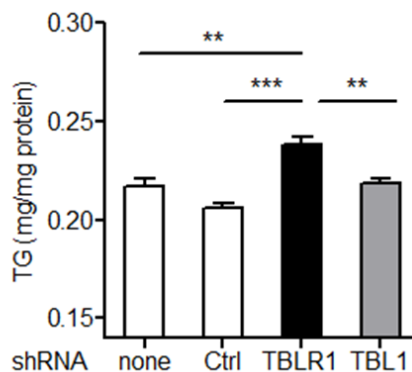
Fig. 23: TBLR1 knock down in 3T3-L1 adipocytes leads to increased triglyceride content of the cells. *3T3-L1 adipocytes with or without TBL1, TBLR1, or control shRNA were harvested in Tx lysis buffer and triglyceride and protein content were measured. Triglyceride levels are calculated relative to protein content. n=6, means ±SEM, *indicates significance.*

2.4.2 TBLR1 knock down inhibits induction of lipolysis

Increased triglyceride content in adipocytes lacking TBLR1 can be due to increased storage or impaired release of triglycerides in these cells. To analyze whether TBL1/TBLR1 are implicated in adipocyte triglyceride breakdown, the impact of the co-factors on β-adrenergic receptor (β-AR) mediated lipolysis was investigated. Isoproterenol, which is structurally similar to epinephrine, activates all three β-adrenergic receptors (Lass, A., 2011). Isoproterenol-stimulated adipocytes hydrolyze triglycerides into glycerol and fatty acids and secrete them into the surrounding medium.
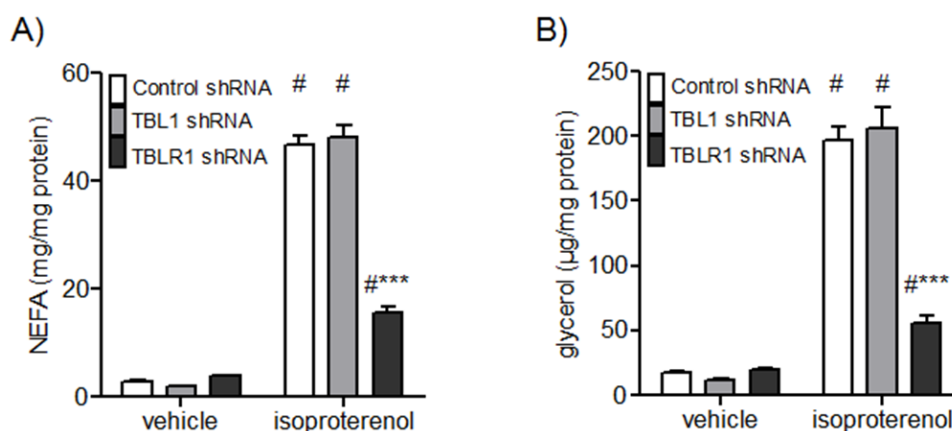
Fig. 24: TBLR1 knock down leads to reduced isoproterenol-stimulated lipolysis. *Lipolysis is stimulated in 3T3-L1 adipocytes with TBL1, TBLR1 or control shRNA by 10 µM isoproterenol for 3 hrs. Rate of lipolysis is estimated by NEFA (A) and glycerol (B) levels in the medium surrounding the cells. n=4, means ±SEM, # indicates significance between basal and stimulated, *indicates significance between Ctrl and specific shRNA.*

Increased secretion of non-esterified fatty acids (NEFAs) and glycerol was measured in 3T3-L1 adipocytes treated with 10 µM isoproterenol for 3 hrs after 2 hrs serum deprivation. The same degree of stimulation was observed in both control cells and cells lacking TBL1. In contrast, TBLR1 knock down led to decreased isoproterenol-mediated induction of lipolysis as measured both in NEFA and glycerol levels, pointing towards an activating role of TBLR1 in triglyceride breakdown (Fig. 24).

To analyze whether the effect of TBLR1 on the stimulation of lipolysis was specific for isoproterenol or independent of the stimulus used, 3T3-L1 adipocytes with or without TBLR1 shRNA were stimulated with 10 µM isoproterenol, 10 µM norepinephrine, 1 µM procaterol (a β2-AR agonist), 10 µM CL316,243, or 10 µM forskolin (an adenylate cyclase agonist) for 3 hrs and rate of lipolysis was estimated by NEFA levels in the medium. As seen in Fig. 25, TBLR1 knock down led to reduced induction of lipolysis independent of the stimulus used. Thus, neither of the β-adrenergic receptors alone could be responsible for the reduced lipolysis mediated by TBLR1 knock down, as the effect was observed in both isoproterenol and norepinephrine (unspecific β-AR agonists) and the β2-specific activator procaterol or the β3-specific activator CL316,243 stimulations. Also, TBLR1 does not act via adenylate cyclase (AC), since cells stimulated with the AC activator forskolin showed the same TBLR1 effects as cells stimulated with the β-AR agonists.
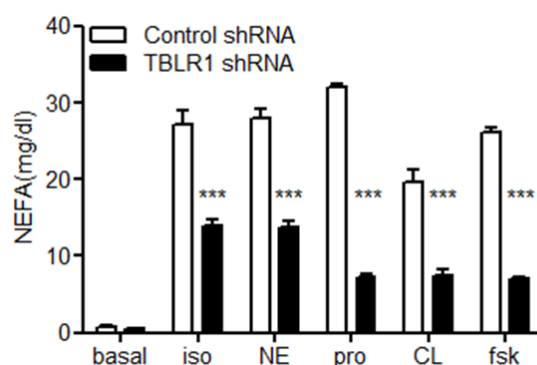
*Fig. 25: TBLR1 knock down leads to decreased stimulation of lipolysis independent of lipolytic stimulus. 3T3-L1 adipocytes with or without TBLR1 shRNA were treated with 10 µM isoproterenol (iso), 10 µM norepinephrine (NE), 100 nM procaterol (pro), 10 µM CL316,243, or 10 µM forskolin (fsk) for 3 hrs and NEFA were measured in the surrounding medium. n=4, means ±SEM, *indicates significance.*

2.4.3 TBLR1 knock down does not activate glucose metabolism or lipogenesis

Adipocytes are able to take up glucose and metabolize it to form novel triglycerides for long- or medium-term storage by the process of lipogenesis, although this is not the major pathway for fat deposition (Strawford, A., 2004). This process is stimulated by insulin, which at the same time inhibits triglyceride hydrolysis. Glucose uptake and metabolism can be studied in vitro using ^{14}C labeled glucose, which is taken up by the cells upon insulin stimulation and metabolized to triglycerides.

3T3-L1 adipocytes transduced with TBLR1 or control shRNA were stimulated with 10 nM insulin in a buffer containing 0.1 µCi D-[[14]C(U)]-Glucose. After 2 hrs incubation, radioactive signal was measured in total cell extracts to estimate glucose uptake and metabolism and in lipid extracts to estimate *de novo* triglyceride formation.

Fig. 26: Insulin-stimulated glucose metabolism and lipogenesis in 3T3-L1 adipocytes upon TBLR1 knock down. 3T3-L1 adipocytes with TBLR1 or control shRNA were treated with 10 nM insulin and 0.1 µCi D-[^{14}C(U)]-Glucose for 2 hrs and disintegrations per minute (DPM) were measured from total cell or lipid extracts. A) Glucose uptake and metabolism measured by DPM in whole cell extracts, B) Lipogenesis measured by DPM in lipid extracts, C) and D) Stimulation of glucose metabolism and lipogenesis shown in percent induction by insulin. n=4, means ±SEM, # indicates significance between basal and stimulated, *indicates significance between Ctrl and specific shRNA..

As shown in Fig. 26 A, insulin efficiently stimulated glucose uptake into 3T3-L1 adipocytes independent of TBLR1 levels. Approximately half of the freshly integrated glucose was incorporated into lipids (Fig. 26 B), but lipogenesis seemed to be reduced in both basal and insulin-stimulated conditions upon TBLR1 knock down. Looking at the percent of induction by insulin (Fig. 26 C-D), both glucose uptake and lipogenesis were unchanged in cells lacking TBLR1. Thus, TBLR1 has no influence on insulin signaling and increased lipogenesis upon TBLR1 knock down cannot account for the increase in triglyceride content of these cells (Fig. 23).

2.4.4 TBLR1 does not influence insulin signaling in 3T3-L1 adipocytes

Insulin is an important regulator of metabolic functions. In adipocytes, insulin regulates triglyceride metabolism by inhibition of lipolysis and activation of lipogenesis. Insulin stimulation of adipocytes leads to an activation of Akt (protein kinase B, PKB) by phosphorylation (Yu, Y. H. and Ginsberg, H. N., 2005), thus investigating phosphorylated Akt levels is a direct measure of insulin action in these cells. Here, 3T3-L1 adipocytes with control or TBLR1 shRNA were stimulated with increasing levels of

insulin in serum-free medium for 10 min. Proteins from whole cell extracts were separated by SDS-PAGE and total and phosphorylated Akt levels were measured by immunoblotting.

Fig. 27: Insulin signaling is not affected by TBLR1 knock down*. 3T3-L1 adipocytes were infected with adenoviruses carrying shRNAs against TBLR1 or a control sequence and three days later stimulated with 0, 0.1, 1, or 10 nM insulin for 10 min in serum-free medium. p-Akt, Akt, TBLR1 and VCP protein levels were detected by immuoblotting using specific antibodies.*

Fig. 27 shows that Akt phosphorylation was efficiently stimulated by increasing doses of insulin (0, 0.1, 1, 10 nM) for 10 min, while total Akt protein levels were constant. Knock down of TBLR1 did not influence Akt protein or phosphorylation levels in these cells. Thus, TBLR1 in 3T3-L1 adipocytes does not influence insulin signaling, which is further supported by the unchanged glucose metabolism and lipogenesis levels upon TBLR1 knock down.

2.4.5 TBLR1 knock down leads to reduced levels of lipases and lipolysis-associated proteins

Since TBLR1 knock down leads to reduced lipolysis, here we analyzed how TBLR1 knock down influences protein expression of the key proteins involved in lipolysis. For this purpose, adipocytes were infected with adenoviruses carrying shRNA against TBLR1 or a scrambled control sequence, and after three days cells were stimulated with 10 µM isoproterenol for 3 hrs prior to cell lysis. Proteins from whole cell lysates were separated by SDS-PAGE and detected by immunoblot using respective antibodies.
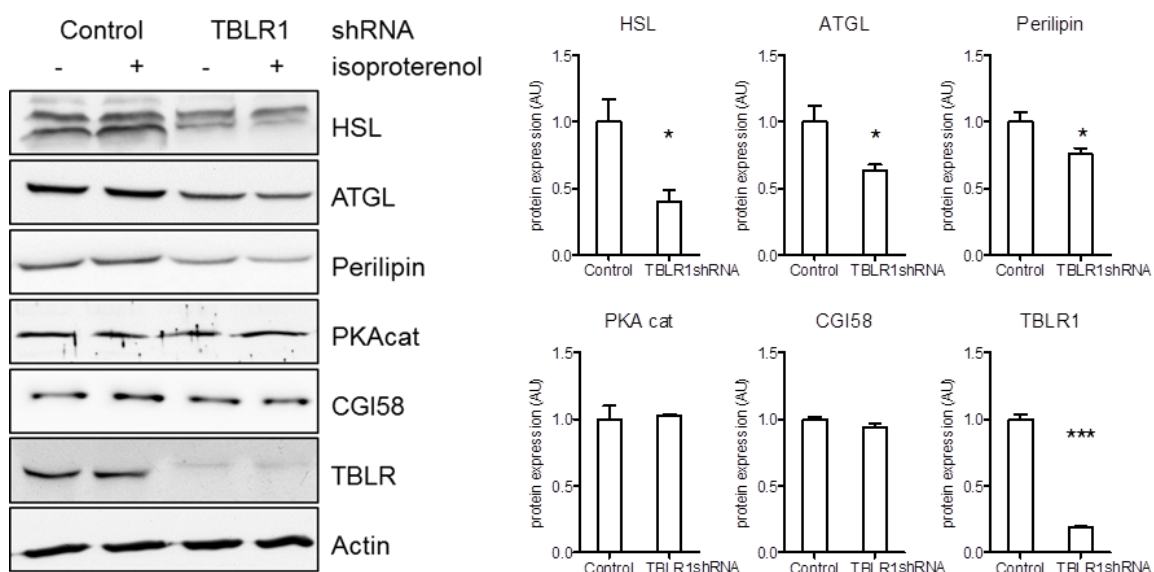
Fig. 28: Protein expression of lipases and lipolysis-associated proteins is decreased in 3T3-L1 adipocytes lacking TBLR1.
*3T3-L1 adipocytes with TBLR1 or unspecific control shRNA were treated with or without 10 µM isoproterenol for 3 hrs and protein levels were analyzed by immunoblot using the respective antibodies. Protein levels were quantified using ImageJ and normalized to actin levels. n=2 from three independent experiments. means ±SEM, * indicates significance.*

As shown in Fig. 28, isoproterenol stimulation in control 3T3-L1 adipocytes did not influence protein levels of the key lipases HSL and ATGL after 3 hrs. Cells lacking TBLR1 however showed strongly reduced protein expression of HSL and ATGL as well as the lipid droplet coating protein perilipin irrespective of isoproterenol treatment. In contrast, protein levels of the catalytic subunit of PKA (PKAcat) and CGI-58, the co-activator of ATGL, were unchanged by either isoproterenol treatment or TBLR1 knock down.

2.4.6 TBLR1 knock down leads to reduced activation (phosphorylation) of hormone sensitive lipase and other PKA targets

To analyze activation of the β-adrenergic signaling cascade, 3T3-L1 adipocytes treated with TBLR1 or control shRNAs were stimulated with 10 µM isoproterenol for 3 hrs, proteins were harvested in a buffer containing phosphatase inhibitors, and phosphorylated HSL (serine660 or serine565) and PKA targets were detected. Phosphorylation was quantified by normalization to actin or HSL protein levels.
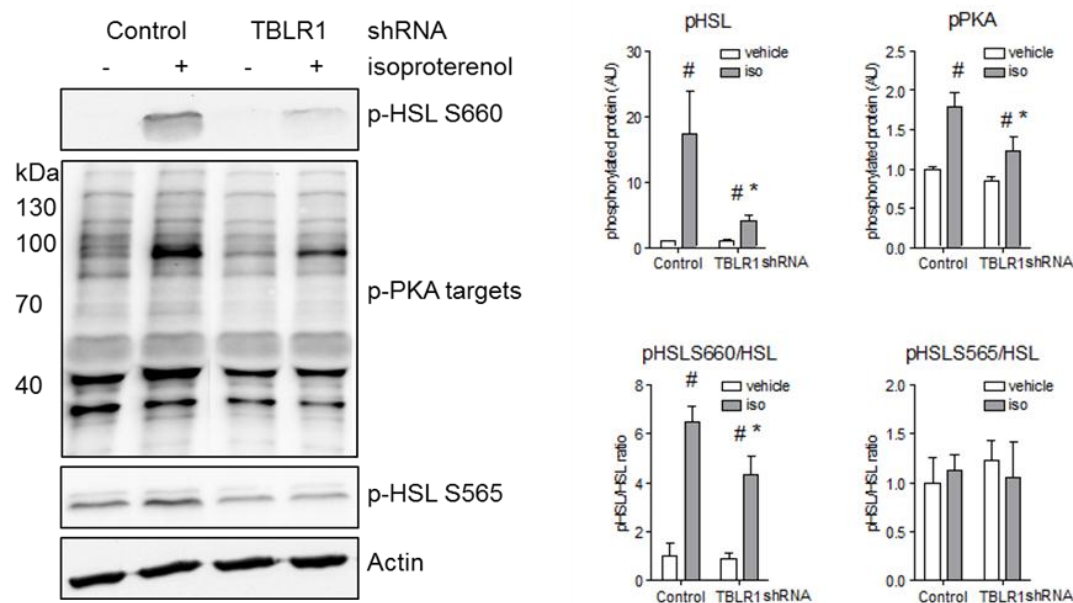
Fig. 29: Phosphorylation of HSL and other PKA targets including perilipin is decreased in 3T3-L1 adipocytes lacking TBLR1.
*3T3-L1 adipocytes with TBLR1 or unspecific control shRNA were treated with or without 10 µM isoproterenol for 3 hrs and protein phosphorylation was analyzed by immunoblot using the respective antibodies. Phosphorylated protein levels were quantified using ImageJ and normalized to actin or HSL protein levels. n=2 from four independent experiments. means ±SEM, # indicates significance between basal and stimulated, *indicates significance between Ctrl and specific shRNA.*

As shown in Fig. 29, serine residue 660 of HSL and other PKA targets, including perilipin, were strongly phosphorylated upon isoproterenol stimulation. HSL was not phosphorylated at the AMPK phosphorylation site (S565) upon isoproterenol stimulation. In cells lacking TBLR1, isoproterenol-stimulated HSL/PKA target phosphorylation was significantly reduced by 70% or 30%, respectively, while basal as well as AMPK-mediated phosphorylation was largely unchanged. As seen in the

quantitation bar graph, in contrast to the AMPK phosphorylation the reduced HSL phosphorylation by PKA cannot be fully attributed to the reduction in overall HSL protein levels, so adipocyte TBLR1 action has to be implicated in events independent of lipase transcription.

2.4.7 Inhibition of lipolysis by TBLR1 is independent of time and concentration of stimulus

Activation of lipolysis by β-adrenergic receptor signaling is dependent on the duration of stimulation and concentration of the stimulus (Lass, A., 2011). The most commonly used condition of 10 µM isoproterenol, 3 hrs represents a rather high concentration and duration of stimulus, so in order to study submaximal effects of the stimulation time- and concentration curves in 3T3-L1 adipocytes transduced with TBLR1 or control shRNA were performed. Stimulation of lipolysis by 10 µM isoproterenol for 15 min yielded no measurable increase in NEFAs, but after 60 min stimulation NEFAs were readily detectable in the supernatant of the cells and accumulated in the medium over time. In cells lacking TBLR1, the increase in NEFAs over time of isoproterenol stimulation was strongly reduced at all time points. The same was true for stimulation of the cells with submaximal doses of isoproterenol. HSL phosphorylation at serine660 was also strongly dependent on isoproterenol concentration, and was attenuated by TBLR1 knock down at all concentrations (Fig. 30).
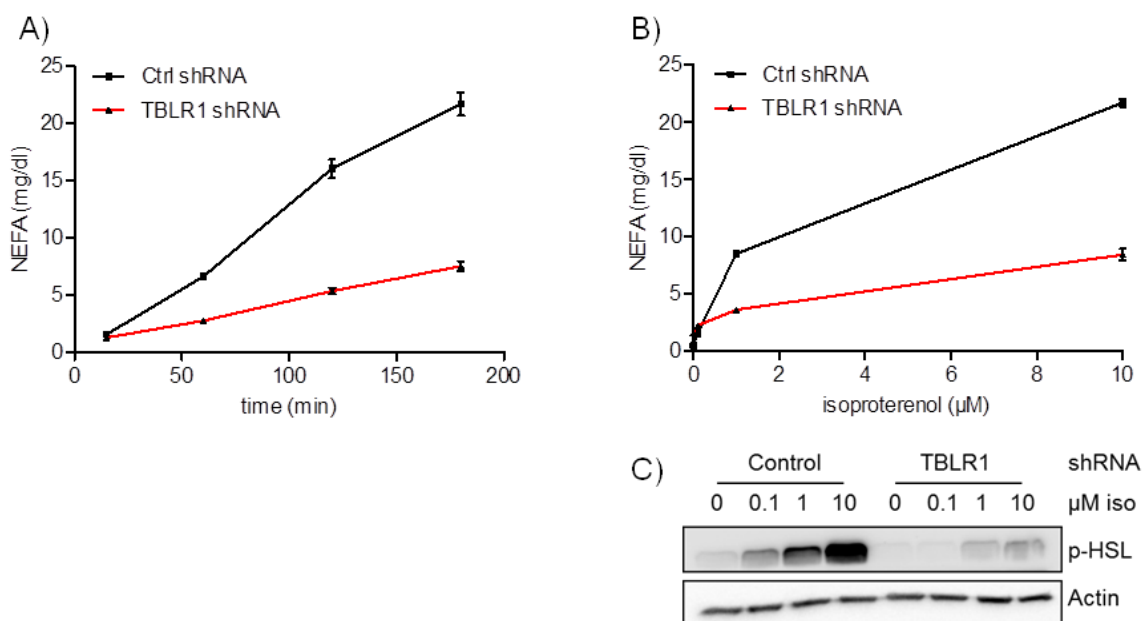
Fig. 30: TBLR1 knock down inhibits lipolysis independent of the duration of stimulation and the concentration of isoproterenol. 3T3-L1 adipocytes treated with TBLR1 or control shRNA were stimulated with 10 µM isoproterenol and media was collected after 15, 60, 120, and 180 min for NEFA measurement (A), or the cells were treated with 0.1, 1, or 10 µM isoproterenol for 180 min, supernatants were collected for NEFA measurements (B) and proteins were harvested for immunoblotting using Actin and p-HSL S660 antibodies (C). (A, B) means ±SEM, n=3.

2.4.8 Reduced PKA-mediated phosphorylation upon TBLR1 knock down is due to decreased cAMP levels

Phosphorylation of HSL at the serine 660 residue is dependent on the action of the cAMP dependent kinase PKA (Lampidonis, A.D., 2011). HSL and other PKA targets including perilipin were shown to be

less phosphorylated upon TBLR1 knock down. Activation of PKA can be regulated by the amounts of available cAMP, which is the most straightforward mechanism. Alternatively it can be regulated by the subunit composition of PKA: Mammals have four distinct regulatory PKA subunits (RIα, RIβ, RIIα und RIIβ), of which certain subunits have a higher affinity for cAMP than others. Thus, depending on the subunit composition of PKA, equal amounts of cAMP may lead to differential activation of the enzyme (Aye, T.T., 2009).
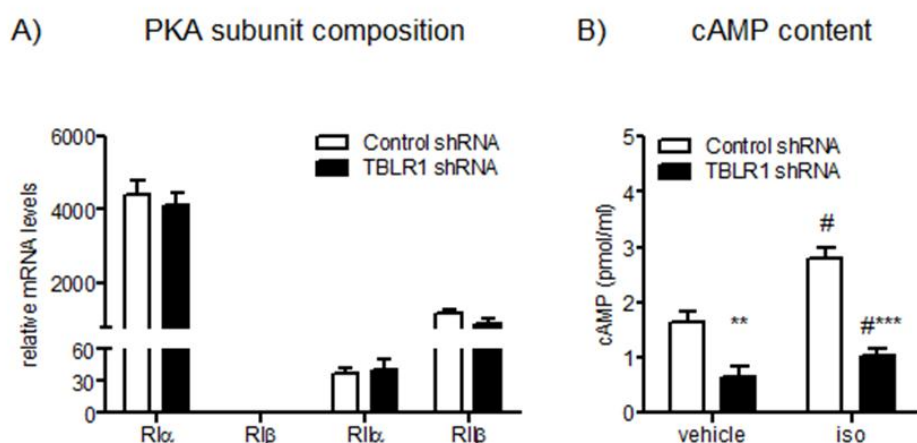
*Fig. 31: PKA subunit composition is unchanged in 3T3-L1 adipocytes with or without TBLR1. cAMP levels are strongly reduced upon TBLR1 knock down both in basal and isoproterenol-stimulated states. A) mRNA levels of protein kinase A regulatory subunits (RIα, RIβ, RIIα und RIIβ) were measured by qPCR in 3T3-L1 adipocytes with or without TBLR1 shRNA. mRNA levels are expressed relative to TBP and RIβ levels. B) cAMP content of 3T3-L1 adipocytes with or without TBLR1 shRNA, treated with 10 µM isoproterenol for 3 hrs. n=4, means ±SEM, # indicates significance between basal and stimulated, *indicates significance between Ctrl and specific shRNA.*

PKA regulatory subunit composition of 3T3-L1 adipocytes treated with TBLR1 or control shRNA was analyzed by qPCR and showed no significant differences between the two groups (Fig. 31 A). However, 3T3-L1 adipocytes treated with isoproterenol had significantly increased cAMP content, which was strongly decreased in 3T3-L1 adipocytes lacking TBLR1 (Fig. 31 B). Thus, reduced cAMP content in adipocytes lacking TBLR1 was responsible for the attenuated phosphorylation of HSL and other PKA targets in these cells.

2.4.9 Reduced cAMP content in adipocytes lacking TBLR1 is not due to increased phosphodiesterase levels

Protein kinase A is negatively regulated by phosphodiesterase PDE3B, which hydrolyzes cAMP to AMP, thereby reducing cAMP concentration and leading to reduced levels of active, dissociated PKA subunits. PDE3B mediates the inhibition of the lipolysis pathway stimulated by insulin (Yu, Y. H. and Ginsberg, H. N., 2005). Analysis of PDE3B mRNA levels in 3T3-L1 adipocytes with or without TBLR1 shRNA revealed that there was no change in PDE3B mRNA expression upon TBLR1 knock down (Fig. 32 A). Apart from this, the phosphodiesterase inhibitor IBMX stimulated lipolysis with or without 10 µM isoproterenol independent of TBLR1 expression levels (Fig. 32 B). This excludes PDE3B regulation as the mechanism mediating TBLR1 knock down dependent reduction in cAMP levels.
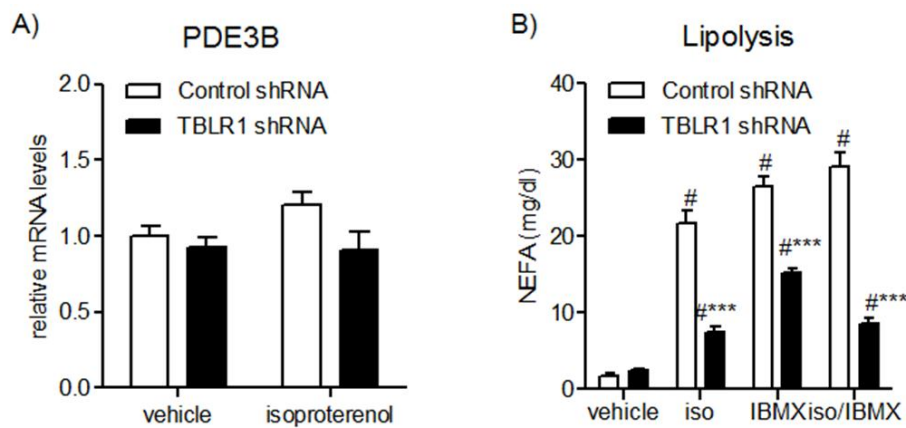
Fig. 32: TBLR1 knock down does not change expression or activity of phoshodiesterase. *A) 3T3-L1 adipocytes transduced with control or TBLR1 specific shRNA were treated with 10 µM isoproterenol for 3 hrs and PDE3B mRNA expression was analyzed by qPCR. B) 3T3-L1 adipocytes transduced with control or TBLR1 specific shRNA were stimulated with 10 µM isoproterenol, 0.5 mM IBMX, or both for 3 hrs and NEFA levels were measured from the medium. n=4, means ±SEM, # indicates significance between basal and stimulated, *indicates significance between Ctrl and specific shRNA.*

2.4.10 Reduced cAMP content in adipocytes lacking TBLR1 is due to decreased levels of β-adrenergic receptors

Adipocytes lacking TBLR1 show a reduced cAMP content, leading to attenuated activation of PKA and thus PKA phosphorylation targets like HSL. Since reduced cAMP levels upon TBLR1 knock down are not due to increased levels or activation of phosphodiesterase PDE3B, there has to be a defect in signaling events upstream of cAMP production. As lipolysis is stimulated by catecholamines binding to β-adrenergic receptors, here we analyzed mRNA and protein expression of the receptors in 3T3-L1 adipocytes with TBLR1 or control shRNA, treated with or without 10 µM isoproterenol for 3 hrs.
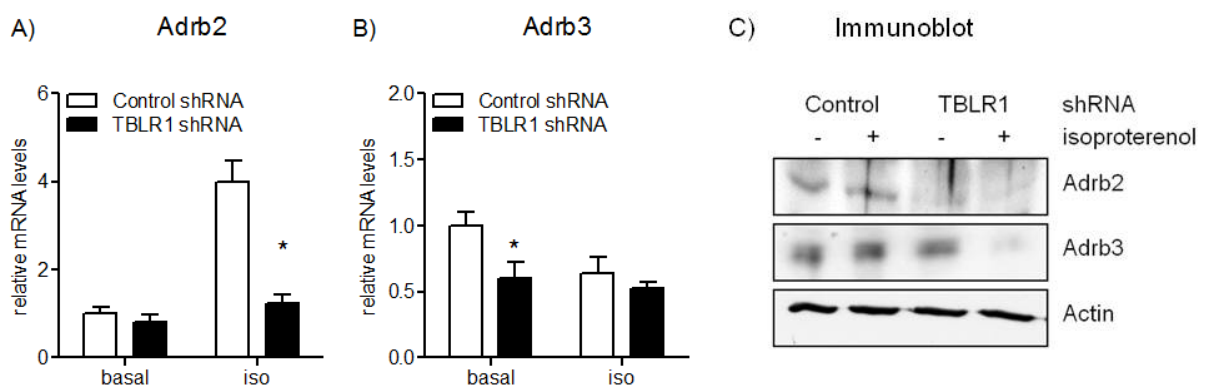
Fig. 33: β-adrenergic receptor levels are decreased in adipocytes lacking TBLR1. *3T3-L1 adipocytes with control or TBLR1 specific shRNAs were stimulated with or without 10 µM isoproterenol for 3 hrs. β2-adrenergic receptor (Adrb2, A) and β3-adrenergic receptor (Adrb3, B) mRNA levels were analyzed by qPCR, protein levels (C) were detected using specific antibodies. (A, B) n=4, means ±SEM, * indicates significance.*

There are three different β-adrenergic receptors involved in catecholamine signaling, β1, 2 and 3 adrenergic receptors (Zechner, R., 2012). mRNA or protein expression of the β-adrenergic receptor 1 could not be detected in 3T3-L1 adipocytes (data not shown). In contrast, β2 and β3 receptors were readily detectable in 3T3-L1 adipocytes by qPCR and immunoblotting. As seen in Fig. 33, the β-adrenergic receptor 2 (Adrb2) expression was increased on mRNA but not protein levels upon

isoproterenol treatment. In cells lacking TBLR1, Adrb2 expression was significantly decreased both on mRNA and protein levels. The β-adrenergic receptor 3 (Adrb3) expression was slightly reduced after isoproterenol treatment on mRNA levels in the control shRNA group, and as observed for Adrb2, Adrb3 levels were also decreased upon TBLR1 knock down. Isoproterenol treatment raises receptor turnover, which may explain why reduced protein expression of the Adrb3 upon TBLR1 knock down was only observed in the isoproterenol treated cells. The decreased receptor levels in cells lacking TBLR1 may explain the reduced cAMP levels leading to attenuated activation of phosphorylation mediated by PKA, which ultimately results in reduced activation of lipolysis.

2.4.11 TBLR1 is a transcriptional activator of HSL and ATGL transcription

As shown earlier in this thesis, TBLR1 knock down led to reduced protein levels of HSL and ATGL. With TBLR1 being a transcriptional co-factor it is tempting to speculate that TBLR1 influences transcription of these genes. To test this hypothesis, we performed luciferase assays and investigated if TBLR1 expression influenced HSL and ATGL promoter activity. For this purpose, 3T3-L1 adipocytes were transfected with vectors containing HSL or ATGL promoters in front of the luciferase coding sequence and co-transfected with plasmids carrying a non-specific control sequence or a sequence mediating TBLR1 knock down. β-galactosidase expression vector with the constitutive CMV promoter was co-transfected to normalize for transfection efficiency.
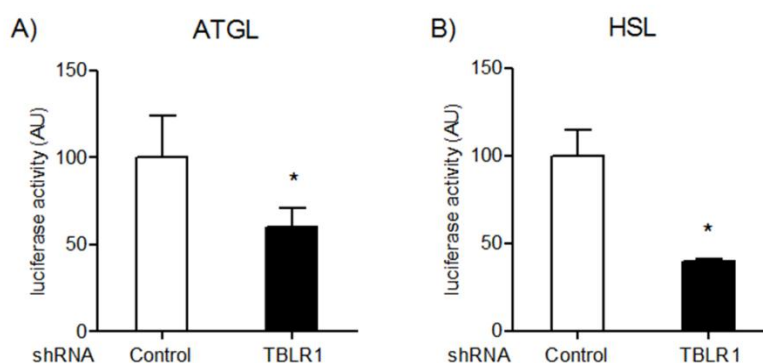
Fig. 34: ATGL and HSL promoter activities are reduced upon knock down of TBLR1. *3T3-L1 adipocytes transfected with luciferase constructs driven by ATGL and HSL promoters were co-transfected with plasmids mediating TBLR1 knock down and luciferase activity was measured; the values were normalized to β-galactosidase activity and expressed in arbitrary units (AU). A) ATGL promoter activity, B) HSL promoter activity. n=3, means ±SEM, * indicates significance.*

As seen in Fig. 34, reduced TBLR1 levels led to approximately 50% reduced activity of both ATGL and HSL promoters, further supporting the notion that TBLR1 is necessary for the transcription of the lipases.

2.4.12 Gene expression profiling of adipocytes lacking TBLR1 reveals strong implication of TBLR1 in PPAR and adipocytokine signaling pathways and lipid metabolism

Global gene expression profiling is a potent tool to analyze genes regulated by a certain transcription factor or transcriptional co-factor. Knowing that TBLR1 is implicated in cytokine signaling and lipid metabolism, we performed gene expression profiling of 3T3-L1 adipocytes transduced with TBLR1 or

a control shRNA and stimulated with or without 10 µM isoproterenol for 3 hrs. We compared four groups (Fig. 35 A) with a sample size of three.

As seen from the hierarchical heat map (Fig. 35 B), the four groups were very homogenous but distinct from one another, and the difference in global gene expression between control and TBLR1 shRNA was much higher than between basal and isoproterenol stimulated groups. In total, more than 7000 genes were alternatively regulated, of which 4714 were regulated both in vehicle and isoproterenol-treated cells (Fig. 35 C). The volcano plots (Fig. 35 D, E) show all genes on the microarray, all significantly altered genes (p < 0.05) are above the threshold.
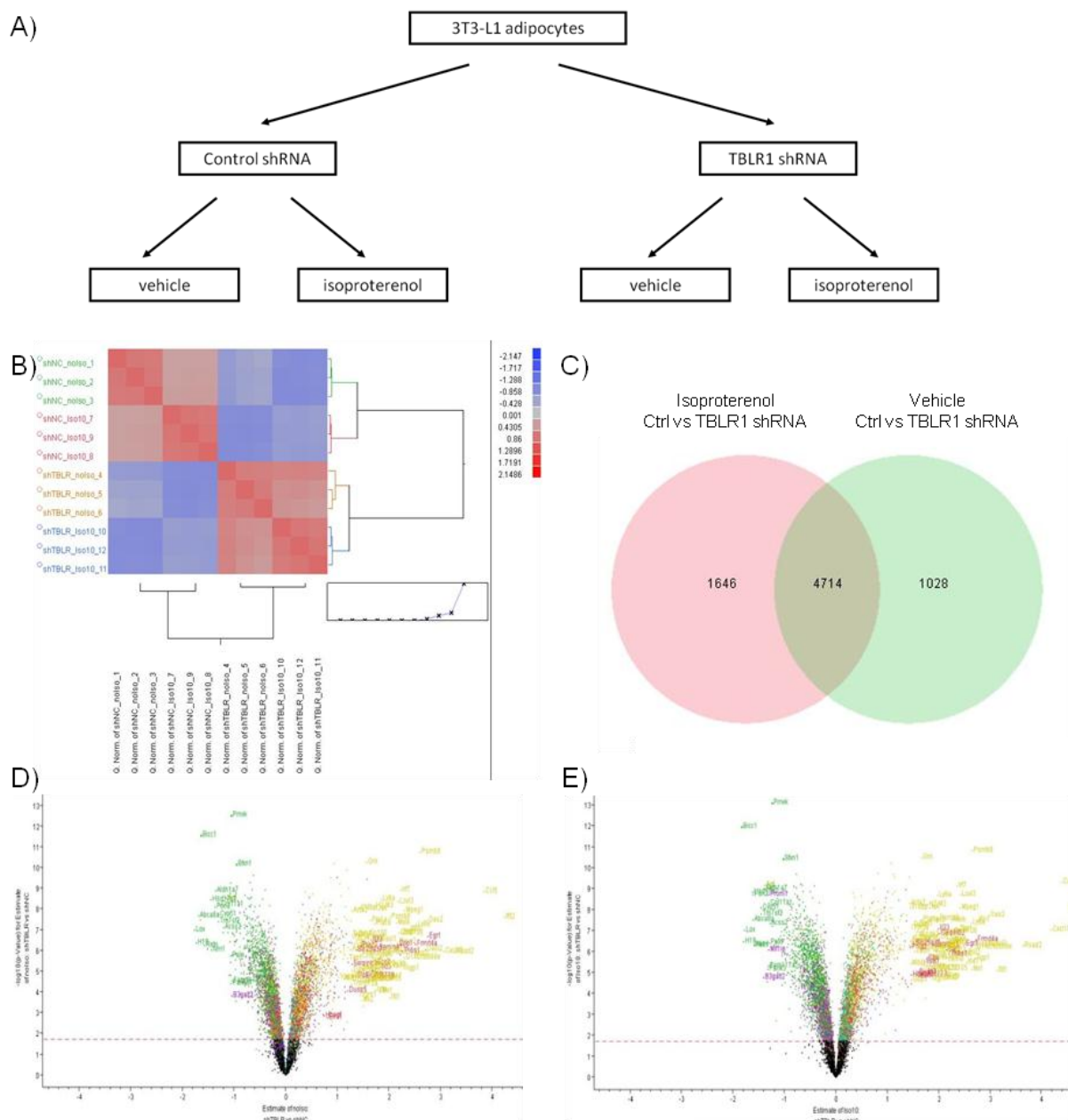
Fig. 35: Gene expression profiling of 3T3-L1 adipocytes transduced with TBLR1 or control shRNA and treated with or without 10 µM isoproterenol for 3 hrs. *A) Experimental setup, B) Hierarchical heat map cluster of the samples, C) Venn diagram of alternatively regulated genes, D) Volcano Plot of control vs. TBLR1 shRNA treated cells without isoproterenol, E) Volcano Plot of control vs. TBLR1 shRNA treated cells with isoproterenol. n=3.*

As expected from immunoblotting, HSL, ATGL and perilipin levels were reduced in cells lacking TBLR1 both in basal and isoproterenol-stimulated states. Apart from that, performing KEGG pathway analysis, we found that the most highly enriched cluster of pathways containing TBLR1 regulated genes consisted of the PPAR and adipocytokine signaling pathways and the lipid metabolism pathway (Tab. 1). All three pathways in this cluster were highly affected by TBLR1 knock down, indicating that TBLR1 regulates genes within these pathways, thereby influencing the whole signaling path.

Annotation Cluster 1 Enrichment Score: 3.14

	Term	Count	PValue	List total	Pop Hits	Pop Total	FDR
mmu03320	PPAR signaling pathway	25	0,0004	866	79	5738	0,49
mmu04920	Adipocytokine signaling pathway	22	0,0006	866	67	5738	0,70
mmu00071	Fatty acid metabolism	16	0,0017	866	45	5738	2,09

Annotation Cluster 2 Enrichment Score: 2.00

	Term	Count	PValue	List Total	Pop Hits	Pop Total	FDR
mmu00020	Citrate cycle (TCA cycle)	13	0,0011	866	31	5738	1,39
mmu00620	Pyruvate metabolism	15	0,0019	866	41	5738	2,28
mmu00010	Glycolysis / Gluconeogenesis	12	0,4508	866	68	5738	99,94

Annotation Cluster 3 Enrichment Score: 1.66

	Term	Count	PValue	List Total	Pop Hits	Pop Total	FDR
mmu00280	Valine, leucine and isoleucine degradation	17	0,0007	866	46	5738	0,88
mmu00071	Fatty acid metabolism	16	0,0017	866	45	5738	2,09
mmu00640	Propanoate metabolism	11	0,0098	866	30	5738	11,53
mmu00010	Glycolysis / Gluconeogenesis	12	0,4508	866	68	5738	99,94
mmu00410	beta-Alanine metabolism	3	0,8658	866	22	5738	100,00

Annotation Cluster 4 Enrichment Score: 1.52

	Term	Count	PValue	List Total	Pop Hits	Pop Total	FDR
mmu05010	Alzheimer's disease	41	0,0074	866	182	5738	8,83
mmu05012	Parkinson's disease	31	0,0132	866	133	5738	15,20
mmu00190	Oxidative phosphorylation	30	0,0170	866	130	5738	19,17
mmu05016	Huntington's disease	37	0,0519	866	183	5738	48,39
mmu04260	Cardiac muscle contraction	15	0,2811	866	78	5738	98,34

Annotation Cluster 5 Enrichment Score: 1.31

	Term	Count	PValue	List Total	Pop Hits	Pop Total	FDR
mmu00280	Valine, leucine and isoleucine degradation	17	0,0007	866	46	5738	0,88
mmu00071	Fatty acid metabolism	16	0,0017	866	45	5738	2,09
mmu00310	Lysine degradation	8	0,4248	866	41	5738	99,90
mmu00650	Butanoate metabolism	6	0,6750	866	37	5738	100,00
mmu00380	Tryptophan metabolism	6	0,7418	866	40	5738	100,00

Tab. 1: KEGG pathway analysis of genes regulated by TBLR1 knock down in both isoproterenol treated and untreated adipocytes. *Enrichment score: measure of pathway cluster enrichment over the other clusters; count: number of regulated genes within the pathway; pvalue: significance of pathway enrichment; list total: number of genes within the analyzed list of target genes having at least one KEGG annotation; pop hits: number of genes available on the entire microarray, annotated by the considered KEGG category or annotation cluster; pop total: number of genes available on the entire microarray and having at least one KEGG annotation; FDR: false discovery rate.*

Enrichment scores in the microarray are not necessarily comparable with qPCR expression values. In order to quantify the changes observed in the array we validated some genes that were found to be regulated by TBLR1 in gene expression profiling by quantitative PCR using the same RNA as for the microarray. As seen in Fig. 36, many genes involved in PPAR signaling, adipocytokine signaling, and lipid metabolism were found to be regulated by TBLR1 also by qPCR, while some other regulated genes could not be validated. Clustered to the adipocytokine signaling pathway, adiponectin, nuclear factor of κ light polypeptide gene enhancer in B-cells inhibitor α (IkappaB), and glucose transporter type 4 (Glut4) were down regulated upon TBLR1 knock down independent of isoproterenol

stimulation. Within the same pathway cluster, insulin receptor substrate 2 (Irs2), peroxisome proliferator-activated receptor γ coactivator 1-α (PGC-1α), and AMPK activator liver kinase B1 (Lkb1) were down regulated upon TBLR1 knock down only in cells stimulated with isoproterenol. Other cytokines like monocyte chemoattractant protein 1 (Mcp1) were upregulated upon TBLR1 knock down, as was the glucose transporter Glut1.

Looking at the PPAR signaling pathway, we observed a robust reduction in expression of many pathway associated genes including PPARγ itself as well as stearoyl-CoA desaturase-1 (Scd1), the transporters cluster of differentiation 36 (CD36) and aquaporin 7 (Aqp 7), lipoprotein lipase (Lpl), liver x receptor (Lxr) and fatty acid binding protein 4 (Fabp4). Phosphoenolpyruvate carboxykinase (PEPCK) was only regulated in isoproterenol stimulated cells as observed in the microarray.

In the fatty acid metabolism pathway, acyl-Coenzyme A dehydrogenase, medium chain (Acadm) and fatty acid synthase (Fasn) were down regulated upon TBLR1 knock down. In contrast to what was observed in the microarray, acyl-Coenzyme A dehydrogenase, long chain (Acadl) was not regulated by TBLR1. Apart from the genes that were clustered in pathways, we observed gene regulation of the β2- and β3-adrenergic receptors, hormone sensitive lipase and adipocyte triglyceride lipase, which was consistent with the regulation observed before on protein levels. Thus, microarray data could be validated by qPCR and confirmed a role of TBLR1 in the regulation of adipocytokine, PPAR and fatty acid metabolism pathways.
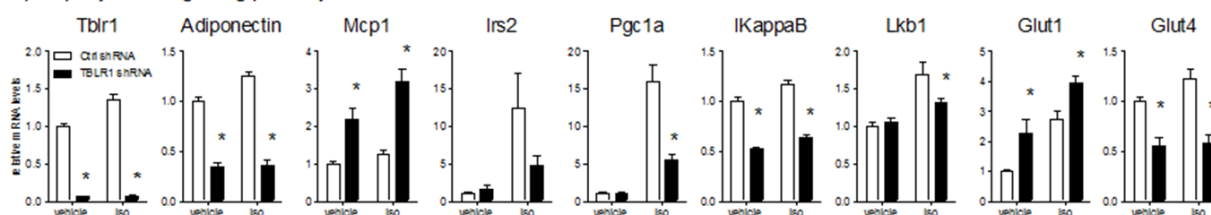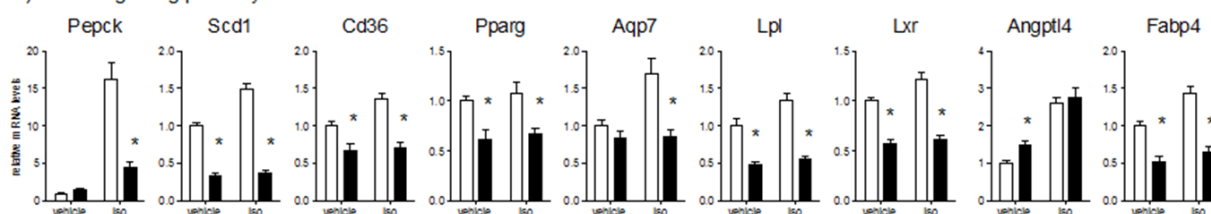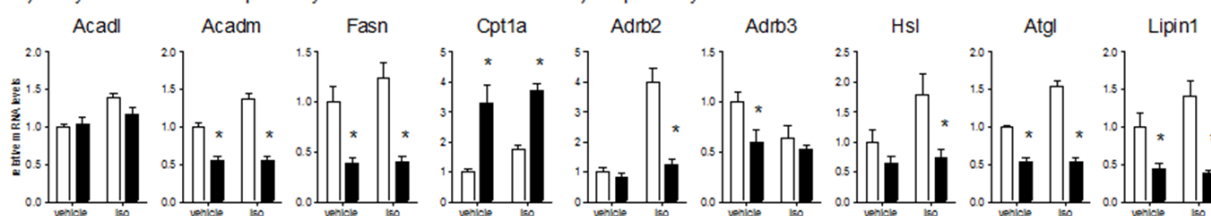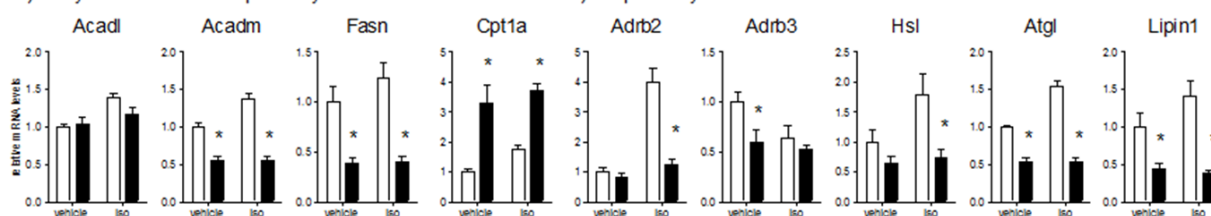
Fig. 36: Validation of microarray data by quantitative PCR reveals involvement of the co-factor in adipocytokine, PPAR and fatty acid metabolism pathways. 3T3-L1 adipocytes were transduced with adenoviruses carrying shRNA against TBLR1 or a control sequence. Adipocytes were stimulated with 10 µM isoproterenol for 3 hrs and induction of lipolysis was monitored by measuring NEFAs and glycerol from the supernatant. RNA isolation was performed using RNeasy mini kit. qPCRs were performed using the Taqman system. A) TBLR1 mRNA expression and expression of genes clustered to the adipocytokine pathway. B) mRNA expression of genes clustered to the PPAR signaling pathway. C) mRNA expression of genes clustered to the fatty acid metabolism pathway. D) mRNA expression of genes regulated by TBLR1 but not clustered to a pathway by the KEGG pathway analysis tool. n=4, means ±SEM, * indicates significance.

2.4.13 TBLR1 acts in part through PPARγ

Gene expression profiling revealed a large impact of PPARs on TBLR1-mediated regulation of gene expression, since the PPAR signaling pathway is most regulated by TBLR1 knock down in adipocytes. To investigate whether PPARs are able to compensate for the loss of TBLR1, we stimulated adipocytes with the PPAR agonists GW7647 (PPARα), GW0742 (PPARβ/δ) and rosiglitazone (PPARγ), and analyzed the effect of TBLR1 knock down on lipolysis as measured by NEFA and glycerol in the surrounding media.
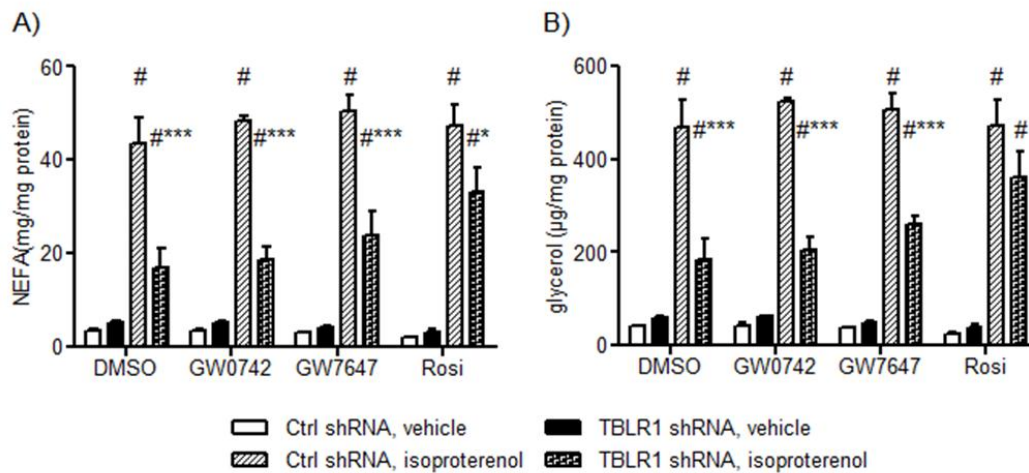
Fig. 37: Inhibition of lipolysis by TBLR1 knock down is in part rescued by rosiglitazone stimulation. 3T3-L1 adipocytes transduced with control or TBLR1 shRNA were stimulated with 10 μM isoproterenol for 3 hrs in the presence or absence of 1 μM GW0742, GW7647 or rosiglitazone for 24 hrs. A) NEFAs and B) glycerol measured from the supernatants of the cells and normalized to intracellular protein levels. n=4, means ±SEM, # indicates significance between basal and isoproterenol-stimulated, *indicates significance between Ctrl and specific shRNA.

As seen in Fig. 37, PPAR agonists alone did not stimulate lipolysis, nor did they influence the efficiency of isoproterenol to induce lipolysis. As seen before, TBLR1 knock down partially inhibited the isoproterenol-induced stimulation of lipolysis, which was independent on GW7647 or GW0742 treatment. In cells pretreated with rosiglitazone, however, the inhibitory effect of TBLR1 knock down on induction of lipolysis was blunted. Thus, PPARγ activation in part rescues the lipolytic response of these cells and renders them insensitive to TBLR1, which means that TBLR1 may normally act via activation of PPARγ-dependent genes.

Looking at protein expression of the main lipases and β-adrenergic receptors, TBLR1 knock down decreased protein expression of HSL, ATGL, perilipin, and β2- and β3- adrenergic receptors as it was observed before. This was not the case when cells were pre-treated with rosiglitazone for 24 hrs (Fig. 38), which was in line with the partial rescue of the TBLR1 deficency phenotype by rosiglitazone treatment. Constant activation of PPARγ by the agonist rosiglitazone therefore leads to a state where TBLR1 is no longer needed for transcriptional activation of the target genes.
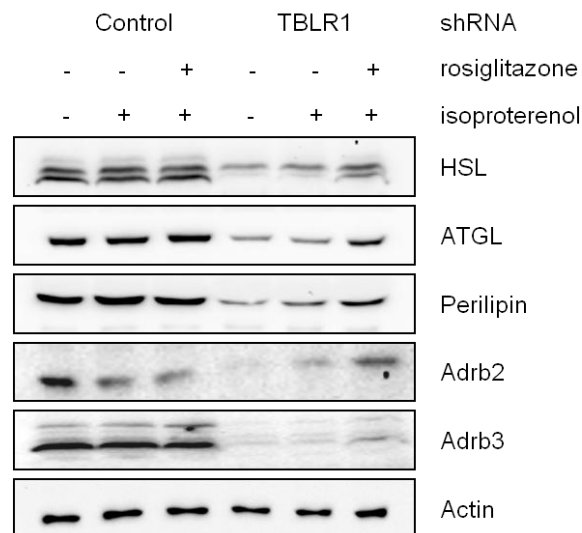
Fig. 38: Rosiglitazone partially rescues the effects of TBLR1 knock down on lipase and receptor expression*. 3T3-L1 adipocytes were transduced with adenoviruses carrying shRNA against TBLR1 or a control sequence and stimulated with 2.5 µM rosiglitazone for 24 hrs or with rosiglitazone for 24 hrs plus 10 µM isoproterenol for 3 hrs. Hormone sensitive lipase, adipocyte triglyceride lipase, perilipin, β2- and β3- adrenergic receptor and actin protein levels were detected by immunoblotting using specific antibodies.*

Indeed, TBLR1 is most likely a regulator of PPARγ, as it interacted both with PPARγ and its obligate dimerization partner RXR in mature adipocytes (Fig. 39 A). In addition, over expression of TBLR1 in 3T3-L1 adipocytes led to an increased activity of the PPAR response element in luciferase assays (Fig. 39 B), further supporting the idea of TBLR1 as a PPAR co-activator.
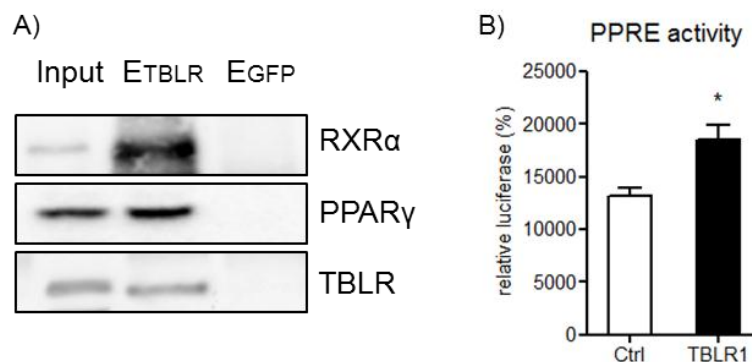
Fig. 39: TBLR1 interacts with RXRα and PPARγ and increased PPRE activity. *(A) Endogenous immunoprecipitation from 3T3-L1 adipocytes using monoclonal TBLR1 antibody pulls down RXRα and PPARγ as detected by immunoblotting with the respective antibodies in eluates (E_{TBLR}, E_{GFP}). Immunoprecipitation with GFP antibody serves as a negative control. (B) Luciferase assay from 3T3-L1 adipocytes transfected with TBLR1 over expression construct. TBLR1 OE increases the activity of the PPAR response element (% over pGL3 background). n=4, means ±SEM, *indicates significance.*

2.4.14 TBLR1 knock down in primary adipocytes leads to reduced stimulation of lipolysis

In 3T3-L1 adipocytes, it was shown that reduction of TBLR1 but not TBL1 levels leads to an attenuated lipolytic response to isoproterenol and other lipolytic stimuli. To investigate whether the same was true in primary adipocytes, we isolated preadipocytes from inguinal fat depots of young male mice and differentiated them *in vitro*. Adipocytes were transduced with adenoviruses carrying shRNA against TBL1, TBLR1 or a scrambled control sequence to mediate TBLR1 knock down. Cells

were stimulated with 10 µM isoproterenol for 3 hrs and NEFAs and glycerol were measured from the medium. As observed in 3T3-L1 adipocytes, isoproterenol potently stimulated lipolysis in control and TBL1 shRNA transduced primary adipocytes. In contrast, the isoproterenol-stimulated increase in fatty acid breakdown was significantly reduced in cells lacking TBLR1. As in 3T3-L1 adipocytes, this effect of TBLR1 knock down was in part mediated by reduced protein levels of perilipin, hormone sensitive lipase (HSL) and their phosphorylation by PKA (Fig. 40).
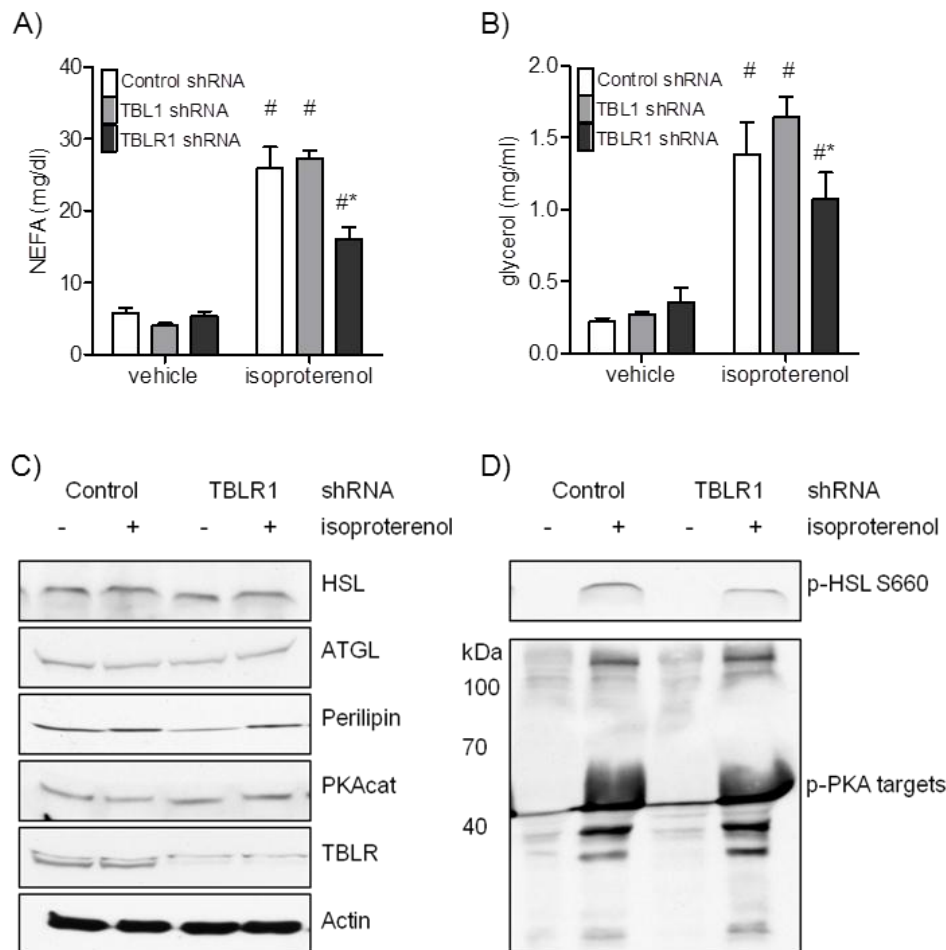
Fig. 40: TBLR1 knock down inhibits stimulation of lipolysis in primary adipocytes. *Preadipocytes isolated from inguinal WAT of 8-week old male mice were differentiated into adipocytes and transduced with TBL1, TBLR1 or unspecific control shRNA carrying adenovirus. Cells were treated with or without 10 µM isoproterenol for 3 hrs and NEFAs and glycerol were measured from the supernatant (A, B). n=4, means ±SEM, # indicates significance between basal and stimulated, *indicates significance between Ctrl and specific shRNA. Protein levels of HSL, ATGL, perilipin, the catalytic subunit of PKA, TBLR and actin as well as HSL and PKA target phosphorylation were measured by immunoblotting using specific antibodies (C, D).*

2.4.15 Ectopic expression of TBLR1 leads to decreased triglyceride content and increased lipolysis in 3T3-L1 adipocytes

TBLR1 knock down in adipocytes has been shown to increase intracellular triglyceride levels and decrease isoproterenol-induced lipolysis while not affecting glucose metabolism or lipogenesis. Here it was investigated whether ectopic expression of TBLR1 in adipocytes led to the opposite effects. For this purpose, 3T3-L1 adipocytes were transduced with adenoviruses carrying the TBLR1 cDNA sequence or a scrambled control sequence fused to a flag-tag under the control of the CMV promoter. This mediated strong over expression of TBLR1 in these cells (Fig. 42 A).
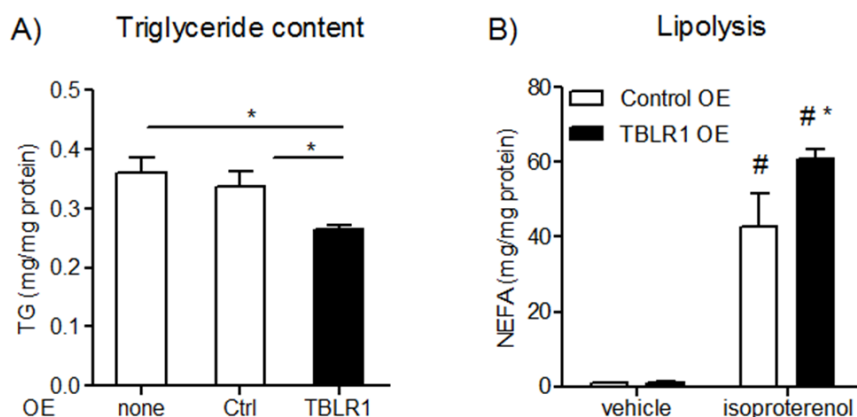
Fig. 41: Over expression of TBLR1 leads to decreased triglyceride content and increased lipolysis. *3T3-L1 adipocytes were transduced with adenoviruses mediating over expression of TBLR1 or a nonsense control. A) Triglyceride content of the adipocytes. B) Lipolysis was stimulated with 10 µM isoproterenol for 3 hrs and NEFAs were measured from the supernatants of the cells. n=4, means ±SEM. # indicates significance between basal and stimulated, *indicates significance between Ctrl and specific OE.*

As seen in Fig. 41 A, adipocytes contained 0.35 mg triglycerides per mg protein and virus infection did not influence triglyceride content. Over expression of TBLR1 significantly reduced triglyceride content, which was opposite of what was observed in cells with reduced TBLR1 levels. In line with reduced lipolysis upon TBLR1 knock down, 3T3-L1 adipocytes transduced with adenoviruses mediating TBLR1 over expression showed increased isoproterenol-stimulated lipolysis (Fig. 41 B) as measured by NEFA levels in the supernatants.

2.4.16 Increased lipolysis in adipocytes over expressing TBLR1 is a result of increased lipase expression and activity

Attenuated lipolysis upon TBLR1 knock down was mediated by a reduction in lipase expression and activity. Thus, we wanted to investigate next whether the increased lipolysis we observed in adipocytes over expressing TBLR1 was due to increased lipase activity.

Indeed, when 3T3-L1 adipocytes were transduced with adenoviruses mediating over expression of TBLR1 or a control sequence, protein levels of HSL and ATGL, the main lipases involved in adipocyte lipolysis, were increased in cells with ectopic TBLR1 (Fig. 42 A). Apart from that, activation (phosphorylation) of HSL and other PKA targets including perilipin was increased in cells over expressing TBLR1 (Fig. 42 B). Thus, increased lipolysis in cells with high TBLR1 levels was due to increased lipase expression and activation, which is opposite to the effects observed in TBLR1 knock down cells. This further supports the notion that TBLR1 is a regulator of adipocyte triglyceride metabolism by regulating key protein expression and activation.
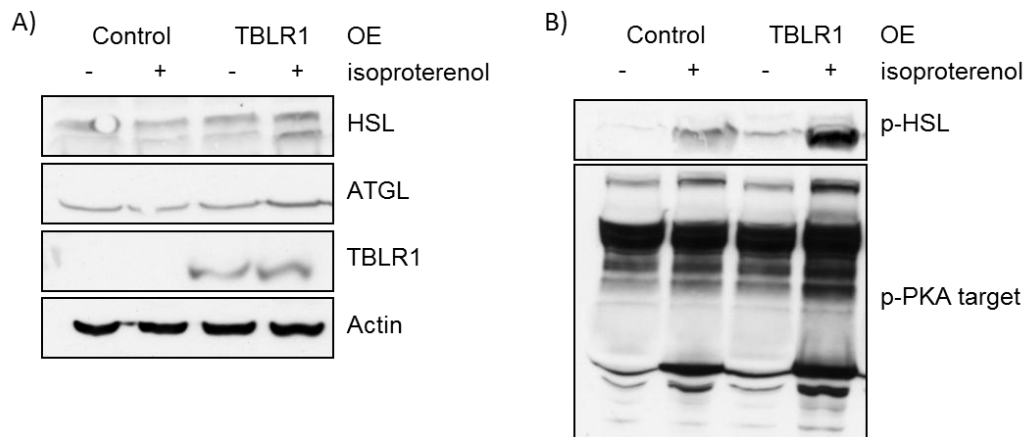
Fig. 42: TBLR1 over expression leads to increased protein expression and activation of key lipases. *3T3-L1 adipocytes transduced with TBLR1 or control over expression mediating adenoviruses were stimulated with 10 µM isoproterenol and total (A) or phosphorylated (B) protein levels of HSL, ATGL, TBLR1, Actin, and p-PKA targets were detected by immunoblotting.*

2.5 TBLR1 gene manipulation *in vivo*

2.5.1 TBLR1 cannot be efficiently knocked down or over expressed in adipose tissue *in vivo* using adenoviruses, siRNAs or morpholinos

In order to study gene function *in vivo*, many approaches to transiently over express or knock down gene expression have been established in the past, including virus-mediated shRNA or cDNA delivery, siRNA or morpholino treatment. These methods have been successfully applied in many organs including liver (Kulozik, P., 2011), kidney (Zhu, G., 1996), or brain (Koda, M., 2004), but are not commonly used for adipose tissue. Thus, we tried to establish a protocol for efficient knock down or over expression of TBLR1 in adipose tissue.

First, we injected *in vivo* siRNAs against TBLR1 or a scrambled control sequence intraperitoneally at a dose of 1.5 µg/g - 20 µg/g BW using DOTAP or Invivofectamine transfection reagents and analyzed knock down after 2, 5, and 8 days. No knock down in any adipose tissue depot on mRNA or protein levels was achieved by this method (data not shown). Since siRNAs have been tested in cell culture before and mediated knock down of TBLR1 in this setting, we hypothesized that they did not reach the adipose tissue depots to mediate knock down.

Second, we injected mice intraperitoneally with morpholinos, which are antisense oligos or nucleic acid analogs commonly used to mediate knock down in zebrafish or xenopus (Draper, B.W., 2001, Heasman, J., 2000). For use in mice, special *in vivo* morpholinos have been designed in order to increase stability and decrease toxicity of the antisense oligos (Morcos, P.A., 2008). We injected mice with the maximum suggested dose of 12.5 µg/g BW intraperitoneally on two consecutive days and analyzed gene expression after 3, 7, and 14 days. Knock down of TBLR1 in abdominal WAT was detectable 3 days after the first injection on protein and on mRNA levels (Fig. 43 D-E). In contrast, no knock down could be detected after 7 and 14 days or in any other tissue investigated (liver, intestine, gastrocnemius muscle, inguinal WAT, BAT, heart; data not shown). We analyzed body weight and body composition of mice injected with *in vivo* morpholinos (Fig. 43 A-C) and found that mice showed severely reduced body weight and adipose tissue weight upon injection with control or

TBLR1 morpholino but not upon PBS injection, pointing towards a high toxicity of the morpholinos independent of the targeted sequence. Thus, *in vivo* morpholinos could not be used for long-term or metabolic studies.
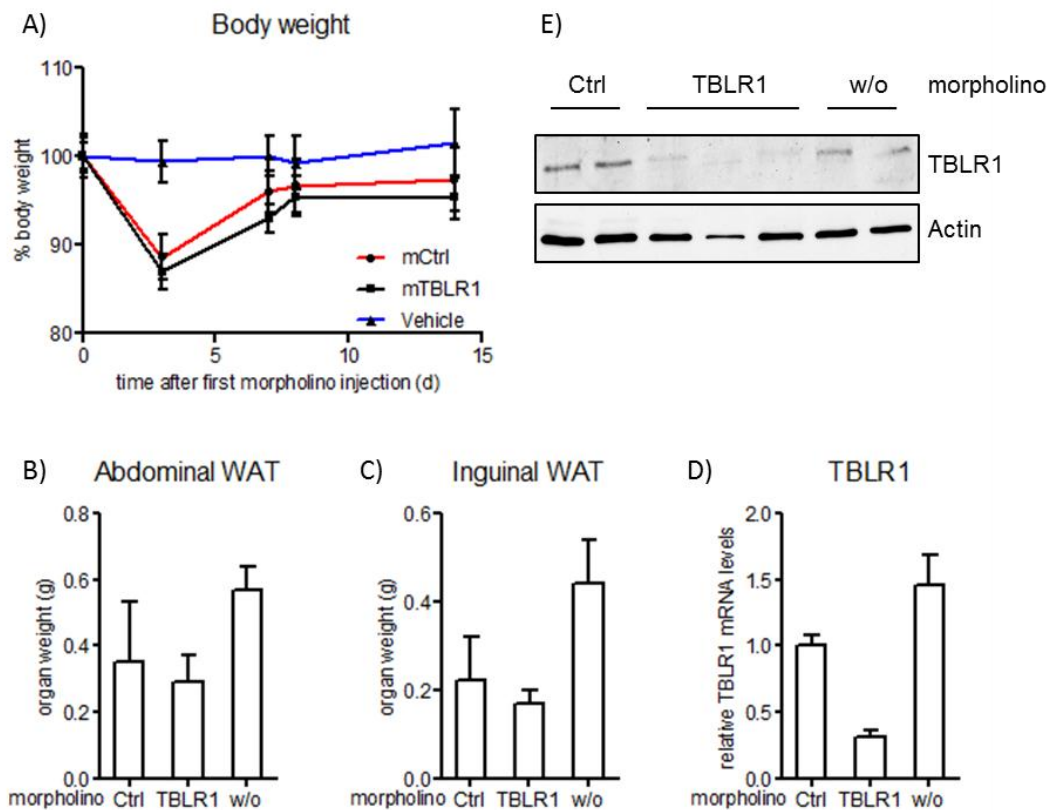
Fig. 43: Intraperitoneal injection of in vivo morpholinos causes transient weight loss and fat mass loss and mediates mild reduction of target gene expression. Male C57Bl6 mice were injected intraperitoneally with 12.5 µg/g BW in vivo morpholinos directed against TBLR1 or a scrambled control sequence or vehicle (0.9% saline) on two consecutive days. Body weight was monitored over 14 days (A). Some of the mice were prepped on day 3 after the first injection. (B) Abdominal and (C) inguinal adipose tissue mass was measured 3 days after the first injection. TBLR1 mRNA expression (D) and protein expression (E) in abdominal adipose tissue was measured by qPCR and immunoblotting.

In the past, *in vivo* knock down techniques using adenoviral systems have been shown to be very efficient. Thus, we next tried to knock down or over express TBLR1 in adipose tissue by injecting adenoviruses carrying shRNA against TBLR1 or cDNA mediating over expression of TBLR1 directly into abdominal fat pads. For this, abdominal adipose tissue depots were exposed and adenoviruses (5 x 10^9-2 x 10^{10} ifu/ml) were injected in a volume of 50 µl for each fat pad, either by normal injection or by microinjection as described in 'Methods'. Knock down or over expression of TBLR1 was assessed one week after injection by qPCR or immunoblotting; changes in TBLR1 expression could not be detected in adipose tissue (data not shown). Injection of an adenovirus mediating GFP expression and subsequent analysis of tissue slices revealed that adenoviruses were not equally distributed throughout the tissue (Fig. 44), which may explain the lack of functionality.
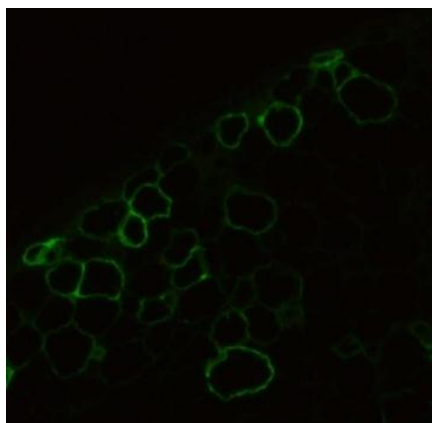
Fig. 44: Few cells express GFP after microinjection of GFP-adenovirus into fat pad*. GFP overexpression mediating adenoviruses (5x10^8 ifu/fat pad) were injected into abdominal fat pads by microinjection. GFP expression was analysed 1 week following the injection by immunohistochemistry using a GFP antibody (20x magnification).*

Lastly, the microinjection technique was applied to inject siRNAs and morpholinos into abdominal adipose tissue. Injecting the maximal dose of either siRNAs (7 mg/kg BW) or morpholinos (12.5 mg/kg BW) into abdominal fat pads did not lead to a measurable knock down of TBLR1 in this tissue.

In conclusion, we did not succeed in establishing a technique to efficiently over express or knock down TBLR1 in adipose tissue due to limitations in accessibility of the tissue and distribution of the agent. Thus, to alter gene expression in adipose tissue, it is inevitable to generate genetic over expression or knock out mouse lines by using floxed mice and adipocyte-specific cre-lines such as the adiponectin- or aP2-cre line (Eguchi, J., 2011; He, W., 2003).

2.6 Adipocyte specific TBLR1 knockout (ATKO) mice display a lipid metabolism phenotype

As it is not possible to manipulate TBLR1 gene expression in adipose tissue *in vivo* using standard knock down or over expression techniques, we generated adipocyte specific TBLR1 knockout mice on C57Bl6 background (C57BL/6-Tbl1xr1(tm2273Arte) Tg(Fabp4-Cre)1Rev), hereafter referred to as ATKO mice (**A**dipocyte specific **T**BLR1 **K**nock**O**ut mice).

The translational start site of TBLR1 (ENSMUST00000063988) lies within exon 3. Floxed TBLR1 mice were created by *TaconicArtemis* by introducing LoxP sites in a region containing exon 5 (size of LoxP-flanked region approx. 1 kb). Positive selection markers flanked by FRT (Neomycin resistance - NeoR) and F3 (Puromycin resistance - PuroR) sites were inserted into intron 4 and intron 5, respectively. Homologous recombinant clones were isolated using double positive selection (NeoR and PuroR). The targeting vector was generated using BAC clones from the C57BL/6J RPCI-23 BAC library and transfected into *TaconicArtemis* C57BL/6N Tac ES cell line. Mice contained the conditional KO allele after Flp-mediated removal of the selection markers. The constitutive KO allele was present in adipose tissues after Cre-mediated recombination with B6.Cg-Tg(Fabp4-cre)1Rev/J mice purchased at *The Jackson Laboratory*. Deletion of exon 5 resulted in loss of function of the TBLR1 gene by deleting part of the F-box-like domain and by generating a frameshift from exon 4 to exons 6 and 7 (premature stop codon in exon 6) (for targeting strategy, see Fig. 45).
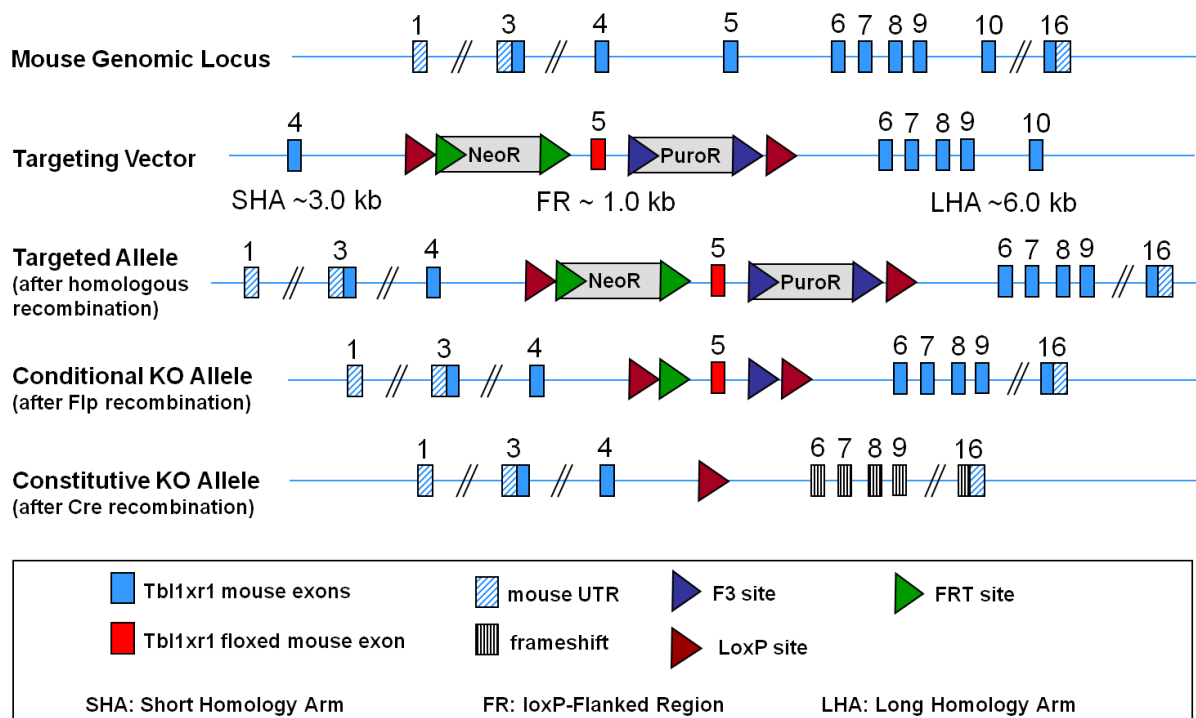
Fig. 45: Targeting strategy for the creation of adipose tissue specific TBLR1 KO (ATKO) mice. *Exon 5 was flanked by LoxP sites in a targeting vector containing double positive selection markers (NeoR, PuroR). Upon Flp recombination the selection markers were removed. Exon 5 was removed by Cre recombination, thereby introducing a stop codon in exon 6. AT specific TBLR1 KO mice were generated by breeding floxed TBLR1 mice with Fabp4-cre mice.*

Here we show only data of female ATKO mice. Male and female mice were highly similar in all the analyzed parameters, but since C57Bl6/N male mice are very prone to developing obesity and glucose intolerance at young age even without a certain stimulus, only female mice were analyzed in detail.

2.6.1 Mice heterozygous for TBLR1 in adipose tissue display normal body weight, organ weight and lipolytic response

In an initial experiment, mice heterozygous for flox-TBLR1 and carriers of Cre (referred to as adipocyte specific TBLR1 heterozygous, ATKO+/- mice) were analyzed to investigate the effects of reduced AT TBLR1 levels. Mice were born at a mendelian ratio and with normal birth weight and size. By 15 weeks of age, mice showed similar body weight, body composition and food consumption and did not significantly differ in blood glucose levels (Fig. 46).
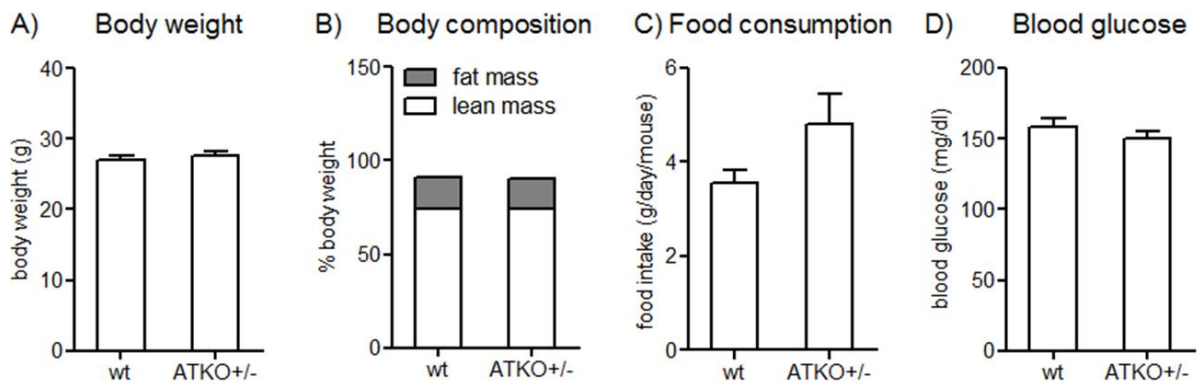
Fig. 46: ATKO+/- mice at the age of 15 weeks are indistinguishable from wt mice at the same age. *Body weight (A), body composition (B), food consumption (C) and blood glucose (D) of 15 week old ATKO+/- mice or wt littermates from TaconicArtemis. Fat mass and lean mass were analyzed by ECHO-MRI and plotted relative to body weight. n=10, means ±SEM.*

Cell sizes of adipocytes from abdominal WAT depots were determined in H&E stained tissue slices. Slices were taken from three different layers of the tissue and cell sizes were determined by measuring the cell area of 30 cells on every slide using ImageJ. As seen in Fig. 47, abdominal adipocyte size was slightly but significantly increased in the ATKO+/- animals.
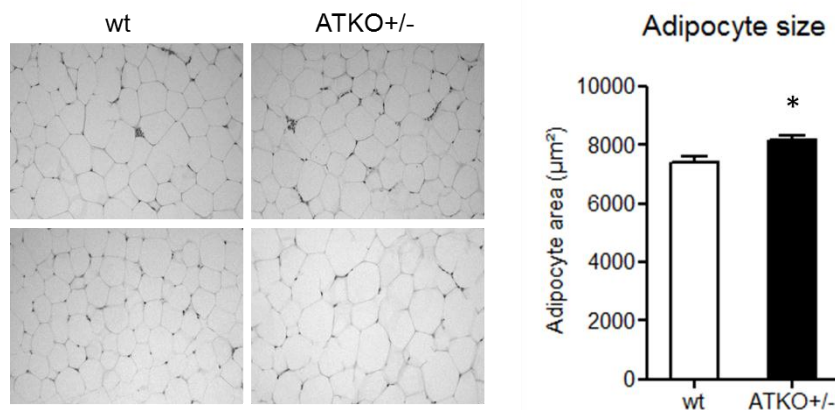
Fig. 47: Abdominal adipocyte size is slightly increased in ATKO+/- animals compared to wt control mice. *H&E staining of abdominal WAT slices. Cell size was quantified with ImageJ by measuring cell area of 30 cells each slide, 3 slides of each WAT were taken. n=7, means ±SEM, *indicates significance.*

To investigate effects of adipose tissue TBLR1 reduction on fasting, we performed a fasting time course experiment where animals were fasted for 3, 8, and 24 hrs. Body composition during that time was monitored using ECHO-MRI, and glycerol and free fatty acid levels were measured in the serum. During 24 hrs fasting, wt and ATKO+/- mice lost equal amounts of body weight, fat mass and lean mass and displayed normal serum glycerol and free fatty acid levels (Fig. 48). The weights of the different adipose tissues of 24 hrs fasted animals were equal in both groups.
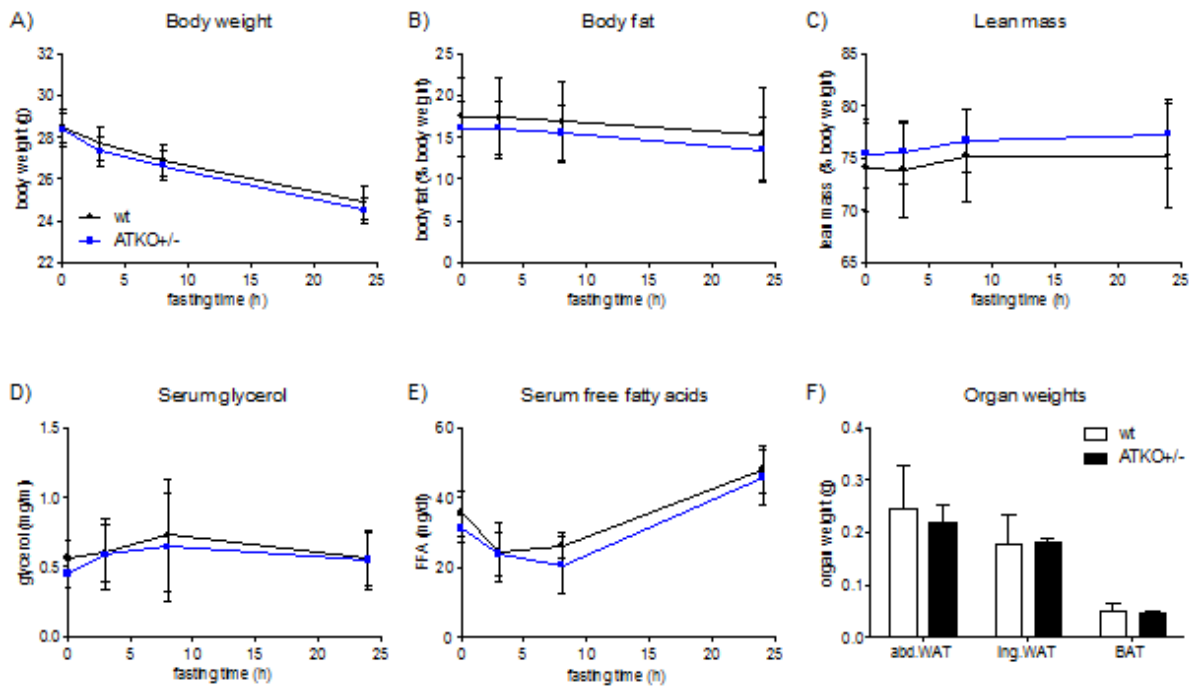
Fig. 48: ATKO+/- mice display normal body weight, body composition and serum FFA and glycerol levels upon fasting. (A) Body weight loss during 24 hrs fasting. Proportion of (B) body fat and (C) lean mass on body weight during a 24 hrs fasting period. (D), (E) Serum glycerol and FFA levels in 24 hrs fasted mice. (F) Organ weights of abdominal and inguinal WAT and BAT after 24 hrs fasting. n=5, means ±SEM.

Gene expression analysis revealed that TBLR1 mRNA levels were reduced by approx. 30% in abdominal, inguinal and brown adipose tissues (Fig. 49 A-C). Protein levels were only slightly reduced in AT of ATKO+/- mice as seen in immunoblotting (Fig. 49 D), which may explain why no major phenotypic changes were observed between wt and ATKO+/- animals.
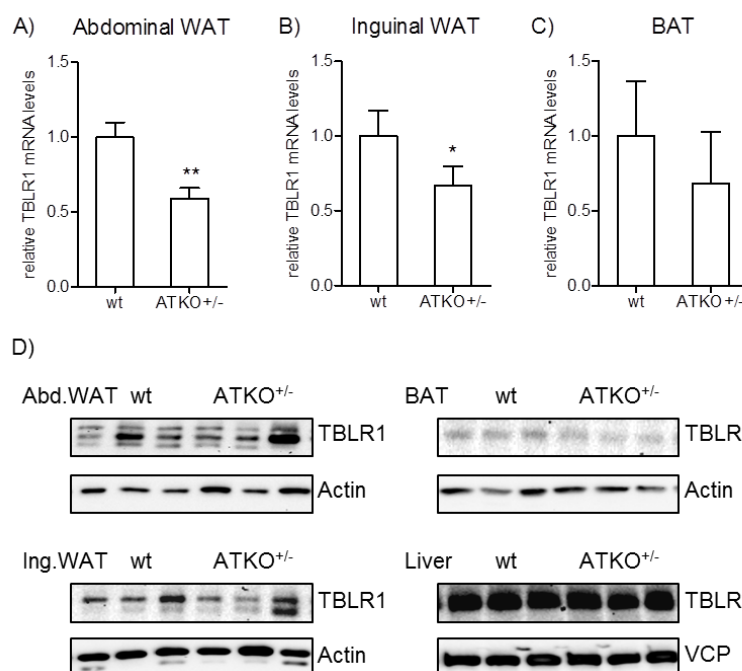
Fig. 49: TBLR1 expression is reduced in ATKO+/- mice in abdominal and inguinal white adipose tissue and brown adipose tissue. TBLR1 mRNA expression in (A) abd. WAT, (B) ing. WAT and (C) BAT of 24 hrs fasted ATKO+/- animals, measured by qPCR. D) TBLR1, actin and VCP protein levels in abdominal, inguinal and brown adipose tissues and liver, measured by immunoblotting using TBLR1, actin or VCP antibodies. n=3, means ±SEM, * indicates significance.

2.6.2 Adipocyte specific knockout of TBLR1 leads to increased body weight and body fat content and enlarged adipose tissue depots

Homozygous adipocyte specific TBLR1 knockout animals (ATKO mice) were bred by TaconicArtemis as described before for the heterozygous animals. To test for specificity of the knockout, we analyzed TBLR1 mRNA expression in various tissues including WAT and BAT using qPCR primers targeting exon 5 (Fig. 50). Reductions in TBLR1 mRNA levels were found in abdominal and inguinal WAT depots and isolated adipocyets as well as in BAT, but could not be detected in the stromal vascular fraction (SVF) isolated from abdominal or inguinal white adipose depots, spleen, kidney, liver, and GC muscle. Opposite of what has been described before (Makowski, L., 2001), we could not observe reduced TBLR1 levels in bone marrow derived macrophages.
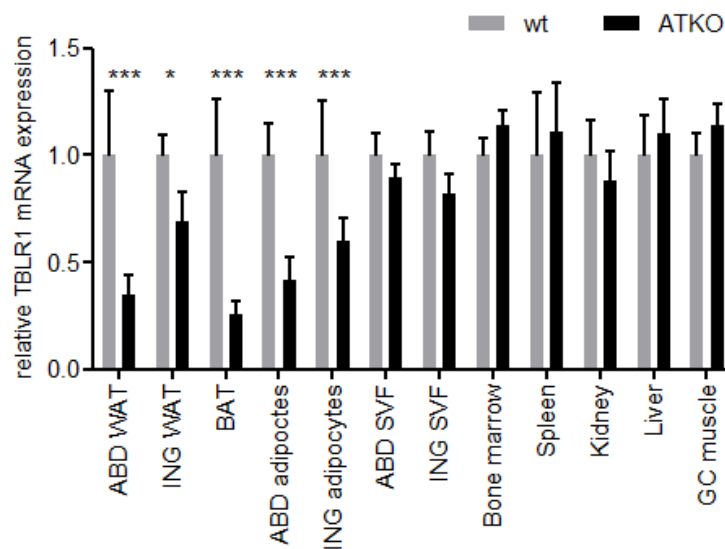
Fig. 50: TBLR1 mRNA levels are specifically reduced in brown and white adipose tissues of ATKO mice. *Indicated tissues or cells of wt and ATKO mice aged 16 weeks were isolated and snap-frozen. TBLR1 mRNA levels were determined by qPCR. Means ±SEM, n=3, * indicates significance.*

While body weight was equal in ATKO and wt animals in young age, ATKO mice were significantly heavier starting from 10 weeks of age onwards. Analysis of body weight composition by ECHO-MRI revealed that increased body weight was largely due to a higher body fat content in the ATKO animals, while the relative contribution of lean mass to the body weight was decreased (Fig. 51 A, B). Similar to the ATKO+/- animals, we could not observe any differences in food intake or blood glucose levels (Fig. 51 C, D).
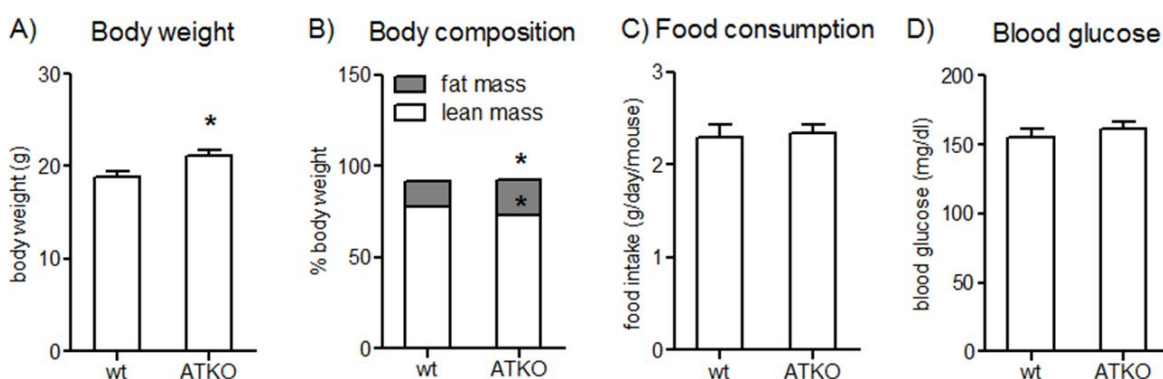
*Fig. 51: ATKO mice at the age of 10 weeks have increased body weight due to higher body fat mass. Body weight (A), body composition (B), food consumption (C) and blood glucose (D) of 10 week old female ATKO mice or wt littermates from TaconicArtemis. Fat mass and lean mass were analyzed by ECHO-MRI and plotted relative to body weight. n=10, means ±SEM, * indicates significance.*

By 3 months of age, ATKO animals were visibly more obese than wt littermates on a normal chow diet and showed extremely enlarged abdominal and inguinal fat pads (by ~50%, Fig. 52).
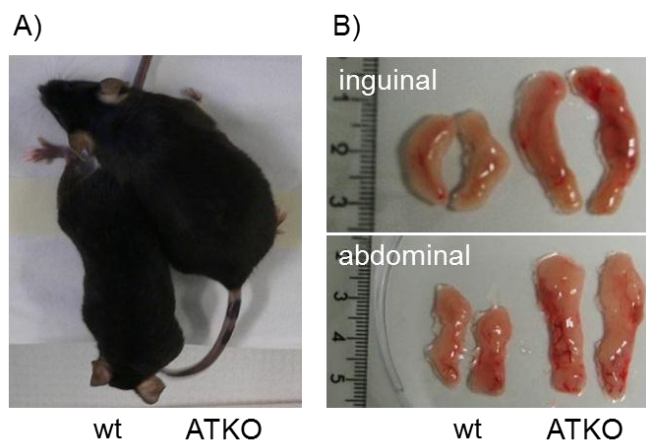
Fig. 52: 3 months old ATKO mice are heavier that their wt littermates which is due to enlarged fat pad size. A) Female wt (left) and ATKO (right) mice aged 3 months. B) Isolated inguinal and abdominal fat pads of female wt (left) and ATKO (right) mice aged 3 months.

2.6.3 Adipose tissue explants isolated from ATKO mice show reduced lipolysis

In order to get a first hint whether the data obtained by *in vitro* studies could be validated in the *in vivo* situation, explants of abdominal, inguinal and interscapular brown adipose tissues of ATKO and wt mice were isolated and lipolysis was stimulated by the addition of 10µM isoproterenol for 3 hrs.

Measuring FFA and glycerol in the supernatants of the explants revealed a reduced FFA and glycerol release in explants isolated from ATKO mice and a diminished lipolytic response to the stimulus in all three tissues (Fig. 53 A-F). Other than in the *in vitro* situation, we could not see reduced ATGL levels in the ATKO explants. In contrast, blunted triglyceride breakdown in the explants isolated from ATKO animals was due to reduced HSL protein levels as well as PKA-mediated HSL and other target protein phosphorylation (Fig. 53 G), eventually caused by reduced beta-adrenergic receptor expression (Fig. 53 H). Thus, TBLR1 is responsible for efficient lipolytic response also in the *ex vivo* situation. Next we sought to assess the physiological relevance of these findings *in vivo*.
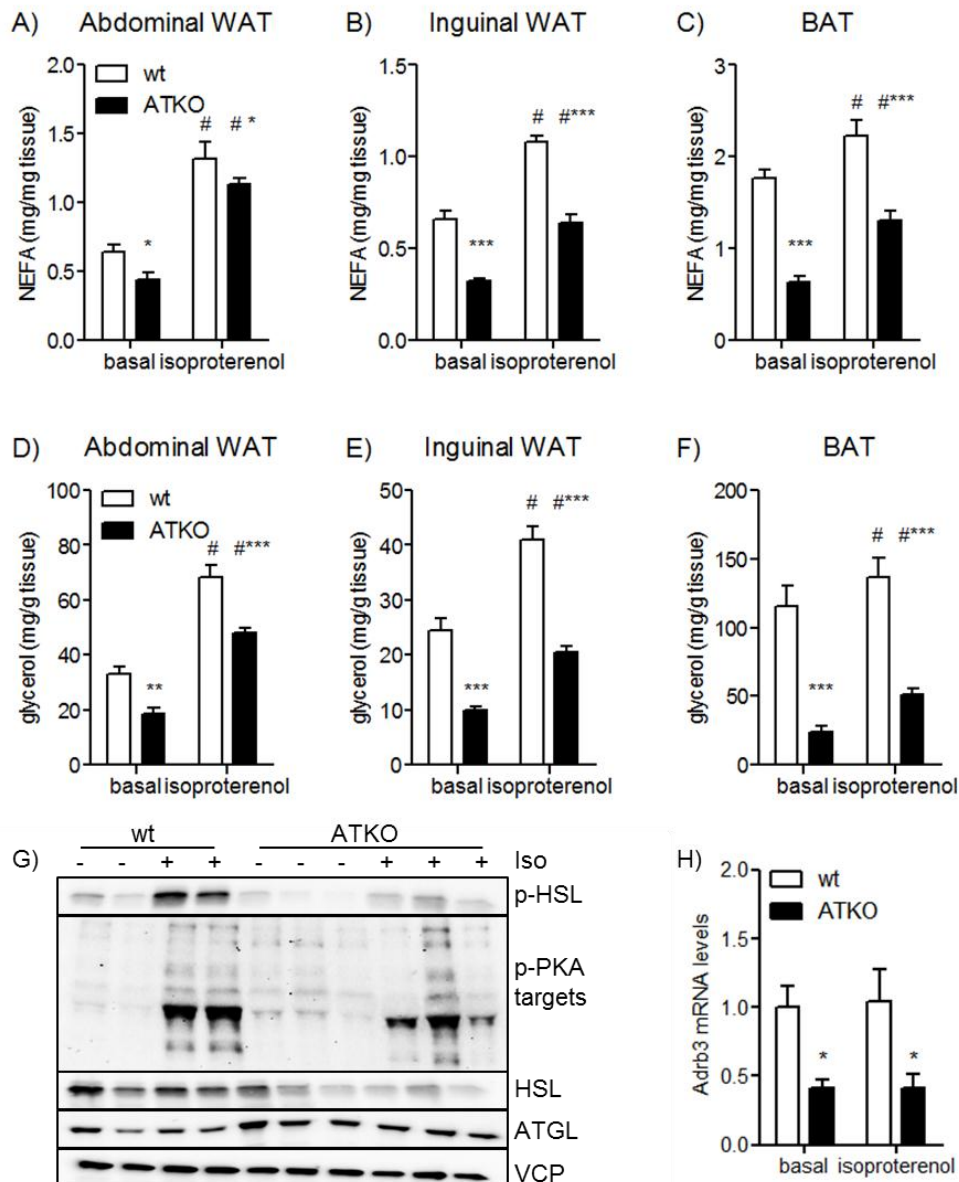
Fig. 53: Adipose tissue explants isolated from ATKO mice show reduced basal and isoproterenol-induced lipolysis due to reduced HSL expression and activation. *Explants isolated from abdominal, inguinal and brown adipose tissues of 3 months old female ATKO or wt mice. Equally sized pieces were treated with or without 10 µM isoproterenol for 4 hrs and FFA (A-C) and glycerol (D-F) were measured from the supernatants. G) p-HSL, HSL, ATGL and VCP were detected by immunoblotting from protein lysates of abdominal WAT explants. H) Adrb3 mRNA levels were detected by qPCR from abdominal WAT explants. n=6, means ±SEM, # indicates significance between basal and stimulated, *indicates significance between wt and ATKO.*

2.6.4 ATKO animals show a disturbed adipose tissue lipolytic response to fasting

To investigate effects of adipocyte TBLR1 knockout on fasting, we performed a time course experiment with the ATKO mice by fasting the animals for 3, 8, 24 and 48 hrs. Half of the animals where subsequently refed for 6 hrs. Body composition during that time was monitored using ECHO-MRI, and glycerol and free fatty acid levels were measured in the serum. As observed before, ATKO mice showed the tendency towards higher body weight and body fat content compared to wt mice at the beginning of the experiment. However, there was no significant difference between ATKO and

wt animals owed to the young age of the mice (8 weeks). During 48 hrs fasting, wt and ATKO mice lost equal amounts of body weight, fat mass and lean mass and displayed normal serum glycerol and free fatty acid levels (Fig. 54 A-E). Adipocyte lipolysis as calculated by total serum FFAs divided by body fat was reduced in the ATKO mice (Fig. 54 F).
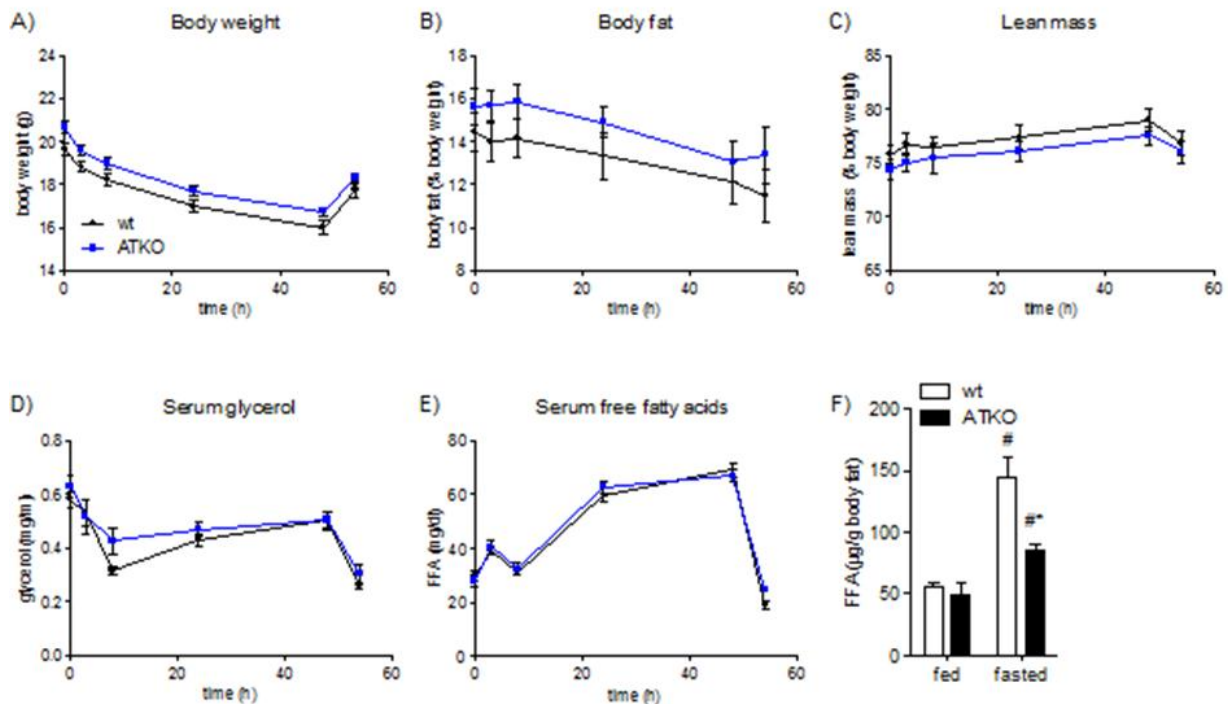
Fig. 54: ATKO mice display normal body weight, body composition and serum FFA and glycerol levels upon fasting*. (A) Body weight loss during 48 hrs fasting and 6 hrs refeeding. Proportion of (B) body fat and (C) lean mass on body weight during the same period. (D), (E) Serum glycerol and FFA levels in 48 hrs fasted and 6 hrs refed mice. (F) Lipolysis calculated by total serum FFA divided by body fat in the fed state. n=6, means ±SEM, # indicates significance between fed and fasted, *indicates significance between wt and ATKO.*

When measuring organ weights, ATKO animals showed enlarged abdominal and inguinal white fat pads compared to wt animals in the fasted state while adipose tissue weights were similar in wt and ATKO animals in the refed state. BAT weights were unchanged in both the fasted and refed states (Fig. 55 A-C). Liver weights were unaltered between wt and ATKO mice and increased by feeding (Fig. 55 D).

In agreement with the increase in white adipose tissue weights, ATKO animals in the fasted state in average had enlarged adipocytes as well as a shift towards a bigger population of larger cells as shown in hematoxylin and eosin (H&E) stained abdominal WAT (Fig. 55 E, F). The reduction in abdominal and inguinal WAT mass with total body fat loss during fasting being unaltered points towards a depot-specific role of TBLR1 in this setting.
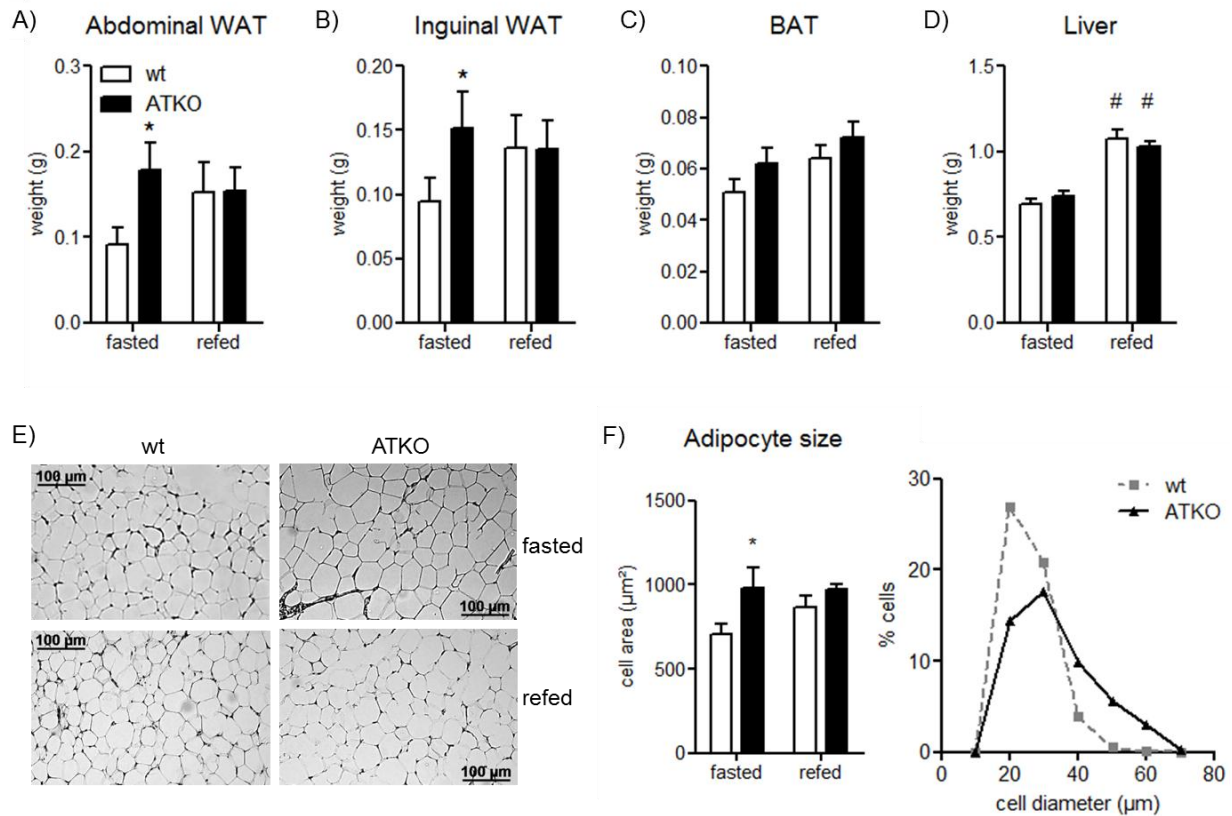
Fig. 55: Abdominal and inguinal WAT weights as well as adipocyte diameter are increased in ATKO mice in the fasted state. *Abdominal WAT (A), inguinal WAT (B), BAT (C) and liver (D) weights of 8 week old ATKO mice and their wt littermates that were fasted for 48 hrs or fasted for 48 hrs and subsequently refed for 6 hrs. E) H&E stained abdominal WAT slices of the same animals. (F) Adipocyte sizes and size distribution were analyzed in three pictures corresponding to three layers of the tissue. n=6, means ±SEM, # indicates significance between fed and fasted, *indicates significance between wt and ATKO.*

In accordance with the enlarged abdominal fat pads in the fasted state in the ATKO mice, we observed reduced levels of p-HSL and p-PKA in these animals when compared to the wt controls (Fig. 56). The reduced levels of phosphorylated PKA and HSL were probably due to a decrease in beta2-adrenergic receptor levels (Fig. 56), which interferes with a normal lipolytic response. Total protein levels of HSL and ATGL were largely unchanged by either fasting or TBLR1 knockout. The same was observed in inguinal adipose tissue (not shown). The reduced adrenergic receptor expression and activation of hormone sensitive lipase and other PKA targets including perilipin strengthened the notion that TBLR1 is involved in adipocyte lipolysis in response to fasting.
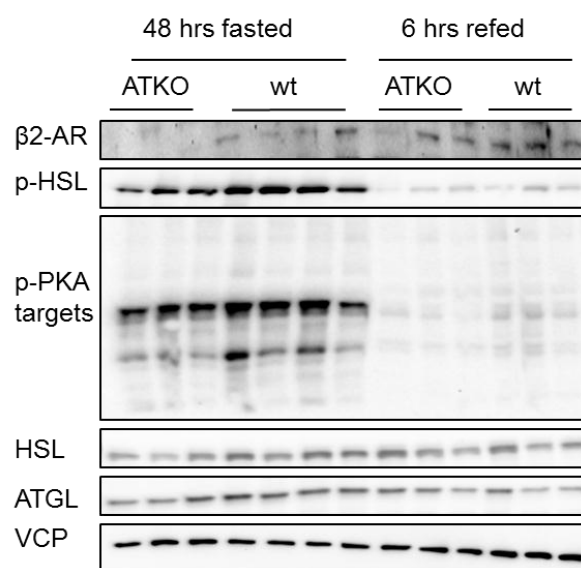
Fig. 56: Immunoblot of 48 hrs fasted or 6 hrs refed ATKO and wt animals. *8 week old female ATKO mice and their wt littermates were fasted for 48 hrs and subsequently refed for 6 hrs. Proteins were detected from protein lysates of abdominal WAT by immunoblotting using beta-2-adrenergic receptor (β2-AR), phospho-HSL, phospho-PKA targets, hormone-sensitive lipase (HSL), adipocyte triglyceride lipase (ATGL), and valosin containing protein (VCP) antibodies, respectively. n=3-4.*

2.6.5 ATKO mice gain more weight during high fat diet feeding and reveal a strong increase in body fat content

So far our data indicate that TBLR1 may play a role in adipose tissue triglyceride homeostasis by regulating transcriptional events leading to basal or stimulated lipolysis. As lipolysis is dysregulated in obesity (Gaidhu, M.P., 2010), we posed the question whether the lipolytic regulator TBLR1 could influence the development of obesity in a mouse model where adiposity is induced by diet.

To investigate this, ATKO or wt mice were fed a high fat diet (HFD) containing 60% calories from fat for 8 weeks to induce obesity, starting at the age of 6 weeks. A low fat diet (LFD) containing 10% calories from fat served as control diet. While body weights were undistiguishable between ATKO and wt mice at the beginning of the experiment, ATKO mice on a low fat diet were heavier than their wt littermates starting from 10 weeks of age onwards. Wild type mice on a high fat diet gained significantly more weight than littermates on a LFD. ATKO mice on the same diet gained even more weight than their wt littermates (Fig. 57).

The higher body weight gain in ATKO compared to wt animals was largely attributed to an increase in body fat mass, which was higher in ATKO animals than in wt animals in both LFD and HFD feeding, as measured by body composition analysis with an ECHO-MRI. Lean mass increased steadily with age in all four groups. Thus, both high fat diet and TBLR1 deficiency promote the development of obesity and act synergistically (Fig. 57).
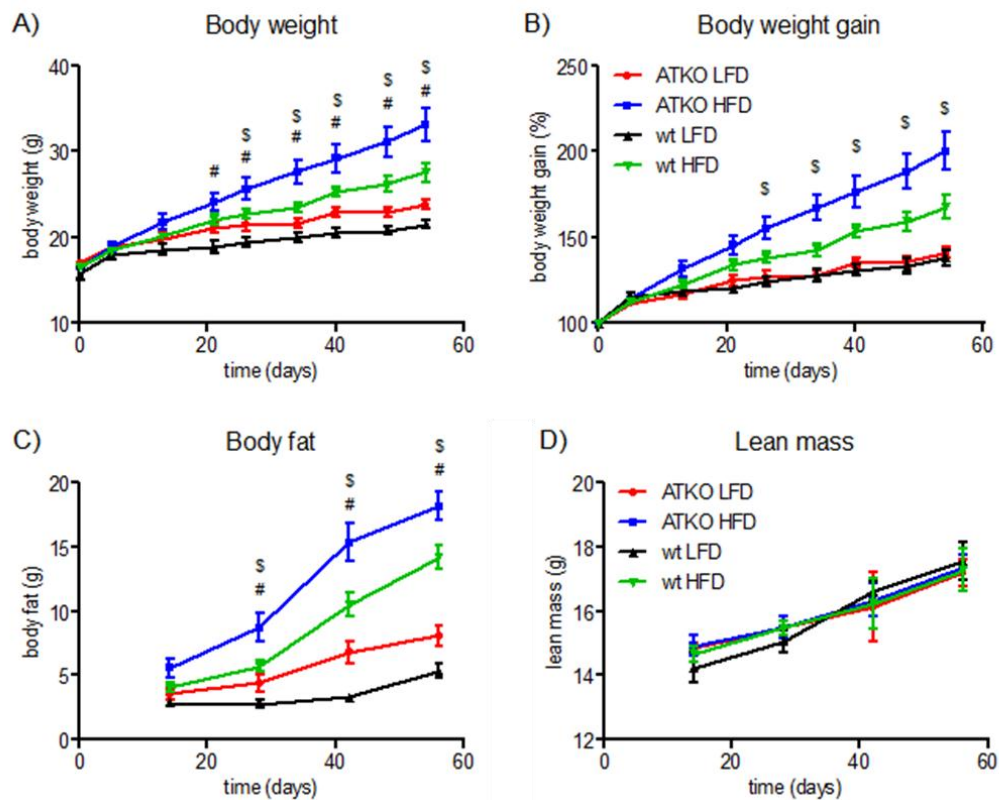
Fig. 57: ATKO mice on a HFD gain significantly more weight and body fat than their wt littermates. *6-week-old female ATKO and wt mice were fed a LFD or HFD for 8 weeks. Body weight (A) was measured weekly. Body weight gain (B) was calculated as % starting weight. Body fat (C) and lean mass (D) were measured after 2, 4, 6, and 8 weeks of HFD/LFD feeding by ECHO-MRI. n=8, means ±SEM, student's t: #p < 0.05 LFD, $p < 0.05 HFD.*

Blood glucose levels were higher in HFD fed mice irrespective of genotype (Fig. 58 A). Interestingly, even after 4 weeks HFD feeding core body temperature of HFD fed mice was lower than that of LFD fed mice in wt animals, whereas ATKO mice showed equally low temperatures in both LFD and HFD feeding, indicating that LFD fed ATKO mice displayed typical signs of obesity. Apart from that, ATKO mice showed increased serum leptin and resistin levels even after 4 weeks HFD feeding (Fig. 58 C-D), which is usually sign of adiposity. This effect was even more prominent after 8 weeks HFD feeding (data not shown), further supporting the idea that TBLR1 deficiency worsens obesity and accompanying symptoms.
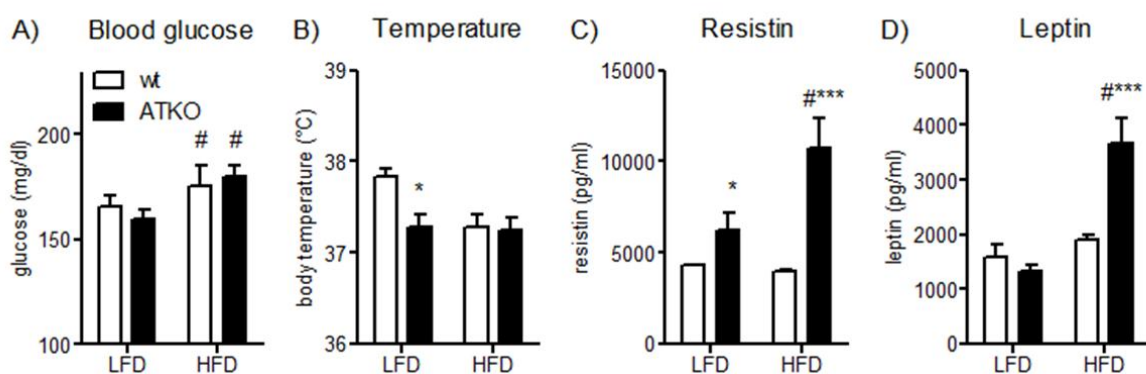
Fig. 58: ATKO mice reveal normal postprandial blood glucose, reduced body temperature and increased serum markers of obesity. *Female ATKO or wt mice were fed a HFD or LFD beginning at 6 weeks of age. Postprandial blood glucose (random fed, 8 am; A), body temperature (B) and serum resistin (C) or leptin (D) levels were measured after 4 weeks LFD/HFD feeding. n=8, means ±SEM, # indicates significance between LFD and HFD, *indicates significance between wt and ATKO.*

After 8 weeks of high fat diet feeding, HFD led to significantly increased body weight in both wt and ATKO mice, but the increase in ATKO mice was still significantly larger than that in wt animals. In both wt and HFD mice, HFD feeding led to an increased nose-to-anus body length, but it did not differ between the genotypes. As expected from the ECHO-MRI data showing increased fat content in the ATKO mice we could observe enlarged abdominal, inguinal and brown adipose tissue depots. The increased WAT depot size was attributed to adipocyte hypertrophy in ATKO mice in both LFD and HFD fed states (Fig. 59 A-G) Cell size distribution revealed a shift towards a larger population of enlarged adipocytes in the ATKO mice (Fig. 59 H).

In accordance to what we observed before, when analyzing abdominal WAT protein expression we saw reduced protein levels of phosphorylated HSL and other PKA targets including perilipin under both LFD and HFD as well as reduced levels of the key lipases ATGL and HSL. Protein levels of the beta2- and beta3-adrenergic receptors were also dysregulated in the ATKO mice, with no clear regulation pattern in the beta2-adrenoceptor but a clear reduction of the beta3-adrenoceptor in the ATKO mice (Fig. 60). Thus, TBLR1 depletion in adipocytes led to increased susceptibility to HFD and increased body fat gain due to decreased triglyceride hydrolysis.
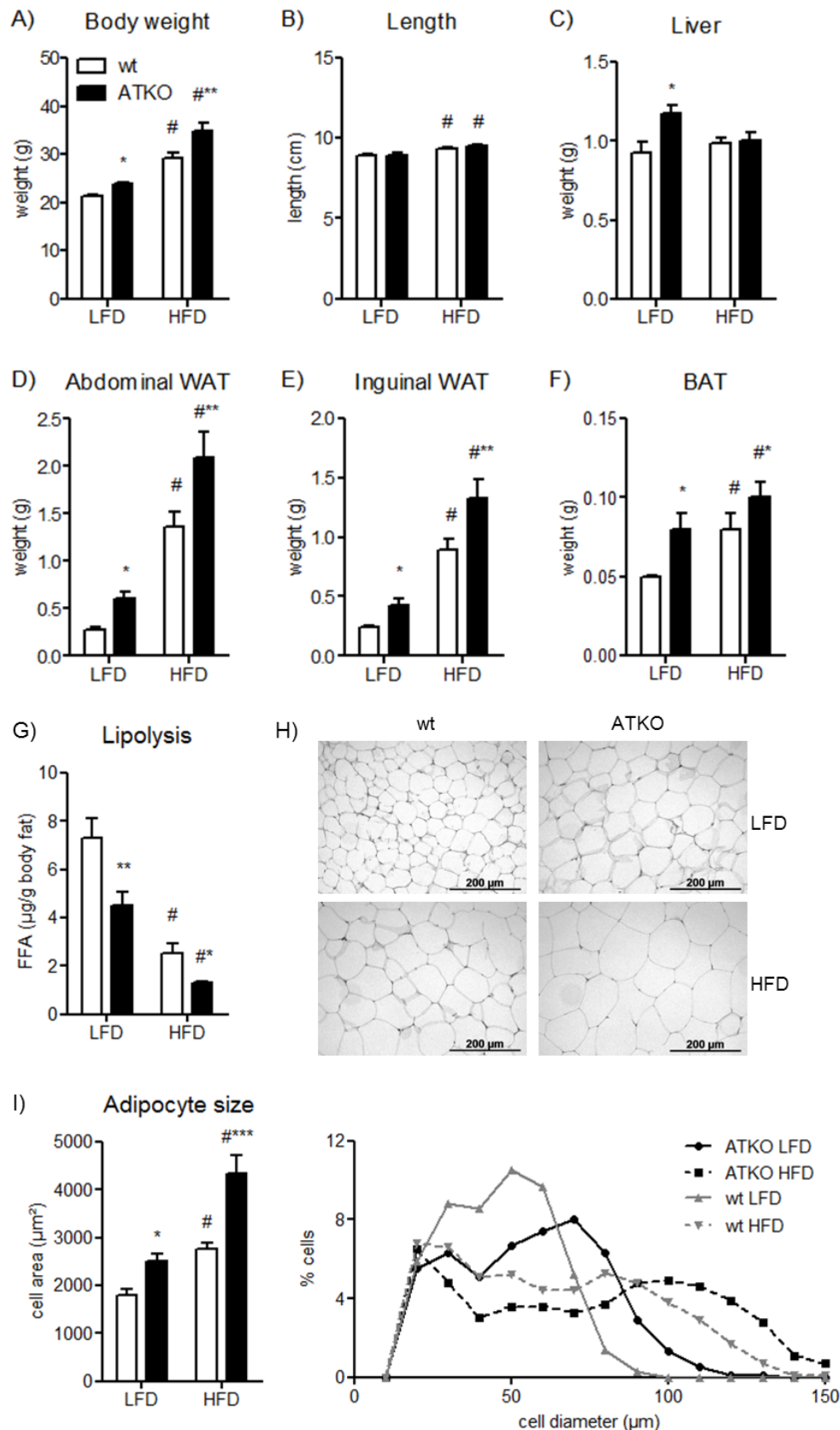
Fig. 59: Fat pad weight and adipocyte size is increased in ATKO mice while liver weights and body length are largely unaltered. *Female ATKO or wt mice were fed a LFD/HFD for 8 weeks starting from the age of 6 weeks onwards. Shown are body weight (A), body length (B), liver (C), abdominal WAT (D), inguinal WAT (E) and BAT (F) weights. (G) Lipolysis calculated by total FFAs divided by body fat. (H) H&E stained abdominal WAT slices. (I) Quantification of 100-200 cells/picture in 2 layers of tissue and cell size distribution in the same samples. n=8, means ±SEM, # indicates significance between LFD and HFD, *indicates significance between wt and ATKO.*
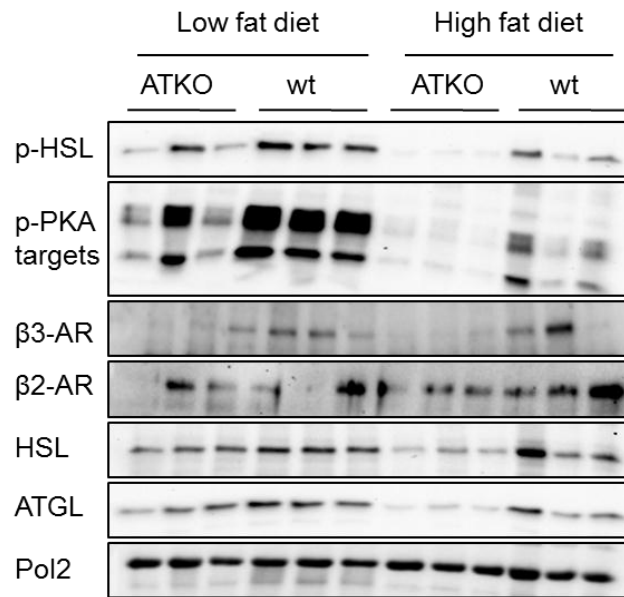
Fig. 60: ATKO mice have reduced levels of phosphorylated HSL and PKA targets and decreased protein expression of adrenergic receptors, HSL and ATGL compared with wt littermates. *ATKO and wt female mice were fed a LFD/HFD for 8 weeks starting at the age of 6 weeks. Protein lysates were prepared from pulverized abdominal WAT and protein levels were detected using the respective antibodies. RNA Polymerase 2 was used as a loading control as both VCP and Actin were regulated by HFD feeding.*

2.6.6 ATKO mice show impaired glucose tolerance and insulin sensitivity and increased subacute inflammation

Obesity often leads to the development of hyperglycemia and reduced insulin sensitivity. In order to investigate glucose homeostasis in LFD and HFD fed ATKO and wt mice, we measured the homeostasis model assessment of insulin resistance (HOMA-IR, HOMA-%B) index and performed an intraperitoneal glucose tolerance test, measuring both insulin and glucose levels after injection of 2 mg/kg glucose over a time period of 2 hrs.

As seen in Fig. 61, HOMA-IR as calculated by fasting glucose and insulin levels (Matthews, D.R., 1985) was significantly increased by HFD and even higher in ATKO animals, pointing towards a beginning insulin resistance of the ATKO animals on a HFD (typically, HOMA-IR values > 2 indicate insulin resistance). HOMA-%B, a measure of beta-cell activity, was unchanged by both feeding and genotype. Insulin Sensitivity Index (ISI, Matsuda, M. and DeFronzo, D.R., 1999) was strongly reduced by HFD feeding and even worse in the ATKO animals. Accordingly, fasting glucose and insulin levels were elevated in HFD fed ATKO mice, and glucose and insulin levels measured during an IPGTT (intraperitoneal glucose tolerance test) show impaired glucose tolerance and insulin sensitivity in the ATKO animals on a HFD.
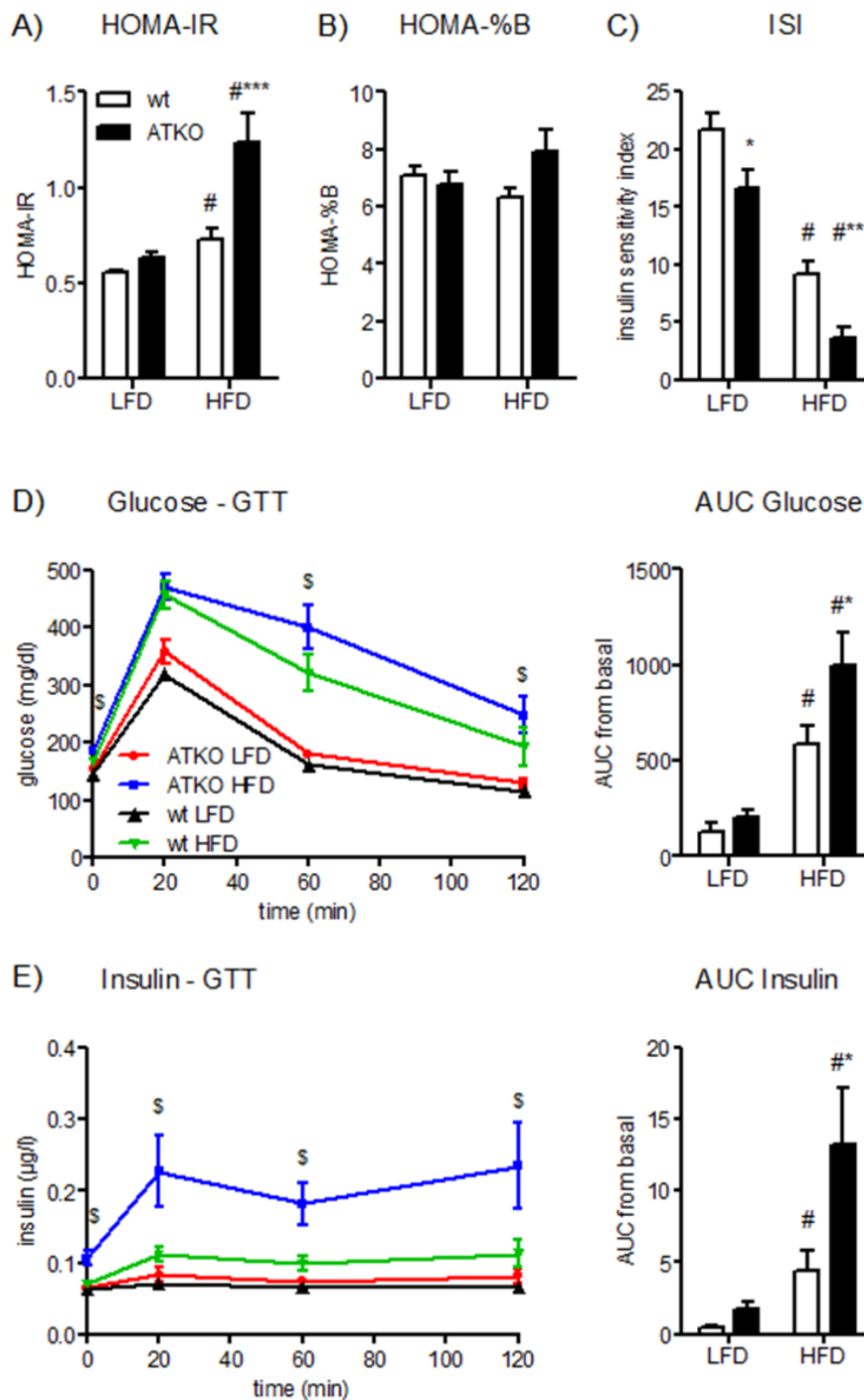
Fig. 61: ATKO mice show impaired glucose tolerance and insulin sensitivity compared to wt mice, which is worsened by HFD feeding. *12 week old female ATKO or wt mice, fed a HFD or LFD for 6 weeks, were starved for 6 hrs beginning at 8am and fasting glucose and insulin levels were measured in the serum. HOMA-IR (A) and HOMA-%B (B) were calculated from the fasted glucose and insulin levels. Mice were then injected intraperitoneally with 2 mg/kg glucose, and blood glucose and serum insulin levels were measured 20, 60, and 120 min after injection. Insulin sensitivity index (ISI, C) was calculated as described (Matsuda M. and DeFronzo D.R., 1999) using the 0 and 120 min time points. Glucose (D) and insulin (E) levels were plotted over the time course of the experiment. Student's t test: $p < 0.05$ HFD. Areas under the curve for glucose and insulin levels were calculated from basal values. n=8, means ±SEM, # indicates significance between LFD and HFD, *indicates significance between wt and ATKO.*

Increased triglyceride storage in adipocytes is described to be beneficial to whole body insulin sensitivity due to reduced lipotoxicity in other organs (Samocha-Bonet, D., 2012). However, obesity is also often accompanied by increased inflammation of the adipose tissue due to hypoxia and endoplasmatic reticulum stress of the adipocytes (Iyer, A., Brown, L., 2010). In these stages,

adipocytes can secrete cytokines to recruit macrophages to the tissue, which leads to chronic subacute inflammation and may cause glucose intolerance and insulin resistance (Iyer, A., Brown, L., 2010). To analyze adipose tissue inflammation, we measured inflammatory marker gene expression in abdominal WAT of LFD and HFD wt and ATKO mice by qPCR. As was described before, we observed increased expression of the inflammatory marker genes TNFα, IL6 and monocyte chemoattractant protein (MCP)-1 in the obese state. ATKO mice revealed a higher inflammatory marker gene expression than their wt littermates in LFD feeding, and TNFα, MCP-1 and F4/80 levels were further increased by HFD feeding (Tab. 2). Thus, adipose tissue of ATKO mice shows signs of increased macrophage infiltration and inflammation that may account for the reduced glucose tolerance of these animals.

Gene	Wt LFD	ATKO LFD	Wt HFD	ATKO HFD
TNFa	1,00 ± 0,33	2,17 ± 0,61*	1,45 ± 0,40	2,60 ± 0,86*
IL6	1,00 ± 0,31	1,45 ± 0,50	3,67 ± 0,96	3,04 ± 0,67
F4/80	1,00 ± 0,11	1,30 ± 0,12*	0,95 ± 0,15	2,49 ± 0,40***
MCP1	1,00 ± 0,12	1,37 ± 0,16*	2,55 ± 0,48	6,01 ± 1,21**

*Tab.2: ATKO mice show increased expression of the inflammatory markers TNFα, IL6, F4/80 and MCP1. means ± SEM, n=8. Student's t-test * indicates significance between wt LFD and ATKO LFD or between wt HFD and ATKO HFD.*

2.7 TBLR1 is implicated in human obesity

2.7.1 TBLR1 expression is increased in obese patients who underwent a weight reduction program

In mice, adipose tissue TBLR1 is implicated in fasting response and obesity by regulating lipolysis, thereby potentially controlling metabolic health and body weight of the animals. In the next step we wanted to investigate whether adipose tissue TBLR1 was also involved in human metabolic disorders, i.e. obesity and weight reduction by fasting.

In a first study, we analyzed TBL1 and TBLR1 mRNA levels in visceral WAT of 25 obese nondiabetic patients (BMI > 30 kg/ m²) who underwent a weight reduction program for 52 weeks (OPTIFAST®52, Rudofsky, G. et al. 2011). This program was divided into three parts: In the first three months, all meals were substituted by special 'Formula' drinks with a total of 800 calories per day (fasting phase). Following this, the drinks were substituted one by one with healthy meals for the next 6 weeks (adjustment phase). In the last 34 weeks, nutrition changed to normal, healthy meals with controlled energy intake (stabilization phase). In average, the subjects lost 22.2 ± 1.5 kg (17.5 %) body weight within the first fasting phase and 23.6 ± 3.0 kg (18.6 %) body weight after a total of 52 weeks. Body weights and serum parameters at the beginning and end point of the study are shown in Table 3.

	before weight loss	after weight loss
Age (years)	41.8 ± 2.6	
Sex	12 f / 11 m	
WAT TBLR1	1.0 ± 0.1	1.29 ± 0.1
BMI (kg/m²)	42.9 ± 1.6	35.2 ± 1.5
Glucose (mg/dl)	113.1 ± 8.8	112.8 ± 12.8
Insulin (mU/l)	31.2 ± 2.1	12.3 ± 1.7

Serum Cholesterol (mg/dl)	202.0 ± 8.4	189.3 ± 6.3
Serum triglycerides (mg/dl)	132.1 ± 15.6	96.7 ± 10.2
Body fat (%)	45.7 ± 1.9	36.6 ± 2.8

Tab. 3: Characteristics of patients participating in 1-year-weight loss study (Optifast) before the study and after 52 weeks of the program. All values are means ± SEM.

As seen in Fig. 62, TBL1 mRNA expression in visceral WAT was not significantly changed upon 12 or 52 weeks of fasting. In contrast, TBLR1 expression increased significantly after 52 weeks of fasting during the stabilization phase of the program, i.e. when acute fasting lay behind and weight reduction was achieved by constantly reduced calorie intake. This fits to the observation that, while acute fasting did not strongly alter TBLR1 levels in mice, long term food restriction lead to increased TBLR1 expression.
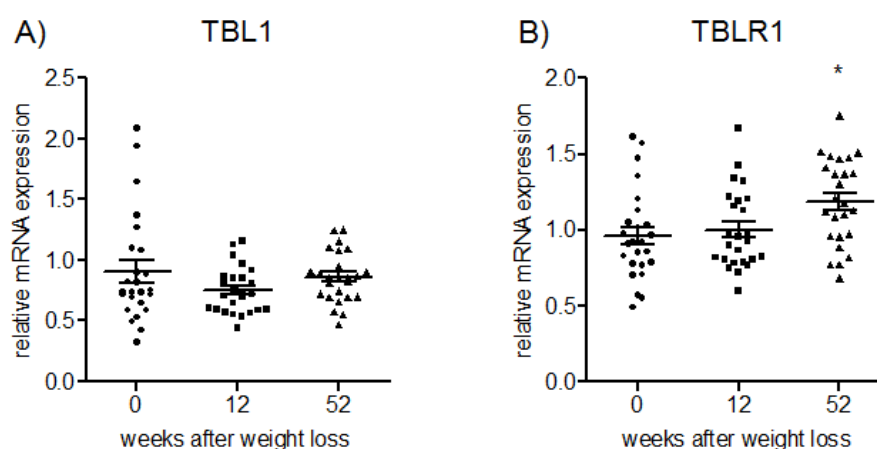
*Fig.62: TBLR1 mRNA expression is increased in obese patients after 52 weeks of restricted calorie intake. 25 obese, nondiabetic patients (BMI > 30 kg/ m²) underwent a 52 weeks weight reduction program. Visceral WAT samples were taken before the start of the study and after 12 and 52 weeks of weight reduction, respectively. TBL1 (A) and TBLR1 (B) mRNA levels were measured by qPCR and normalized to 3dg4 expression levels. n=25, 1-way ANOVA, Bonferroni pt, * indicates significance.*

2.7.2 TBLR1 but not TBL1 expression levels in visceral WAT are increased in obese patients

In mice, TBLR1 mRNA expression in adipose tissue was found to be increased in several genetic and diet-induced mouse models of obesity, while WAT TBL1 levels were largely unchanged. In humans, obesity is an increasing health risk with many genetic and environmental causes that in most cases cannot be attributed to a single genetic defect (Popkin, B.M., 2012). Here we analyzed whether TBL1 and TBLR1 mRNA expression in WAT of obese patients was altered in comparison to lean control patients, similar to what was observed before in obese and lean mice.

For this study we analyzed mRNA expression of TBL1 and TBLR1 in visceral WAT of 21 morbidly obese (BMI = 46.4 ± 1.5 kg/m²) and 20 age- and sex-matched non-obese (BMI = 25.1 ± 0.75 kg/m²) patients (characteristics, see Tab. 4). As expected from the mouse data showing elevated TBLR1 levels in obesity models (Fig. 9), TBLR1 levels were significantly increased in visceral WAT of obese patients, while TBL1 levels were unchanged (Fig. 63). Thus, TBLR1 but not TBL1 was upregulated in mice and humans in various states with increased lipolysis including obesity.

	lean	obese
Age (years)	43.5 ± 1.9	42.1 ± 2.3
Sex	15 f / 5 m	15 f / 6 m
WAT TBLR1	1.00 ± 0.09	1.2 ± 0.10
BMI (kg/m²)	25.1 ± 0.75	46.4 ± 1.5
Glucose (mg/dl)	84.1 ± 2.5	91.6 ± 2.0
Insulin (mU/l)		17.9 ± 2.2
Serum cholesterol (mg/dl)	218.7 ± 11.5	214.5 ± 9.6
Serum triglycerides (mg/dl)	125.2 ± 29.1	177.5 ± 18.8
Serum free fatty acids (mmol/l)		440.6 ± 40.3
Serum adiponectin (µg/ml)		7.7 ± 0.5

Tab. 4: Characteristics of lean and obese patients. All values are means ± SEM. Insulin, FFA and adiponectin levels were only measured in the obese group.
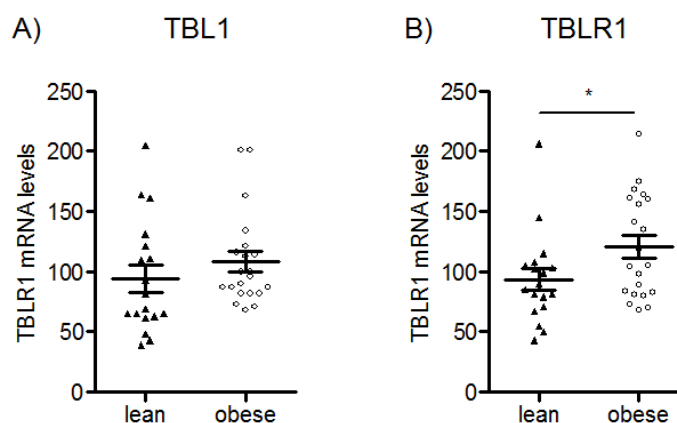
*Fig. 63: TBLR1 but not TBL1 mRNA levels are increased in visceral WAT of obese patients. TBL1 and TBLR1 mRNA levels were measured by qPCR from visceral WAT biopsies of 21 morbidly obese (BMI = 46.4 ± 1.5 kg/m²) and 20 age- and sex-matched non-obese (BMI = 25.1 ± 0.75 kg/m²) patients. n=20-21, student's t-test, * indicates significance.*

2.7.3 TBLR1 expression in WAT correlates with BMI, serum adiponectin, triglyceride and free fatty acid content and with expression of β- adrenoceptors

TBLR1 was found to be upregulated in obese patients. In this respect, calculating Pearson's correlation with body mass index revealed a slight but significant correlation between BMI and TBLR1 expression (Fig. 64 A). As obesity is mostly associated with elevated serum triglycerides and free fatty acids, and TBLR1 was found to be a regulator of lipid metabolism, we also analyzed correlation between TBLR1 levels and serum TG and FFA and indeed observed significant positive correlation (Fig. 64 B-C). Interestingly, TBLR1 expression also correlated with adiponectin levels in this patient cohort (Fig. 64 D). Finally, since TBLR1 has indirectly been shown to regulate beta-adrenergic receptor levels in mice, we analyzed gene expression of β1-, β2-, and β3-adrenergic receptors in visceral WAT of lean and obese patients. mRNA levels of the beta3-receptor yielded very low levels and were undetectable in most patients, indicating that in humans, the beta3- receptor plays only a minor role in WAT lipolysis (data not shown). However, beta1- and beta2-adrenoceptors were readily detectable and correlated with TBLR1 levels (Fig. 64 E, F), giving a further hint that TBLR1 regulates adrenoceptor expression also in humans.
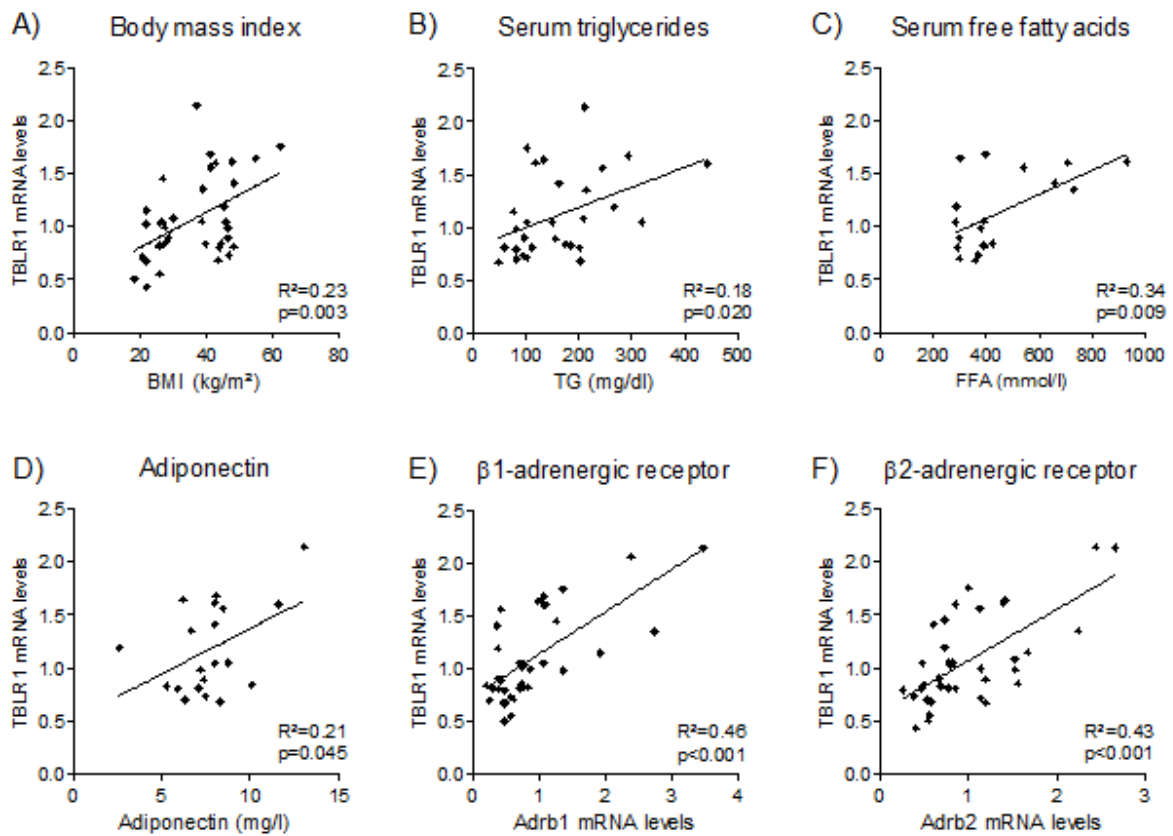
Fig. 64: Pearson correlation of visceral WAT TBLR1 mRNA expression and BMI, serum TG, FFA, and adiponectin levels and visceral WAT beta-adrenergic receptor expression. *Pearson correlation coefficients and significance given in each diagram. n=40 (A, B, E, F) or 20 (C, D).*

3 DISCUSSION

3.1 TBL1 and TBLR1 regulate lipid metabolism through cell-type specific distinct mechanisms

TBLR1 has originally been identified as a TBL1 homolog with redundant functions (Yoon, H.G., 2003). Evidence has accumulated, though, that the two 90% identical proteins may have non-redundant or even antagonistic functions (Perissi, V., 2004; Zhang, X.M., 2006). While their protein structure is largely identical, they differ in phosphorylation sites (Perissi, V., 2008) and tissue-specific expression (Fig. 8), which further supports the notion of non-redundancy.

In accordance with high liver TBL1 levels, previous studies in our lab have showed that TBL1 was a critical determinant of hepatic lipid metabolism, as knock down of this protein led to strong triglyceride accumulation and liver steatosis (Kulozik, P., 2011). Gene expression profiling revealed an implication of TBL1 in PPAR signaling, and TBL1 was shown to mediate beta-oxidation and lipogenesis by interaction with the nuclear receptor PPARα. In states with high lipid challenge, like obesity or acute lipid infusion, as well as in human liver samples from patients with non-alcoholic fatty liver disease (NAFLD), hepatic TBL1 levels were down regulated. Interestingly, while TBLR1 levels were not regulated under these conditions, liver TBLR1 knock down produced a phenocopy of the TBL1 knock down phenotype, and double knock down of both co-factors potentiated liver lipid accumulation (Kulozik, P., 2011). This would point towards a coordinated function of these two proteins eventually via heterodimerization, as it has been proposed by Yoon, H.G. et al., 2003.

Opposite to what has been observed in the liver, TBL1 was not regulated by any metabolic challenge in the adipose tissue. We observed no changes in gene expression irrespective of the stimulation in mice, be it obesity, fasting, or injection of chemicals like LPS or beta-adrenergic receptor agonists. In adipocytes, knock down of TBL1 had no effect on either differentiation or lipid metabolism. This may be explained by a less central role of the nuclear receptor PPARα in adipocytes – PPARα is expressed to a higher extent in tissues with high rates of fatty acid oxidation and peroxisomal metabolism (Lefebvre, P., 2006) like liver. Thus, regulatory mechanisms of lipid metabolism in adipose tissue have to be distinct from those in liver concerning TBL1/TBLR1 action.

In adipose tissue, the co-factor TBLR1 seems to play a more central role to lipid metabolism. Its expression in WAT of mice was tightly regulated by obesity, fasting, beta-adrenergic stimulation and inflammation, and knock down of the protein in adipocytes led to increased triglyceride levels and reduced lipolysis in these cells. When performing gene expression profiling in adipocytes lacking TBLR1, we observed that genes annotated to adipocytokine signaling pathways, such as the body weight regulator adiponectin or the proinflammatory cytokine monocyte chemoattractant protein 1 (MCP1), as well as those annotated to fatty acid metabolism, like e.g. fatty acid synthase, were enriched in the fraction of TBLR1 regulated genes. These pathways are amongst the most central pathways to adipocyte biology (Dahlman, I. and Arner, P., 2010), and their dysregulation in this setting leads to the assumption that adipocyte homeostasis is severely impaired by loss of TBLR1 function.

Pathway analysis of TBLR1 regulated genes revealed an implication of TBLR1 in the PPAR signaling pathway also in adipocytes. Since the KEGG pathway analysis does not discriminate between the three subgroups of PPARs, PPARα, γ, and β/δ, this result was congruent with the described function of TBLR1 as co-factor of the PPAR family of nuclear receptors (Perissi, V., 2004) and our gene

expression profiling results from liver (Kulozik, P., 2011). When we tried to rescue the effects of TBLR1 knock down on triglyceride accumulation and lipolysis, we observed that, while PPARα or PPARβ/δ agonists fail to rescue the TBLR1 knock down phenotype, the PPARγ agonist rosiglitazone restores lipolytic activity of the TBLR1 knock down cells. PPARγ has been shown to be a positive regulator of lipolysis at the level of transcriptional activity before (Rodriguez-Cuenca, S., 2012a and Festuccia, W.T., 2006), so it is intriguing to speculate that TBLR1 in adipose tissue may exert its function by PPARγ activation, or derepression. This is further supported by the finding that TBLR1 knock down specifically led to a downregulation of most genes annotated to the PPAR signaling pathway, arguing for a role of TBLR1 as a co-activator of PPARγ. This fits to the description of TBLR1 as a co-activator of nuclear receptors (Perissi, V., 2004) and is further supported by the finding of a direct interaction of TBLR1 with PPARγ and the obligate PPARγ heterodimerization partner RXR. Indeed, a comparison of genes regulated by adipocyte TBLR1 knock down and in adipose tissue of PPARγ+/- mice (Anghel, S.I., 2007) showed striking similarities: Genes implicated in fatty acid metabolism, like HSL, Aqp7, ACC1, or FAS were down regulated with reduced PPARγ or TBLR1 levels, while genes involved in cell stress or inflammation were increased. In contrast to what was described for the PPARγ+/- mice, however, we could not observe differences in glucose uptake or lipogenesis upon TBLR1 knock down, underlining the notion that mechanisms distinct from PPARγ signaling are involved in TBLR1 function. Thus, TBL1 and TBLR1 exert their functions on lipid metabolism in WAT and liver by different mechanisms and the involvement of distinct transcriptional networks, potentially involving the PPAR family of transcription factors.

3.2 TBLR1 regulates multiple layers of the lipolytic cascade

In adipocytes, TBLR1 is an important regulator of lipid metabolism by influencing adipocyte lipolysis stimulated by hormonal signals. This effect on the cellular level is achieved by the regulation of several key factors involved in the well-described lipolytic cascade. Importantly, adipocytes lacking TBLR1 showed increased triglyceride content without defects in glucose metabolism, insulin signaling or lipogenesis. In cells, TBLR1 knock down led to an impaired expression of beta-adrenoreceptors, representing the most upstream element of the lipolytic cascade, which resulted in decreased cAMP levels and PKA-mediated phosphorylation of target genes like HSL or perilipin. Of note, cAMP signaling efficiency or degradation were unaffected by TBLR1 knock down in these cells, as PKA subunit composition (and as such substrate affinity) was unaltered and treatment with the phosphodiesterase inhibitor IBMX had no further effect on the phenotype of TBLR1 knock down. If the adrenoceptors were the only level at which the lipolytic cascade was regulated by TBLR1, the repressive effect on lipolysis by TBLR1 should largely disappear when stimulating the cells with the adenylate cyclase (AC) agonist forskolin. This agent stimulates cAMP production directly through AC activation and circumvents the beta-adrenoceptors (Garcia-Barrado, M.J., 2011). Interestingly, TBLR1 knock down inhibited forskolin-mediated lipolysis to the same extent as it inhibited lipolysis stimulated by the beta-adrenoceptor agonists isoproterenol, CL316,243 or procaterol. Thus, transcriptional regulation of beta-adrenergic receptors cannot be the only mechanism by which TBLR1 regulates lipolysis.

In addition to reduced adrenoceptor levels, TBLR1 knock down also led to reduced ATGL, HSL and MGL expression in these cells, representing the major lipases involved in lipolysis. As pointed out by HSL and ATGL promoter analysis showing that both lipase promoters were less active without TBLR1,

this is a direct transcriptional effect of TBLR1. Thus, regulation of lipolysis by TBLR1 occurs at multiple sites within the lipolytic cascade on the transcriptional level (Fig. 65). In proof of this principle, TBLR1 over expression had opposing effects on triglyceride accumulation, lipolysis and target gene expression.
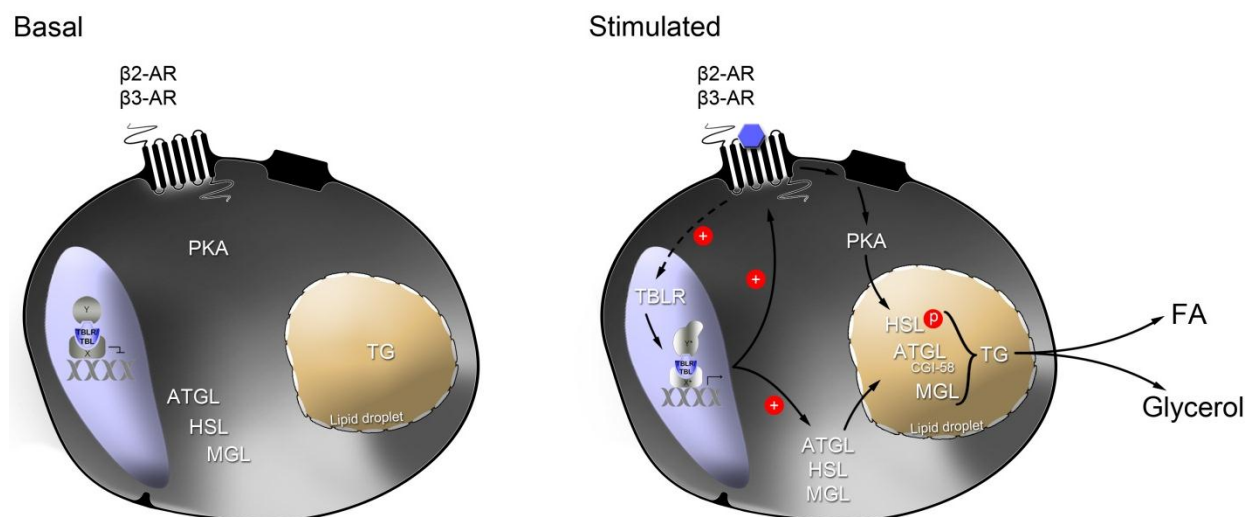
Fig. 65: Transcriptional regulation of the lipolytic cascade by TBLR1. *Under basal conditions, when the lipolytic cascade is shut off, TBLR1 is inactive or bound to co-repressor complexes. Upon ligand binding to the adrenoceptors, TBLR1 is induced and activates transcription of the target genes ATGL, HSL and MGL and the beta-adrenergic receptors, leading to a feed forward mechanism promoting triglyceride breakdown in the adipocyte.*

mRNA levels of ATGL and HSL, however, do not always correlate with cellular lipase activity. For example, Kralisch et al. have shown that isoproterenol or TNFα signals reduce mRNA levels of these lipases, but conversely stimulate lipase activities as measured by FA and glycerol release (Kralisch, S., 2005). Thus, the modern view of lipolysis takes into account that lipolytic regulation involves protein modifications, interactions and subcellular localization (reviewed in Zechner, R., 2012) rather than transcriptional regulation. Indeed, HSL is regulated mainly by phosphorylation by PKA, but enzyme activity can also be influenced by phosphorylation by other kinases, including AMPK, extracellular signal-regulated kinase, or glycogen synthase kinase-4 (Lass, A., 2011). However, TBLR1 knock down did not influence HSL phosphorylation on other sites apart from the PKA target residue Serine660. AMPK-phosphorylated HSL (Serine565) levels were indeed reduced in TBLR1 knock down cells (Fig. 29), yet this reduction can be fully attributed to reductions in HSL protein content, further supporting the notion of a specific alteration in PKA-mediated signaling.

In addition to HSL, PKA also phosphorylates the lipid droplet coating protein perilipin 1, which, in its phosphorylated form, recruits HSL to the lipid droplet to facilitate access to the lipids (Wang, H., 2009). Phosphorylated perilipin also undergoes conformational changes and releases CGI-58, so that CGI-58 can bind to ATGL as a co-activator necessary for full enzyme activity (Lu, X., 2010). The question of subcellular localization was addressed by immunohistochemical approaches showing perilipin, ATGL and HSL localization in relation to the lipid droplet with and without adrenergic receptor stimulation. Interestingly, we were not able to detect any differences in protein localization in cells lacking TBLR1, indicating that TBLR1 is indeed a regulator of transcription rather than acting through protein localization (data not shown). In this respect, we did not observe any changes in CGI-

58 mRNA or protein levels; however, the question if TBLR1 knock down influences CGI-58/ATGL interaction still needs to be addressed.

3.3 TBLR1 is a critical regulator of body weight and adiposity

Mice lacking TBLR1 in adipocytes (adipocyte specific TBLR1 knockout mice (ATKO) mice) showed increased body weight due to strongly increased body fat content, already starting at young age and developing over time. This cannot be attributed to increased adipocyte differentiation, since (a) aP2-mediated genetic knockout was largely present in mature adipocytes, and (b) TBLR1 did not influence adipocyte differentiation as seen in the cellular model. Instead, as expected from *in vitro* data, ATKO mice showed adipocyte hypertrophy as measure of increased triglyceride stores on both low and high fat diet. This was mediated by impaired lipolysis through reduction of adrenoceptor and lipase expression in WAT and subsequently of cAMP signaling strength as measured by PKA target phosphorylation.

In fasting, WAT lipolysis is activated through catecholamine signals to beta-adrenergic receptors and leads to reductions in WAT lipid levels by triglyceride hydrolysis (Yu, Y. H. and Ginsberg, H. N., 2005). The products of this reaction, free fatty acids and glycerol, are then exported from the adipocyte into the blood stream to be used by 'sink' organs like liver or muscle. Defective lipolysis in ATKO mice should therefore result in decreased FFA and glycerol levels in the blood. Interestingly, despite increased adipocyte triglyceride levels we did not observe an effect of TBLR1 knockout on either FFA or glycerol, which seems contradictory at the first glance. However, the ATKO mice are not the only mouse model describing this phenomenon. Mice lacking all three subtypes of activating adrenoceptors (β1/β2/β3 triple KO mice) develop progressive obesity as would be anticipated from mice with defects in lipolysis. Opposite to what would be expected, β1/β2/β3 triple KO mice display increased serum levels of FFA and glycerol in both fasted and fed states, probably due to over-compensation by other hormones activating lipolysis, like glucocorticoids and adrenocorticotropin hormone or by decreased antilipolytic effects through insulin (Jimenez, M., 2002). TBLR1 inactivation in adipocytes did not lead to alterations in glucose metabolism or insulin signaling, so in case of the adipocyte specific TBLR1 knockout mice decreased insulin action cannot be causal for the unchanged FFA and glycerol levels in the blood. Also, liver lipid levels and serum ketone bodies (as measure of liver TG breakdown) were largely unchanged between ATKO and wt mice (data not shown). Thus, compensation for altered FFA or glycerol excretion from the adipose tissue by insulin action or hepatic lipid metabolism is not causal for unchanged FFA/glycerol levels in ATKO mice. One explanation for this phenomenon could be that the reduced FFA/glycerol excretion observed in WAT explants of ATKO mice is not measurable *in vivo* in serum because the excretion occurs from a bigger population of enlarged adipocytes, leading to an equalization of the net effect. Calculating lipolysis relative to adipose tissue content, ATKO mice indeed displayed 2-fold reduced lipolysis when compared to wt animals in both LFD/HFD as well as fasting conditions. In this respect, although obesity has been reported to associate with decreased lipolysis, serum FFA levels are unchanged in this state, indicating that serum free fatty acid levels do not directly mirror lipolysis (McQuaid, S.E., 2011). However, further investigation is required to rule out the involvement of other lipolytic activators compensating for reduced beta-adrenergic receptor expression explaining the unchanged blood FFA and glycerol levels in the ATKO mice.

The best characterized mouse models in the field of lipolysis are the ATGL and HSL knockout mice (summarized in Zechner, R., 2012). Although one could expect a similar phenotype in these two mouse strains – ATGL and HSL represent the key enzymes of the lipolytic cascade – ATGL and HSL KO mice vary in quite a number of physiologic aspects. For decades, HSL was considered to be the only enzyme catalyzing adipocyte triglyceride hydrolysis, so several labs created whole body knockout mice expecting to see a striking fat phenotype (Haemmerle, G., 2002a; Osuga, J., 2000; Wang, S.P., 2001). Surprisingly for that time, these mice had normal lipid and energy metabolism and did not develop adiposity; in contrast they were protected against diet-induced obesity. HSL knockout mice accumulated large amounts of diacylglycerol in adipose- and non-adipose tissues (Haemmerle, G., 2002b), which supported the role of HSL as more important DG hydrolase than TG hydrolase. The creation of ATGL knockout mice has largely helped to improve our picture of the lipolytic processes in WAT. The phenotype of the ATGL knockout mice is in striking contrast to that of the HSL knockout mice. They show severely impaired lipolysis and subsequent accumulation of triglycerides not only in WAT but in all tissues. They develop obesity and – due to severe BAT and heart TG accumulation – impaired thermogenesis and cardiomyopathy (Haemmerle, G., 2006). In this respect, mutations impairing the function of ATGL or its activator CGI-58 have recently been linked to neutral lipid storage disease (NLSD) in humans. NLSD is characterized by systemic triglyceride accumulation in all tissues, leading to skeletal and cardiac myopathies and hepatic steatosis (Pena-Penabad, C., 2001). Adipocyte specific ATGL deletion leads to blunted lipolysis and severe fasting defects leading to proteolysis in other organs including skeletal muscle and heart (Wu, J.W., 2012).

Although we observed stronger reductions in HSL than ATGL protein levels in the ATKO mice, the ATKO phenotype compares more to that of the ATGL KO mice. ATKO and ATGL KO mice parallel in increased body weight and adiposity, enlarged adipocytes, and impaired lipolysis, although the question why we could not observe altered FFA or glycerol levels remains to be elucidated as explained above. In contrast to the whole body ATGL KO mice, we did not see massive triglyceride accumulation in non-adipose tissues, though, which may be explained by the tissue-specific knockout in case of the ATKO mice.

In respect to the described role of TBLR1 as co-factor regulating nuclear receptors, another very interesting mouse model is that of adipocyte specific NCoR knockout mice. The nuclear receptor co-repressor (NCoR) as part of multiprotein complexes has been described to be a negative regulator of PPARγ, one of the key factors in adipose tissue biology (Chen, J.D. and Evans, R.M., 1995). When fed a high fat diet, these mice developed increased adiposity due to increased lipogenesis. Despite the increased fat mass, adipocyte specific NCoR mice showed decreased adipose tissue inflammation, reduced macrophage infiltration, smaller adipocytes, increased adiponectin and reduced leptin and resistin levels. In addition, they exhibited improved glucose tolerance and enhanced systemic insulin sensitivity. The phenotype was explained by enhanced PPARγ activity in these mice (Li, P., 2011). Except for the increased adiposity, this mouse model represents the exact opposite to the adipocyte specific TBLR1 knockout mice with enlarged adipocytes, increased inflammation, increased leptin/resistin levels and impaired glucose tolerance. It is interesting that knockout of a PPARγ co-repressor, leading to increased activity of the nuclear receptor, has the opposite phenotype than the knockout of TBLR1, potentially acting as a co-activator, leading to decreased PPARγ activity. This finding provides another hint for the involvement of PPARγ in TBLR1 specific regulation of adipocyte biology. In this respect, it is noteworthy that PPARγ2 knockout mice show severe defects in lipolysis (Rodriguez-Cuenca, S., 2012b).

We cannot exclude that TBLR1 knockout in brown adipose tissue has influence on the obese phenotype of the ATKO mice. Indeed, aP2-cre mice mediate recombinase expression to the same extent or even stronger in BAT than in WAT (qPCR data and He, W., 2003). We observe reduced beta-adrenergic signaling as measured by FFA and glycerol release also in BAT explants of ATKO mice, and adrenoceptor expression was reduced in this tissue. Accordingly, gene expression of uncoupling protein 1 (UCP1) and PPARγ-coactivaor 1 alpha (PGC1α) was reduced in BAT of ATKO mice (data not shown), which is suggestive of reduced thermogenesis. This in turn may explain increased adiposity due to diminished energy burning (Liang, H. and Ward, W.F., 2006). Indeed, rectal body temperature was lower in ATKO mice on a low fat diet, to the same extent as high fat diet feeding reduces body temperature in wt animals. However, high fat diet fed ATKO mice did not show a further reduction in body temperature despite strongly increased adiposity, which excludes reduced BAT thermogenesis as sole reason for the ATKO phenotype. Experiments involving housing of the ATKO animals under thermoneutrality may help separating between BAT- and WAT-specific effects of adipocyte TBLR1 deletion. Future studies will focus on TBLR1 function in BAT homeostasis and possible implications in the ATKO phenotype.

It has been described that enhanced triglyceride storage in adipose tissue prevents lipotoxicity and is beneficial for glucose tolerance and insulin sensitivity (Samocha-Bonet, D., 2012). This was also observed in the NCoR and ATGL knockout mice. In contrast, TBLR1 knockout in the adipose tissue lead to increased adipocyte triglyceride storage and impaired glucose tolerance and insulin sensitivity. This is a situation typical for the metabolic syndrome, where obesity and impaired glucose homeostasis act in concert to promote the development of serious diseases like type 2 diabetes or cardiovascular disease. This is caused by lipotoxicity through lipid spillover from adipose tissues and a systemic low-grade inflammatory condition and altered adipocytokine profile (Iyer, A. and Brown, L., 2010). While we did not observe changes in lipid or FFA levels, we indeed observed increased inflammatory marker gene expression and altered adipocytokine profile in WAT of ATKO mice. Interestingly, interleukin-6 is not among the genes that were expressed to a higher extent in ATKO adipose tissue, which fits to the *in vitro* data showing reduced IL6 expression upon TBLR1 knock down. In contrast, TNFα expression was increased in WAT of ATKO mice, which at the first glance may contradict the *in vitro* gained data. However, macrophage markers F4/80 and MCP-1 were increased in ATKO adipose tissue, arguing for a higher content of cytokine- especially TNFα- producing adipose tissue macrophages (ATM). By separating ATM from adipocytes and analyzing cytokine expression we will gain deeper insights into the ATM-adipocyte crosstalk and the implication of TBLR1 in the pro-inflammatory condition of obesity.

Impaired glucose tolerance and insulin sensitivity may further be consequence of impaired metabolic flexibility of the ATKO mice. Metabolic flexibility describes the potential of adapting to the nutritional status by switching between different metabolic programs, especially between lipid and carbohydrate oxidation. The inability to do so has been implicated in the development of insulin resistance (Galgani, J.E., 2008). In case of the ATKO mice, the metabolic inflexibility disrupts the equilibrium between lipogenesis and lipolysis, resulting in a net increase in triglycerides in the adipocytes and subsequent glucose intolerance. Thus, lack of TBLR1 in WAT, although enhancing WAT triglyceride storage, leads to glucose intolerance by disturbing the metabolic flexibility of the tissue.

3.4 Outlook and Summary

In summary, these data show that TBLR1 is involved in the regulation of adipocyte lipid metabolism. While TBL1 regulates liver lipid metabolism, TBLR1 is responsible for metabolic flexibility of the adipose tissue. Conditions favoring lipolysis increase TBLR1 levels in WAT. It may be that PPARα is involved in this regulation, as CL injection in PPARα-/- mice failed to induce TBLR1 expression (Fig. 13); however, the detailed mechanism by which TBLR1 expression is regulated remains to be elucidated. We hypothesize that TBLR1 interacts with PPARγ and by this regulates expression of target genes. A direct proof of TBLR1 regulation, e.g. by showing TBLR1 binding to PPRE elements on target promoters, is still pending and is limited by the availability of good antibodies. ChIP-Seq analyses will give first hints on TBLR1 target promoters. TBLR1 is described to function as a nuclear exchange factor. In this respect, the ultimate goal will be to show co-repressor or co-activator binding on target promoters upon ligand binding, e.g. upon beta-adrenergic stimulation.

Apart from the mechanistic details, it will also be of interest to focus more on TBLR1 action in brown adipose tissue. We have evidence that TBLR1 regulates beta-adrenergic signaling also in BAT and influences UCP1 and PGC1α levels. TBLR1 knockout in BAT can be achieved by breeding the floxed TBLR1 mice with a mouse line expressing Cre recombinase under the control of the BAT specific UCP1 promoter and will shed light on BAT specific TBLR1 actions. It is tempting to speculate that BAT specific TBLR1 knockout leads to an obesity phenotype similar to that of the ATKO mice due to reduced lipolysis and thermogenesis in BAT.

Knock down of TBLR1 in adipocytes does not inhibit differentiation but leads to increased triglyceride accumulation due to reduced lipolysis, which is mediated by reduced expression and activation of beta-adrenergic receptors and the key lipases ATGL and HSL. ATGL and HSL are direct target genes of TBLR1. Evidence exists that the regulation of the lipolytic cascade is probably dependent on the interaction partner PPARγ, since stimulation with the PPARγ agonist rosiglitazone partially rescues the effect of TBLR1 knock down on lipolysis. Adipocyte specific TBLR1 knockout mice show increased adiposity that worsens with age, enlarged adipocytes, reduced lipolytic fasting response, and are more susceptible to high fat diet feeding than wt mice. As in cells, TBLR1 knockout reduces beta-adrenergic receptor expression and expression and activation of ATGL and HSL. Thus, increased TBLR1 levels in fasting or obesity lead to increased adrenergic receptor and lipase expression, mediating sufficient energy supply and mirroring energy surplus, respectively, by shifting lipid balance towards lipolysis.

Being upregulated by conditions favoring lipolysis, like obesity, fasting, adrenergic receptor stimulation or LPS injection, TBLR1 plays a critical role in energy handling in WAT in mice and humans. During fasting or different means of adrenoceptor activation, TBLR1 expression is increased to activate the lipolytic program, ensuring sufficient energy supply. In obesity, energy surplus leads to enlargement of adipocytes, which is also seen in the higher amount of β2-adrenoceptors that we and others observe in obesity (e.g. Rasmussen, M., 2003). To compensate for increased adipocyte lipid load, TBLR1 is upregulated to increase lipolysis and counteract obesity (Fig. 66). Thus, high WAT TBLR1 levels are beneficial for fighting obesity and metabolic syndrome and manipulating adipocyte TBLR1 action may represent a future goal in fighting this modern pandemic.
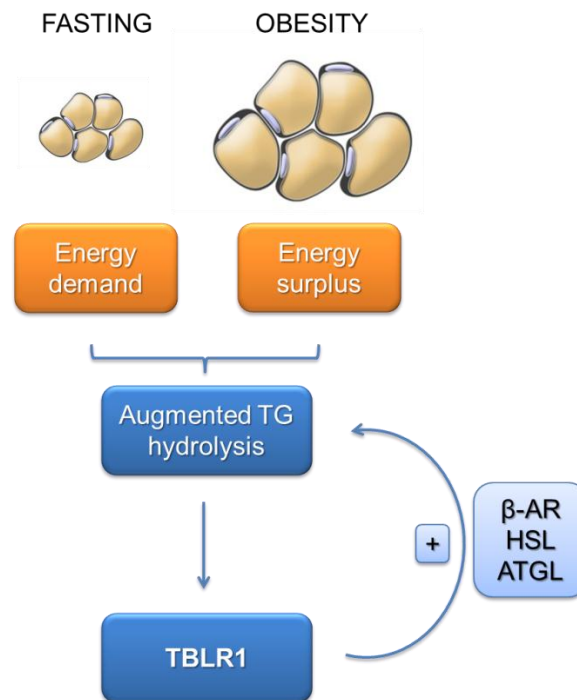
Fig. 66: Situations requiring augmented lipolysis upregulate TBLR1 to allow for efficient triglyceride breakdown*. Energy demand in fasting situations as well as energy surplus in obesity require enhanced TG hydrolysis, in the first case in order to supply the sink organs with enough fuel, in the second case in order to deal with excess fat. Requirement for enhanced lipolysis increases TBLR1 levels, thereby enhancing expression and activation of the key lipolytic players adrenoceptors (β-AR), HSL, and ATGL.*

4 METHODS

4.1 Molecular Biology

Transformation of *E.coli*

TOP10 and XL-1 blue chemically competent (cc) *E.coli* strains were transformed by chemical transformation. 50 µl of cell suspension were thawed on ice and mixed with 0.1-1 µg of plasmid DNA or 2-5 µl of a ligation reaction. After 30 min incubation on ice, a heat shock at 42°C was applied for 30 s. Following addition of 250 µl SOC medium cells were incubated at 37°C under vigorous shaking and subsequently plated onto LB agar plates containing the appropriate antibiotic.

Bacterial liquid cultures

Single colonies were inoculated into LB medium supplemented with the appropriate antibiotic. Depending on the amount of DNA needed, 2-200 ml cultures were inoculated. The cultures were incubated over night at 37°C under vigorous shaking (~160 rpm).

Preparation of plasmid DNA from *E.coli*

Plasmid DNA was isolated from *E.coli* bacterial cultures using commercially available kits, following the manufacturer's instructions (QIAprep Plasmid Miniprep Kit, Qiagen for small scale plasmid preparation; PureLink HiPure Plasmid Maxiprep Kit, Invitrogen for large scale plasmid preparation).

Preparation of genomic DNA from tissues

Tissues were digested in 500 µl proteinase K lysis buffer containing 0.5 mg/ml proteinase K for 3 hrs at 60°C and overnight at 56°C, shaking. Genomic DNA was extracted by phenol chloroform extraction adding 500 µl phenol/chlorophorm/isoamylalcohol (25:24:1), vortexing and centrifugation at 13.000 rpm, 4°C, 10 min. The upper phase was transferred to a new tube and the extraction step was repeated. The upper phase was transferred to a new tube again and 500 µl chloroform were added to it. After spinning, DNA was pelleted by adding the upper phase to 500 µl isopropanol, vortexing, and spinning at 13.000 rpm, 4°C, 45 min. Pellet was washed with 75% ethanol, dried, and resuspended in 100 µl TE buffer. Genomic DNA was stored at 4°C until use.

Determination of DNA concentration

DNA concentration and the degree of contamination were determined by using the NanoDrop ND-1000 spectrophotometer. The concentration was determined by measuring the absorption at 260 nm wavelength, contamination with salts or proteins was assessed by measuring the absorbance spectrum between 220 and 300 nm. A 1.5 µl DNA sample was used for each measurement.

DNA Sequencing

For sequencing DNA was diluted to 800 ng in 10 µl H_2O. Primers at 5 pmol/µl were added either directly or by the company. The samples were sequenced by LGC genomics. The sequencing primers are listed in the material section.

PCR

DNA from plasmids, cDNA or a genomic DNA was amplified by polymerase chain reactions using a thermocycler (PTC 200) and Phusion polymerase (Finnzymes). The primers used are listed in the material section. PCR reactions were set up following the manufacturer's instructions and were programmed according the T_m of each individual primer pair and the length of the PCR product.

Purification of PCR fragments

DNA from PCR reactions was purified applying the QIAquick PCR purification kit provided by Qiagen following the manufacturer's instructions. DNA was eluted in 30 µl H_2O. Alternatively, fragments were purified by gel extraction as described.

Agarose gel electrophoresis

DNA fragments were separated by agarose gel electrophoresis using 1% or 2% agarose and 1 µg/ml ethidium bromide in TBE. DNA samples were mixed with 1x Orange G loading dye and separated at 80-150 V. Gel pictures were taken under UV light (254 nm) with the Gel imager (Intas).

Gel extraction of DNA

DNA extraction following separation by agarose gel electrophoresis was performed using the QIAquick gel extraction kit (Qiagen) following the manufacturer's instructions.

DNA restriction

DNA restriction was performed using restriction enzymes (10-20 U) and corresponding buffers provided by New England Biolabs. Restriction reactions were incubated at 37°C for 1-2 hrs.

DNA dephosphorylation

Self-ligation of plasmid DNA in ligation reactions was avoided by adding 10 U CIP (Calf Intestinal Phosphatase) to restriction reactions after 1 h of restriction. Dephosphorylation occurred in 60 min at 37°C. CIP could be added to every customary restriction enzyme buffer without a loss of activity.

DNA Ligation

Ligation of insert and vector DNA was performed using a T4 DNA ligase (NEB or Fermentas). The molar ratio of insert to vector was adjusted to 3:1 applying the following formula:

ng insert = (100 ng vector x bp insert / bp vector) x 3

1 U enzyme was used in 1x ligase buffer for the ligation reactions according to the manufacturer's instructions. The reactions were performed in 20 µl total volume and incubated for 2-6 h at room temperature. After the ligation reaction, the enzyme was heat inactivated (10 min 65°C). A reaction containing the vector without insert was used as a negative control to determine the degree of vector self-ligation.

Southern Blot

For southern blot, genomic DNA was extracted and digested with EcoRI as described. The restriction enzyme was heat inactivated by incubation at 65°C, 10 min. DNA fragments were separated on a large 0.9% agarose gel in TAE buffer and fixated to the gel by washing in 0.25 M HCl for 15 min followed by two washing steps in 0.4 M NaOH for 20 min. The gel was pre-incubated in 20 x SSC

buffer and the DNA subsequently blotted on a nitrocellulose membrane by capillary force. The DNA was fixated to the membrane by UV crosslinker (600 µJx100) and dried until use. Probes were created by PCR and labelled using ^{32}P-dCTP and hybridized to the membrane during overnight incubation.

RNA isolation

A) From 3T3-L1 adipocytes

Cells were harvested in 1 ml QIAzol (Qiagen) and transferred to RNase free tubes. Lysates were incubated at room temperature for 5 min to release nucleoprotein complexes before adding 200 µl of chloroform. Mixtures were vortexed for 15 sec and then centrifuged for 30 min at 13,000 rpm, 4°C. The upper aqueous solution containing the RNA was transferred into a fresh reaction tube. The RNA phase was then mixed with 1 volume of isopropanol and incubated at room temperature for 10 min, followed by a 10 min centrifugation step at 13,000 rpm, 4°C. The supernatant was aspirated and the pellet was washed once with 1 ml of 75% ethanol. The pellet was dried at 55°C (approx. 10 min) and re-solubilised in 30 µl water. To increase solubilisation, the RNA solution was incubated at 55°C for 10 min. The samples were stored at -80°C until further use.

B) From primary adipocytes

Cells were harvested in 500 µl QIAzol (Qiagen) and transferred to RNase free tubes. Phase separation was performed as described in A). The upper phase was then transferred to a new tube containing 1 volume 100 % ethanol to precipitate nucleic acids. RNA was then purified using the RNeasy micro kit (Qiagen), following the manufacturer's instructions. RNA was eluted in 30 µl H$_2$O and stored at -80°C until further use.

C) From tissue

Frozen tissue samples were transferred into a 2 ml RNase/DNase-free reaction tube containing 1 ml QIAzol (Qiagen) and a pre-cooled stainless steel bead. The samples were lysed using the TissueLyser for 90 sec at a frequency of 30 Hz. Lysates were incubated at room temperature for 5 min to release nucleoprotein complexes before adding 200 µl of chloroform. Phase separation was performed as described in A). The upper phase was then transferred to a new tube containing 1 volume 100 % ethanol to precipitate nucleic acids. RNA was then purified using the RNeasy micro kit (Qiagen), following the manufacturer's instructions. RNA was eluted in 50 µl H$_2$O and stored at -80°C until further use.

Determination of RNA concentration

The RNA concentration was determined spectrophotometrically at 260 nm using the NanoDrop ND-1000 spectrophotometer. In parallel, the ratio 260 nm/280 nm was detected in order to measure protein impurities in the samples.

Assessment of RNA quality

RNA quality way assessed using agarose gel electrophoresis. 1% agarose gels were poured with RNase free agarose in 1x TBE buffer. The RNA samples were denatured in RNA denaturing buffer. 1 µl per RNA sample were added to 10 µl RNA denaturing buffer and incubated for 10 min at 65°C. After

running the gel, quality of the RNA was determined visually by examination of the ratio between 28S to 18S ribosomal RNA, which was 2:1 for intact RNA.

cDNA synthesis

For synthesis of complementary DNA, 200-1000 ng of RNA was used. cDNA synthesis was performed using the cDNA synthesis kit (Fermentas) following the manufacturer's instructions. After completion, cDNA samples were diluted 10 fold in RNase free water and stored at -20°C.

Quantitative PCR

5 µl of the diluted cDNA samples obtained from reverse transcription were used for quantitative PCR. A master mix was prepared containing 10 µl *TaqMan* Gene Expression Assay Supermix, 4.5 µl DNase/RNase free water and 0.5 µl *TaqMan* probe per individual reaction. Technical duplicates of all samples were performed. The *TaqMan* probes used were obtained from Applied Biosystems or MWG and are listed in the material section. Water was used as a negative control and samples containing no reverse transcriptase served as controls for genomic DNA contamination. 20 µl PCR reactions were transferred per well onto a MicroAmp Optical 96 well reaction plate and quantitative PCR was performed using the StepOnePlus Real Time PCR System (Applied Biosystems).

Gene expression profiling

Gene expression profiling was performed in 3T3-L1 adipocytes transduced with TBLR1 or control shRNA carrying adenoviruses. RNA isolation, cRNA synthesis and hybridization to Mouse Genome 430 2.0 arrays (Affymetrix, Freiburg) were performed according to the manufacturer's recommendations. Three arrays per virus were hybridized. CustomCDF by Brainarray with Entrez based gene definitions (Entrez basic version 13) was used to annotate the arrays (Sandberg R., 2007). The raw fluorescence intensity values were normalized applying quantile normalization. Differential gene expression was analyzed based on ANOVA using a commercial software package (SAS JMP8 Genomics, version 4, SAS Institute, Cary, NC). A false positive rate of a=0.05 with FDR correction was taken as the level of significance. Pathways belonging to various cell functions were obtained from public external databases (KEGG, http://www.genome.jp/kegg/). A Fisher's exact test was performed to detect the significantly regulated pathways.

4.2 Cell Biology

All experiments with eukaryotic cells were performed under sterile conditions. Cells were cultivated at 37°C, 5% CO_2 and 95% humidity. All media and additives were warmed to 37°C prior to use. A list of the media used for cell culture experiments is shown in Tab. 5.

Name	Medium	Serum	Antibiotic	Further additives
3T3-L1 culture	DMEM (1 g/l glucose)	10% FCS	1% P/S	-
3T3-L1 differentiation	DMEM	10% FCS	1% P/S	See Tab. 6
3T3-L1 starve 1	DMEM (1 g/l glucose)	1% FCS	-	-
3T3-L1 starve 2	DMEM (1 g/l glucose)	0.1% FCS	-	-

3T3-L1 transfection	DMEM	-	-	-
3T3-L1 virus infection	DMEM (1 g/l glucose)	-	-	-
Freeze medium	DMEM	20% FCS	-	10%DMSO
HEK293 culture	DMEM	10% FCS	1% P/S	-
HEK293A culture	DMEM	10% FCS	1% P/S	1% NAA
Primary adipocyte culture	DMEM	10% FCS	1% P/S	-
Primary adipocyte differentiation	DMEM	5% FCS	1% P/S	See Tab. 6
RAW264.7 culture	DMEM	10% FCS	1% P/S	-
Virus titration	DMEM	2% FCS	1% P/S	1% NAA

Tab. 5: *Media used for cell culture and virus experiments.*

Thawing cells

Eukaryotic cells were stored in liquid nitrogen tanks in 1 ml aliquots containing $5*10^5$ cells in freeze medium. Following thawing at 37°C cells were distributed equally to two 15 cm tissue culture plates containing 25 ml culture medium. 24 h after seeding medium was changed to remove remaining DMSO.

Cultivation of 3T3-L1 fibroblasts

3T3-L1 cells were cultivated on 15 cm tissue culture plates in 20 ml 3T3-L1 culture medium.

A confluency of 70% as well as a passage of 15 was never exceeded to avoid diminished differentiation capacity.

For passaging, the cells were first washed in 1x PBS and trypsinized, then the detached cells were resuspended in 10 ml of fresh medium. Cells were pelleted by centrifugation at 2000 rpm for 3 min and subsequently resuspended in 10 ml fresh medium. After counting in a Neubauer counting chamber, $4x 10^4$ cells were plated onto a 15 cm tissue culture dish containing 20 ml medium. Cells were passaged every 3-4 days.

Differentiation of 3T3-L1 fibroblasts into adipocytes

3T3-L1 fibroblasts can be differentiated into adipocytes by the addition of insulin, 3-isobutyl-1-methylxanthine (IBMX), dexamethasone and ABP (L-ascorbate, d-biotin, pantothenic acid). Cells were cultivated on 10 cm plates until they reached confluency and then induced to undergo differentiation by adding 3T3-L1 differentiation media as shown in Tab. 6.

Differentiation	Medium	Additives
Day 1	3T3-L1 differentiation	1 µg/ml Insulin
		0.25 µM Dexamethasone
		0.5 mM IBMX
		1/1000 ABP stock solution
Day 3	3T3-L1 differentiation	1 µg/ml Insulin
		0.25 µM Dexamethasone

		0.5 mM IBMX
		1/1000 ABP stock solution
Day 5	3T3-L1 differentiation	1 µg/ml Insulin
		1/1000 ABP stock solution
Day 8	3T3-L1 culture	none

Tab. 6. *Media and additives for differentiation of 3T3-L1 adipocytes.*

Experiments could be performed 8-12 days after initiation of differentiation.

OilRedO staining of 3T3-L1 adipocytes

Differentiated 3T3-L1 adipocytes were washed in 1x PBS followed by 10% formalin in PBS for 5 min. Then cells were fixated by the addition of 10% formalin in PBS for 1 h at RT. After washing with 60% isopropanol the wells were dried and subsequently stained with Oil Red O working solution for 10 min. Unbound dye was removed by washing with water and pictures of the stained cells were taken under the microscope.

Transfection of 3T3-L1 adipocytes

3T3-L1 adipocytes were transfected by electroporation using the NEON transfection device (Invitrogen). Cells were trypsinized, washed with PBS and counted. A total of $4x10^5$ cells/well were resuspended in 10 µl buffer R (Invitrogen). After adding DNA, cells were transfected by electroporation in 10 µl NEON tips (Invitrogen) with the settings 1400 V/ 20 ms/ 2 pulses. Experiments were performed 24-48 hrs post transfection.

Luciferase Assays

Transiently transfected cells (12well plates) were washed with cold PBS 48 hrs after transfection and harvested in 150 µl harvest buffer/well. Insoluble cell debris was removed by centrifugation for 3 min at 13,000 rpm. To determine luciferase activity in lysates, 30 µl of lysate were transferred into a well on a black 96-well-plate. Lysates were complemented with 100 µl assay buffer and plates were measured using a luminometer (Mithras 940 Luminescence). Automatic injection of 100 µl luciferin buffer started the reaction. Light emission was measured at a wavelength of 560 nm and harvest buffer alone was used to determine a blank value. All results were normalized to the activity resulting from a co-transfected β-galactosidase expression plasmid harboring a CMV promoter (CMV β-Gal). For the β-Galactosidase assay 50 µl cell lysate/well were transferred into a clear 96-well plate and 50 µl ONPG buffer were added to each well. Harvest buffer was used to obtain a blank value. The plates were incubated at 37°C for 3-60 min until a clear yellow color was visible and the absorption was measured at 405 nm.

Lipolysis Assays

Lipolysis assays were performed in mature adipocytes 8-12 days after induction of differentiation. After preincubation in Krebs Ringer buffer for 2 hrs, cells were stimulated with 0.1-10 µM isoproterenol (Calbiochem, Merck), 0.1-10 µM forskolin (Sigma, Munich), 0.5 mM IBMX (Sigma, Munich) or 1 µM procaterol (Biozol, Heidelberg) for 3 hrs in Krebs Ringer buffer supplemented with 5% BSA, 5 mM glucose, 25 mM HEPES/KOH pH 7.5. Supernatants were harvested for measurement

of NEFAs or glycerol. Cells were harvested in QIAzol (Qiagen) and Tx lysis buffer for RNA and protein extraction, respectively.

Glucose metabolism and lipogenesis Assays

Glucose uptake and lipogenesis assays were performed in 3T3-L1 adipocytes transduced with control or TBLR1 shRNA carrying adenoviruses. Cells were washed with Krebs Ringer buffer and glucose uptake was stimulated by 10 nM insulin in Krebs Ringer buffer supplemented with 3% BSA, 25 mM HEPES/KOH pH 7.5 and 1mM glucose spiked with 0.1 µCi D-[^{14}C(U)]-Glucose (Perkin Elmer, Waltham) for 2 hrs. Cells were lysed using 0.5 M NaOH and defined amounts were used to measure overall glucose uptake or to isolate triglycerides and measure lipogenesis by counting ^{14}C lipid incorporation as disintegrations per minute (DPM) in a scintillation counter. Glucose uptake and lipogenesis were calculated as % induction by insulin.

cAMP Assays

cAMP Assays were performed in mature 3T3-L1 adipocytes using the Cyclic AMP EIA Kit (Cayman Chemicals) following the manufacturer's instructions.

Cultivation of Raw264.7 Macrophages

Raw264.7 cells were cultivated in Raw264.7 culture medium on 10 cm and 15 cm tissue culture plates, respectively, and passaged at a confluency of 70-90 % by trypsinization as described for 3T3-L1 cells.

Stimulation of Raw264.7 Macrophages with LPS

Raw264.7 cells can be stimulated to inflammatory cytokine secretion by addition of LPS to the culture medium. For this purpose 3x 10^6 cells were seeded onto 15 cm tissue culture plates. 100 ng/ml LPS in fresh RAW264.7 culture medium was added 3 days after seeding. As a control, fresh culture medium without LPS was added to the cells. The medium was collected 9 hrs after the addition of LPS and sterile filtered with a 0.45 µm filter. The conditioned macrophage medium (CM) or control macrophage medium (M) was stored at -20°C until use for no longer than 2 weeks.

Cultivation of human embryonic kidney (HEK) cells

HEK293 and HEK293A cells were cultured in HEK293 and HEK293A culture medium, respectively. The cells were cultivated either in 10 cm tissue culture plates containing 10 ml medium or in 15 cm plates with 25 ml medium. Cells were passaged at 70-90% confluency by resuspension in 10 ml fresh medium, centrifugation (3 min, 2000 rpm), resuspension of the pelleted cells in 10 ml medium and subsequent addition of the twentieth part of the cells to a new tissue culture plate. Cell number could be determined by using the Neubauer counting chamber.

Transient transfection of HEK cells

Transfection with calcium phosphate

Cells were seeded 24 h prior to transfection and transfected at 70-80% confluency. DNA was mixed with 0.25 M CaCl$_2$ and the same volume of 2x BBS, the amounts used are listed in Tab. 7. After

incubation for 15-20 min at RT, the mixture was added to the cells in fresh medium. Medium was changed 6-12 h after transfection. Experiments were performed 48-72 hrs after transfection.

Format	Cell number	DNA	CaCl$_2$	2x BBS
15 cm plate	2-8x 10^6	6.25 µg	1.25 ml	1.25 ml
6well plate	2x 10^5	100 ng -1 µg	80 µl	80 µl

Tab. 7: *Reagents used for calcium phosphate transfection.*

Transfection with Lipofectamine 2000

For higher transfection efficiency HEK293 cells were transfected with Lipofectamine 2000 transfection reagent (Invitrogen). 3 µl of the reagent were added to 250 µl of serum free Opti-MEM medium. The mixture was combined with DNA which was diluted in the same medium, and the mixture was incubated at RT for 20 min to allow complex formation. The DNA/Lipofectamine complexes were added dropwise to the cells in antibiotic-free medium. Medium change to the normal culture medium was performed the following day.

Isolation of preadipocytes from adipose tissue

Preadipocytes were isolated from the stromal vascular fraction (SVF) of abdominal or inguinal white adipose tissue or from interscapular brown adipose tissue depots of male C57Bl6/N mice aged 6-9 weeks. Mice were sacrificed by cervical dislocation, sterilized with 70% ethanol and adipose tissue depots were dissected. After cleaning the fat pads, the pads were chopped until no pieces could be observed anymore and subsequently digested in 7 ml collagenase medium (DMEM containing 1.5 mg/ml type II collagenase and 0.5% BSA) for 1 h at 37°C and 180 rpm. To stop the reaction, 6 ml culture medium was added and adipocytes floated to the top of the tube, where they could be removed. If needed, 1 ml QIAzol reagent (Qiagen) was added to 200 µl mature adipocytes to isolate RNA as described. The SVF was harvested by centrifugation at 1000 rpm, 10 min. The cell pellet was resuspended in culture medium, filtered through a 70 µm falcon strainer, and cells were plated to 12 well plates. One mouse harvested one 12 well plate abdominal preadipocytes, one 12 well plate inguinal preadipocytes, and half a 12 well plate brown preadipocytes. Cells were washed every day with warm culture medium until they reached confluency.

Differentiation of primary preadipocytes into adipocytes

Primary preadipocytes are differentiated into adipocytes by the addition of insulin, 3-isobutyl-1-methylxanthine (IBMX), dexamethasone and ABP (L-ascorbate, d-biotin, pantothenic acid). In case of preadipocytes harvested from brown adipose tissue, in addition triiodothyronine (T3) is added. Preadipocytes were cultivated until they reached confluency (approximately 1 week) and then induced to undergo differentiation by adding primary cell differentiation media as shown in Tab. 8.

Differentiation	Medium	Additives
Day 1	Primary adipocyte differentiation	1 µg/ml Insulin
		0.25 µM Dexamethasone
		0.5 mM IBMX
		1/1000 ABP stock solution
		(3 nM T3)

Day 3	Primary adipocyte differentiation	1 µg/ml Insulin
		0.25 µM Dexamethasone
		0.5 mM IBMX
		1/1000 ABP stock solution
		(3 nM T3)
Day 5	Primary adipocyte differentiation	1 µg/ml Insulin
		1/1000 ABP stock solution
Day 8	Primary adipocyte culture	none

Tab. 8: *Media and additives for differentiation of primary adipocytes.*

Experiments could be performed 8-12 days after initiation of differentiation.

Cloning of adenoviruses

The BLOCKiT™ Adenoviral RNAi Expression System was used to generate adenoviruses expressing shRNAs against murine TBL1 and TBLR1 or a non-specific control. Oligonucleotide sequences were chosen using Invitrogen's RNAi Designer tool. Forward and reverse oligonucleotides against the target gene sequence were annealed and cloned into the pENTR™/U6 vector according to the manufacturer's instructions. The resulting constructs were recombined with the pAd/BLOCK-iT™ DEST vector, which contains the adenovirus serotype 5 DNA, but lacks the E1 and E3 genes that are required for viral replication. The viral vector containing the shRNA sequence was linearized by restriction digest using the enzyme PacI and transfected into HEK 239A cells using Lipofectamine 2000 according to the manufacturer's instructions. HEK293A cells express the viral E1 and E3 genes necessary for viral outbreak, allowing the virus to expand in this cell line. Viral plaques appeared 6 to 10 days after transfection and cells started to detach from the cell culture dish. Once about 70% of cells were floating, they were harvested. The same procedure was used to generate viruses overexpressing TBL1 and TBLR1. The cDNAs were cloned into a pENTR vector harboring the CMV promoter and subsequently recombined with the pAd/BLOCK-iT™ DEST vector. An empty adenovirus was used as a negative control in over expression experiments.

Adenovirus harvest

Adenoviruses were harvested when 70-80% of the HEK293A cells were rounded and lost adhesion. For that purpose the remaining adherent cells were rinsed off the tissue culture plate with a pipette and transferred to a centrifuge tube together with the non-adherent cells. Cells were pelleted by centrifugation (2000 rpm, 10 min, RT) and resuspended in 0.5-3 ml PBS-TOSH. The cell suspension was stored at -80°C. For cell disruption and virus release, 3 freeze-and-thaw cycles were performed. To this end the suspension was frozen in liquid nitrogen, thawed at 37°C and vortexed vigorously. Cell debris was removed by centrifugation at 3000 rpm for 5 min and the resulting crude virus lysate could be purified by CsCl gradient or used for further infection of HEK293A cells.

Adenovirus purification using cesium chloride gradient

Cesium chloride (CsCl) gradient centrifugation is a type of density gradient centrifugation for the purification of viral particles (Green et al. 2006). Confluent HEK293A on twenty 15 cm cell culture dishes were infected with crude virus lysate or purified adenovirus (1 µl per plate) and grown until 70-80% of the cells were rounded and lost adhesion, then they were harvested and lysed as

described. PBS-TOSH was added to the crude lysate to a final volume of 20 ml. All solutions were adjusted to pH 7.2. The first gradient was layered with 9 ml 4.4 M CsCl, 9 ml 2.2 M CsCl and 20 ml virus in PBS-TOSH. After ultracentrifugation (2 hrs, 4 °C, 24,000 rpm, SW28 rotor) the virus band was removed and added to the same volume saturated CsCl. The second gradient was layered with 8 ml virus in CsCl, 1.5 ml 4.4 M CsCl und 1.5 ml 2.2 M CsCl. Following the second ultracentrifugation (3 hrs, 4 °C, 35,000 rpm, SW40Ti rotor) the virus band was removed in the smallest possible volume and dialysed against PBS-glycerol over night at 4°C. 10% glycerol was added to the purified virus and aliquots were stored at -80°C.

Virus Titration using the Tissue Culture Infectious Dose 50 (TCID$_{50}$) method

The virus titer (plaque forming units, pfu) could be determined by TCID$_{50}$. For that purpose, 10^4 HEK293A cells were seeded in 100 µl virus titration medium in each well of a 96 well plate and infected with decreasing amounts of virus after 2 hrs of adhesion. Serial dilutions of the virus up to 10^{-14} were prepared in titration medium and added to the cells. Double measurements were performed for each virus. 10-12 days after infection and incubation at 37°C the plaques were counted and the titer was calculated using the following formula:

$$T = 10^{1+(s-0.5)} \times 10 \text{ pfu / ml}$$

(s = sum of positive wells starting from the 10^{-1} dilution; 10 positive wells per dilution = 1)

Titration of virus particles using the OD$_{260nm}$ method

Measurement of the optical density of the virus suspension at 260 nm results in a good estimation of the virus titer. With this method, non-infectious as well as infectious particles are included in the measurement. The virus suspension was diluted 1/10 or 1/20 in 0.1% SDS and heated to 56°C for 10 min, which liberates the DNA of the viral capsid. Following 30 sec centrifugation at 13,000 rpm the OD$_{260nm}$ was determined using a spectrophotometer (NanoDrop ND-1000). The titer was calculated by OD 1 = dilution x 1.1 x 10^{12} particles / ml.

Transduction of 3T3-L1 fibroblasts with adenoviruses

2×10^4 3T3-L1 cells were seeded on 6 well plates and transduced with different amounts of adenovirus 72 hrs after plating. MOIs of 100 to 100,000 were tested, with MOI 1000 being ideal for efficient transduction of the fibroblasts. The desired amounts of virus were diluted in low glucose DMEM without FCS and 0.5 µg/ml poly-L-lysin were added (Orlicky et al. 2001). After incubation at RT for 60-100 min the mixture was added to PBS-washed cells. After 90 min incubation at 37°C, 3T3-L1 culture medium was added and cells were incubated 72-96 hrs until harvest. In case of subsequent differentiation the differentiation process was started 24 hrs after virus transduction.

Transduction of 3T3-L1 adipocytes with adenoviruses

Differentiated 3T3-L1 adipocytes on day 10 of differentiation were washed with PBS and trypsinized. The pelleted cells were then resuspended in 3T3-L1 culture medium and filtered through a 70 µM falcon strainer. Cells were counted, and 4×10^5 cells were plated to each well of a 12 well plate. For larger scale transductions, 4.8×10^6 cells were plated on 10 cm plates. 24 hrs later, floating cells were removed by washing with PBS and 3T3-L1 starve 1 medium was added. After 12 hrs incubation, cells were again washed in PBS and 3T3-L1 starve 2 medium was added for 12 hrs. Adenoviruses at an

MOI of 500 were diluted in 3T3-L1 virus infection medium containing 0.5 µg/ml poly-L-lysin (250 µl medium per well or 2.5 ml per 10 cm plate). After incubation at RT for 60-100 min the mixture was added to PBS-washed cells. After 90 min incubation at 37°C, 3 volumes 3T3-L1 culture medium were added and cells were incubated 72-96 hrs until harvest.

Transduction of primary adipocytes with adenoviruses

Primary adipocytes were differentiated on 12well plates and transduced with adenoviruses 10 days after induction of differentiation. Adenoviruses with an MOI of 1000 were diluted in 250 µl DMEM medium without any supplements, containing 0.5 µg/ml poly-L-lysin. After incubation at RT for 60-100 min the mixture was added to PBS-washed cells. After 90 min incubation at 37°C, 750 µl primary adipocyte culture medium was added and cells were incubated 72-96 hrs until harvest.

4.3 Animal experiments

The animals were housed according to international standard conditions with a 12 hrs dark, 12 hrs light cycle and regular unrestricted diet if not stated otherwise. Animal handling and experimentation was performed in accordance with NIH guidelines and approved by local authorities (Regierungspräsidium Karlsruhe). Blood was taken after cervical dislocation. Organs including liver, kidney, fat pads, and gastrocnemius muscles were collected, weighed, snap-frozen in liquid nitrogen and used for further analysis.

Obesity models

8-12 week old ob/ob, db/db or New Zealand Obese and New Zealand Black (NZO/NZB) mice were obtained from Charles River Laboratories (Brussels, BEL) and maintained on a 12 hrs light-dark cycle with regular unrestricted diet. In high-fat diet experiments, C57Bl6 mice were fed a high-fat diet (45% or 60% energy from fat, New Brunswick, USA) or low-fat control diet (10% energy from fat, New Brunswick, USA) for a period of 12-20 weeks.

Colon26 murine cachexia model

For tumor induction in cachexia models, $1.5x\ 10^6$ Colon 26 cells in PBS were injected subcutaneously into 10 week old Balb/c mice (Charles River Laboratories, Brussels). Control mice were injected with PBS. Mice were sacrificed approximately 2 weeks after injection.

Sepsis model

10 week old male wild type C57Bl6 mice were fasted for 12 hrs and subsequently injected with 20 mg LPS / kg body weight (E. Chichelnitskiy). As a control, mice were injected with PBS and kept at fasting conditions for the same time. 8 hrs after LPS or PBS injection, mice were sacrificed.

Fasting and Refeeding

For an extensive fasting and refeeding study, male C57Bl6 mice at the age of 13 weeks were used. Different groups of mice were fasted for 8 hrs, 24 hrs and 48 hrs, respectively, and subsequently refed for 1 hr, 6 hrs or 24 hrs before the sacrifice.

CL and NE injections

For CL and NE treatments, 8-week-old female NMRI mice or PPARα-/-, PPARβ/δ-/- or PPARγ+/- mice (obtained from W. Wahli) were injected intraperitoneally with 1 mg/kg CL316,243 (Tocris Bioscience) in 0.9% NaCl, 1 mg/kg Norepinephrine bitartrate (Sigma) in 0.9% NaCl or vehicle and sacrificed 3 or 8 hrs later.

Mice for isolation of primary preadipocytes

Male wt C57Bl6/J purchased from Charles River or C57Bl6/N mice from Barrier 2 within DKFZ at the age of 6-9 weeks were used for the isolation of primary preadipocytes.

siRNA injection

siRNAs obtained from MWG or Applied Biosystems were diluted in Invivofectamine transfection reagent according to the manufacturer's instructions and diluted with 0.9% NaCl. 7 μg/g body weight were injected either intravenously or intraperitoneally in volumes of 100 μl (i.v.) or 200 μl (i.p.). Mice were prepped after 2-10 days. Alternatively, 1.5 μg/g BW siRNAs were mixed with 150 μl DOTAP transfection reagent per mouse and injected i.v. or i.p. for 10 days every 72 hrs.

Morpholino injection

In vivo morpholinos are artificial siRNA like oligos especially for use in mice and were obtained from Gene Tools, LLC. Morpholinos were diluted in PBS pH 7.2 and a maximum of 12.5 μg/g body weight were injected either intravenously or intraperitoneally in volumes of 100 μl (i.v.) or 200 μl (i.p.) on two consecutive days. Mice were prepped 3 days, 1 week or 2 weeks after the first injection.

Fat pad injection

To place injections exclusively into the epididymal fat pad, the intra-abdominal cavity was opened and the epididymal fat pads were exposed. Adenoviruses (5×10^9 -2×10^{10} ifu/ml), siRNAs or morpholinos were injected into the fat pad at a maximum volume of 50 μl for each fat pad. A microinjector was used in some experiments for stepwise injection of 2 μl volumes. Anesthesia was performed by isofluorane (induction: 3-4 % isofluorane, maintainance: 1-1.5 % isofluorane).

Adipocyte specific TBLR1 knockout mice

Adipocyte specific TBLR1 knockout mice were generated on C57Bl6 background (C57BL/6-Tbl1xr1(tm2273Arte) Tg(Fabp4-Cre)1Rev) by TaconicArtemis as described in 'Results'. Adipocyte specific knockout was assessed by Southern Blot in various tissues with probes created by primers shown in 'Materials'.

Adipose tissue explants

Adipose tissue explants were isolated by excising inguinal and abdominal WAT or BAT, washing it in PBS and cutting it into equally sized pieces of 20-40 mg. One explant was transferred to one well of a 24-well plate and cultured in 300 μl Krebs-Ringer buffer supplemented with 5% BSA, 5 mM glucose, 25 mM HEPES/KOH pH 7.5 with or without 10 μM isoproterenol for 4 hrs. Supernatants were harvested for measurement of FFA and glycerol and explants were frozen in liquid nitrogen and used for RNA or protein extraction as described.

Body composition analysis using EchoMRI

Mice were weighed and body composition was determined using magnetic resonance (EchoMRI, Echo Medical Systems, Houston).

Blood serum

Blood serum was obtained by incubation of blood samples at room temperature for 30 min and subsequent centrifugation for 1 hr at 3,000 rpm, 4°C. The serum (upper phase) was transferred to a new tube and stored at -80°C.

Glucose tolerance test

In a glucose tolerance test, glucose is injected in the peritoneum of fasted mice and blood samples are taken to determine how quickly the sugar can be cleared from the blood. Improved insulin signaling results in lower glucose levels as the sugar load induces a better clearance from the blood stream. Mice were fasted for 16 hrs prior to the experiment. The animals were transferred into fresh cages equipped with fresh water but no food. The following morning, the body weight and the initial blood glucose levels were determined by nicking the tail with a razor blade. Blood glucose was measured using a glucometer strip. 10 µl/g body weight of a 20% glucose solution were then injected intraperitoneally. Blood glucose was measured before injection and 20, 60, and 120 min after injection.

Insulin tolerance test

An insulin tolerance test (ITT) is a procedure in which insulin is injected into a mouse to assess if it can still induce its full function. If mice are insulin resistant, blood glucose levels are elevated over time. For the insulin tolerance test a stock solution of 0.75 U insulin/ml was prepared using 0.9% sodium chloride. The body weight of all animals was determined and the blood glucose levels were measured by nicking the tail with a razor blade. The blood drop was put onto a glucometer strip and measured. 1 U insulin/kg body weight was injected intraperitoneally. The blood glucose levels were monitored before injection and 20, 60, and 120 min after injection.

4.4 Biochemistry

Preparation of protein extracts

Cell lysis using 2 x SDS sample buffer

3T3-L1 and primary preadipocytes or adipocytes were washed once with PBS and lysed by the addition of an appropriate volume of 2 x SDS sample buffer. Samples were boiled for 10 min at 95°C and stored at -20°C until further use.

Cell lysis using Tx lysis buffer

3T3-L1 and primary preadipocytes or adipocytes were washed once with PBS and lysed by the addition of an appropriate volume of Tx lysis buffer containing protease and phosphatase inhibitors. Still on the plates, cells were frozen to -80°C for at least one hour, thawed, and transferred to a tube on ice. Cell debris was removed by centrifugation (10 min, 13,000 rpm, 4°C) and supernatants were

transferred to new tubes. Protein concentration was determined using the BCA kit (Pierce) and samples were diluted in 5x SDS sample buffer and boiled for 10 min at 95°C.

Protein extracts from tissue samples

Protein extracts from tissue samples were prepared using the Tissue Lyzer. Frozen tissue pieces or powder were transferred to 2 ml safe lock tubes containing ice-cold protein lysis buffer A containing protease and phosphatase inhibitors and a pre-cooled steel bead. The samples were immediately homogenized using the Tissue Lyser for 2 min at 30 Hz. The extracts were incubated on a rotating wheel for 1 hour and then transferred to fresh tubes (if using adipose tissues, the fat remains in the old tube). Then, extracts were supplemented with high salt supplement buffer and incubated for an additional hour on the wheel at 4°C. The protein concentration was determined using the BCA kit (Pierce) and samples were diluted in 5x SDS sample buffer and boiled for 10 min at 95°C.

Isolation of Nuclear Extracts

For preparation of nuclear extracts from 3T3-L1 adipocytes, cells on 10 cm plates were first washed in PBS and then lysed in 500 µl hypotonic buffer including protease and phosphatase inhibitors / plate. After 15 min incubation on ice, cells were homogenized by 20 strokes in a dounce homogenizer. Samples were transferred to 1.5 ml tubes and centrifuged at 4°C, 10 min, 4,000 rpm. The supernatant (=cytoplasmic extract) was removed, centrifuged 10 min at 4°C, 13,000 rpm, and boiled with SDS sample buffer. The pellet (=nuclei containing fraction) was resuspended in 150 µl high salt buffer. Nuclei were extracted by incubation for 30 min at 4°C on a rotating wheel. Samples were centrifuged 30 min at 4°C and 13,000 rpm and the supernatant (=nuclear extracts) was mixed with SDS sample buffer and boiled for use in immunoblot. For IPs, nuclear extracts were diluted 1:10 in dilution buffer and used as input for the immunoprecipitation.

Determination of Protein Concentration

Protein concentrations were determined using the BCA kit (Pierce) following the manufacturer's instructions. If SDS concentration of the samples was higher than 0.1 %, protein concentration had to be determined using the 2D-Quant kit (Amersham Biosciences) following the manufacturer's instructions. All measurements were performed in duplicates within the linear range of the BSA standard curves (0.1-2 mg/ml).

SDS Polyacrylamide Gel Electrophoresis (SDS-PAGE) and Immunoblotting

Protein samples in SDS sample buffer were loaded onto 6-12 % SDS-polyacrylamide gels and blotted onto nitrocellulose membranes using a wet blot system. Blotting was performed at 80 V for 70 minutes or 30 V overnight in transfer buffer. Membranes were subsequently blocked by incubation in 5% milk or 5% BSA dissolved in PBS-T for 1 hour. Specific primary antibodies diluted in milk or BSA, according to the manufacturer's recommendations, were incubated with the membranes overnight at 4°C. The membranes were washed with PBS-T the next day and incubated with the secondary antibody conjugated to horse radish peroxidase (HRP) at a dilution of 1:5,000 for 1 hour. To detect specific bands the enhanced chemiluminescence system (ECL) Western Blotting Detection Reagent was applied. The chemiluminescent signal produced by the blots was detected with the ChemiDoc detector (BioRad). Exposure times differed based on the quality of specific antibodies and protein concentrations.

Endogenous IP

3T3-L1 cells were lysed in Co-IP lysis buffer containing protease and phosphatase inhibitors and centrifuged at 13,000 rpm, 4°C, 15 min. The supernatant was incubated with protein A/G agarose beads and 4 µg of the respective antibody over night at 4°C on a rotating wheel. Beads were washed in Co-IP buffer and proteins were eluted by the addition of 50 µl 2 x SDS sample buffer. Protein samples were boiled for 10 min at 95°C prior to immunoblotting.

Flag-IP

3T3-L1 cells on 10 cm plates were transduced with Flag-TBLR1 or an empty Flag plasmid. Subsequently, cells were lysed with Co-IP lysis buffer containing protease and phosphatase inhibitors and centrifuged at 13,000 rpm, 4°C, 15 min. The supernatant was incubated with anti-FLAG M2 Agarose beads for 2 hours at 4°C and washed vigorously to remove unspecific binding. Precipitated proteins were eluted using excess Flag peptide. The immunoprecipitates were subsequently analyzed by immunoblotting as described.

Chromatin-IP

3T3-L1 adipocytes on 10 cm plates were transduced with Flag-TBLR1 or an empty Flag plasmid and incubated for 3 days. For ChIP, cells were washed once in 1 x PBS, then 4.5 ml PBS were added to each plate and 37% formaldehyde was added to a final concentration of 1% (135 µl). Cells were fixed on a shaker for 15 min and the reaction was stopped by adding 663 µl of 1 M glycine. After 5 min incubation, supernatant was removed and cells were harvested in ice-cold 1 x PBS. Cells were washed twice in cold PBS and then lysed in 1.5 ml/plate simple tissue fractionation buffer with 20 strokes of a dounce homogenizer. Lysates were centrifuged at 8,000 g for 10 min at 4°C, supernatants were discarded and the pelleted nuclei were re-suspended in 500 µl ChIP lysis buffer using a micropestle. Following 30 min incubation at 4°C on a rotating wheel, samples were aliquoted in 250 µl aliquots and sonicated in a BioRuptor (Diagenode) with 12 cycles 30 sec on, 45 sec off and a maximum of two tubes at a time. Samples were centrifuged at 3,000 g, 4°C, 10 min and supernatants were pooled. Protein concentrations were measured of 1:10 dilutions using the BCA kit (Pierce). 500 µg protein containing extracts were diluted 1:10 in ChIP dilution buffer and pre-cleared with 50 µl salmon-sperm agarose beads for 30 min on a rotating wheel. Beads were removed by centrifugation and the pre-cleared input was added to anti-FLAG M2 Agarose beads or salmon sperm agarose beads and 4 µg of the respective antibodies. IP was performed over night at 4°C on a rotating wheel. Beads were then washed vigorously (1 x wash buffer A, 1 x wash buffer B, 1 x wash buffer C, 1 x wash buffer A) and protein complexes were eluted from the beads by adding 300 µl elution buffer. Elution took place at 30°C and 750 rpm and was repeated using 200 µl elution buffer, so the final volume was 500 µl. Reversal of the crosslinks was achieved by incubating the samples for 2 hrs at 65°C, 750 rpm. Then, 100 µg Proteinase K were added followed by an overnight incubation at 56°C. DNA was extracted by phenol/chloroform extraction. 100 µg protein inputs were used as controls. DNA was used for SYBR-PCR or ChIP-Sequencing.

Isolation of Hepatic Triglycerides

Lipids were extracted from frozen liver tissue using chloroform/methanol (2:1 v/v). About 100 mg (the exact weight was noted) of frozen, pulverized liver were transferred into a 2 ml tube containing 1.5 ml chloroform/methanol and a steel bead. The tissue was homogenized using a tissue lyzer for 1

min at a frequency of 30 Hz. For the lipid extraction, samples were incubated on a rotating wheel at room temperature for 20 min. Reactions were centrifuged at 4,000 rpm for 10 min and supernatants were transferred to fresh tubes. The organic layer was mixed with 0.9% sodium chloride and the aqueous solution was carefully discarded. 50 µl of the organic layer were transferred to a fresh tube and 10 µl of triton-X 100/chloroform (1:1 v/v) were added. The reagents were mixed and the solvent was evaporated. The residue containing the hydrophobic contents of the liver was resuspended in 50 µl water and stored at -20°C until further use.

Determination of Free Fatty Acid Levels

Free Fatty Acids were determined in serum samples or cell supernatants using a colorimetric assay from WAKO (NEFA kit) following the manufacturer's instructions. 4 µl of serum samples or 20 µl of cell supernatants were measured in duplicates. A standard curve was determined using a dilution series of oleic acid. OD-values were determined at 540 nm.

Determination of Glycerol Levels

Glycerol content of serum or cell supernatants was measured using a calorimetric assay. The Free Glycerol component of the serum TG determination kit from Sigma was used for this assay. 4 µl of serum or 20 µl of supernatants were transferred to a 96well plate, 100 µl Free Glycerol Reagent were added and glycerol levels were measured at 540 nm against a glycerol standard.

Determination of Triglyceride Levels

TG levels were determined by separating TGs into one glycerol and three fatty acid molecules and measuring the glycerol using a colorimetric assay. The serum TG determination kit from Sigma was used for this assay. 4 µl of isolated hepatic TG, 4 µl of serum or 20 µl of cell supernatants were transferred to a 96well plate. In order to determine a blank value, 100 µl Free Glycerol Reagent were added to each well and the plate was incubated at 37°C for 5 min. Free glycerol levels were measured at 540 nm. In a second reaction (assay), 100 µl TG Reagent were added. This mixture contains the enzyme lipase, which catalyses the release of fatty acids from TGs. Plates were incubated at 37°C for 5 min and measured at 540 nm. TG content (TG-bound glycerol) was determined by subtracting the free glycerol (blank) from the second measurement of total glycerol (assay).

Determination of Cholesterol Levels

Liver or serum cholesterol concentrations were determined using a total cholesterol determination kit (Randox Laboratories) following the manufacturer's instructions. 4 µl of each sample were mixed with 100µl assay reagent and incubated at 37°C for 5 min. The optical density was measured at 492 nm and the sample concentration was determined using a standard curve resulting from a serial dilution of cholesterol (200 mg/dl; provided with the kit).

Determination of Blood Glucose Levels

Blood glucose levels were determined using a drop of blood obtained from the tail vein and an automatic glucose monitor (One Touch, Lifescan).

Insulin measurement

Insulin levels were determined using an ELISA kit (Mercodia). Plates containing the insulin antibody were provided and were activated using a buffer contained in the kit. 5 µl of each sample or standard (provided in the kit) were added to each well. Plates were then incubated at 4°C for 2 hours. Plates were washed five times in the provided buffer and 100 µl of anti-insulin conjugate were added to each well. Reactions were incubated at room temperature for a further 30 min and then washed several times. 100 µl of enzyme substrate solution were added to each well and the plates were incubated at room temperature for 40 min. Reactions were stopped by adding 100 µl of stop solution to each well and measuring the absorbance at 450 nm. Insulin concentrations were determined using a standard curve resulting from a serial dilution of insulin.

Serum ALT measurement

Serum levels of Alanine Aminotransferase (ALT) were determined by a calorimetric assay in order to estimate liver damage. Serum ALT levels were determined using the Infinity ALT Liquid Stable Reagent (Thermo Electron, Melbourne) following the manufacturer's instructions, measuring absorbance at 340 nm.

Serum adipocytokine measurement

Serum levels of adipocytokines were determined in duplicates from 10 µl mouse serum using the Magpix Luminex machine and the mouse metablic hormone magnetic bead multiplex assay kit (Millipore) following the manufaturer's instructions.

4.5 Human subjects

For the fasting study, 23 obese subjects underwent a weight reduction program (OPTIFAST®52, Rudofsky, G., 2011) for 52 weeks (BMI = 42.9 ±1.6 kg/ m² before, 35.2 ±1.5 kg/ m² after) and WAT TBLR1 mRNA expression was measured before and after the weight reduction. This study has been approved by the ethics committee at the Heidelberg University, and all patients gave written informed consent. For the obesity study, TBLR1 mRNA expression in subcutaneous and visceral WAT of 21 morbidly obese (BMI > 35 kg/m²) and 20 age- matched non-obese (BMI < 30 kg/m²) subjects was measured. Expression levels were correlated to BMI, serum parameters or gene expression using Pearson correlation. This study was conducted by M. Zeyda, Medical University of Vienna (unpublished data) and has been approved by the ethics committee of the Medical University of Vienna and the General Hospital Vienna, and all patients gave written informed consent.

4.6 Statistical Analysis

Statistical analyses were performed using a 1- or 2-way analysis of variance (ANOVA) with Bonferroni-adjusted post-tests, or t-test in one-factorial designs, respectively. Correlation was determined using Pearson's correlation coefficient. $p < 0.05$ was considered statistically significant. $*p < 0.05$, $**p < 0.01$, $***p < 0.001$.

5 MATERIAL

5.1 Solutions and Buffers

All buffers were diluted in H_2O, unless otherwise stated.

10x MOPS	200 mM MOPS 50 mM NaAc 10 mM EDTA pH 7	**10x PBS**	1.4 M NaCl 27 mM KCl 100 mM Na_2HPO_4 8 mM KH_2PO_4 pH 6.8
2x BBS	280 mM NaCl 50 mM BES 1.5 mM Na_2HPO_4 pH 6.95	**2x SDS sample buffer**	120 mM Tris /HCl pH 6.8 4% SDS 20% glycerol 200 mM DTT 0.01% bromphenol blue
5x SDS sample buffer	250 mM Tris/HCl pH 6.8 0.5 M DTT 10 % SDS 50 % glycerol 0.01% bromphenol blue	**ABP stock solution**	50 mg/ml L-Ascorbate 1 mM d-Biotin 17 mM Pantothenic acid
Block buffer	1x PBS 0.1% Tween 20 5% milk powder	**ChIP Dilution buffer**	As ChIP Wash buffer A
ChIP Lysis buffer	50 mM Tris pH 6.8 150 mM Nacl 1 mM EDTA 1 % SDS 1 x PIC Adjust pH to 7.2	**ChIP Wash buffer A**	50 mM Tris pH 6.8 150 mM NaCl 1 mM EDTA 1 % NP40
ChIP Wash buffer B	50 mM Tris pH 6.8 500 mM NaCl 1 mM EDTA 1 % NP40 0.1 % SDS	**ChIP Wash buffer C**	50 mM Tris pH 6.8 250 mM LiCl 1 % NP40
ChIP Elution buffer	1 % SDS 100 mM $NaHCO_3$	**CoIP Lysis buffer**	20 mM HEPES/KOH pH 7.4 125 mM NaCl 0.5 mM EDTA 0.1% NP-40 10% Glycerol
Coomassie stain	4 parts Coomassie Colloidal Blue 1 part Methanol	**Destain for Coomassie stained gels**	25% Isopropanol 10% Acetic acid
Gly-Gly buffer	25 mM Gly-Gly pH 7.8	**High Salt Buffer**	20 mM HEPES/KOH pH

	15 mM MgSO4 4 mM EGTA		7.9 1.5 mM $MgCl_2$ 380 mM KCL 25% glycerol 0.2 mM EDTA 1 mM DTT 1x PIC
Hypotonic Buffer	10 mM HEPES/KOH pH 7.9 10 mM KCl 1.5 mM $MgCl_2$ 0.2 mM EDTA 0.5 mM DTT 1x PIC	**Krebs-Ringer Buffer**	115 mM NaCl 5.9 mM KCl 1.2 mM $MgCl_2$ 1.2 mM NaH_2PO_4 1.2 mM Na_2SO_4 2.5 mM $CaCl_2$ 25 mM $NaHCO_3$ Adjust pH to 7.4
LB medium	10 g/l Trypton 5 g/l Yeast extract 10 g/l NaCl pH 7.0	**Oil Red O stock solution**	0.7 g Oil Red O 200 ml Isopropanol Stirred overnight, sterile filtrated
Luciferase Harvest Buffer	100% Gly-Gly buffer; 1% Triton X-100 1 mM DTT	**Luciferase Assay Buffer**	20 mM K3PO4 pH 7.8 80% (v/v) Gly-Gly buffer 1.6 mM DTT 2mM ATP
Luciferase Luciferin Buffer	1 mM Luciferin 10 mM DTT in Gly-Gly buffer	**Oil Red O working solution**	6 parts Oil Red O stock solution 4 parts H_2O
ONPG buffer	0.1 M NaP pH 7.5 1 mM $MgCl_2$ 10 mM KCl 1 mg/ml ONPG 100 mM ß-mercaptoethanol (added freshly)	**Orange G loading dye (6x)**	10 mM EDTA 70% Glycerol A pinch Orange G
PBS-Glycerol	1x PBS 10% Glycerol pH 7.2, sterile	**PBS-T**	1x PBS with 0.1 % Tween-20
PBS-TOSH	30.8 mM NaCl 120.7 mM KCl 8.1 mM Na_2HPO_4 1.46 mM KH_2PO_4 10 mM $MgCl_2$ pH 7.2, sterile filtrated	**Protease Inhibitor (50x)**	50 mM PMSF 50 mM NaF 0.5 mg/ml Leupeptin 0.5 mg/ml Aprotinin 0.5 mg/ml Pepstatin A Dissolved in ethanol
Proteinase K lysis buffer	10 mM Tris pH 8.0 100 mM NaCl 15 mM EDTA 1 % SDS	**Protein lysis buffer A**	50 mM Tris/HCl pH 6.8 1 mM EDTA 10 mM NaF 2 mM Na_3VO_4 1 mM DTT 1 x PIC

1 x PPI

RNA denaturing buffer	0.5 µl 1/10 Ethidium bromide 0.5 µl 10x MOPS 5 µl Formamide 1.75 µl Formaldehyde 1.7 µl 6x loading dye 0.55 µl RNase free H_2O	**SDS gel fixation buffer**	25% Isopropanol 10% Acetic acid
SDS running buffer (10x)	0.25 M Tris 1.92 M Glycin 1% SDS	**Simple tissue fractionation buffer**	50 mM Tris/HCl pH 7.2 1 mM EDTA 10 mM NaF 2 mM Na_3VO_4 1 x PIC
Supplement buffer	1.5 M NaCl 10 % NP-40	**TBE buffer (10x)**	100 mM Tris 1 mM EDTA 90 mM Boric acid pH 8.0
TE buffer (10x)	1 mM EDTA 10 mM Tris HCl pH 8.0	**TENS buffer**	1x TE pH 8.0 0.1 M NaOH 0.5% SDS
Transfer buffer	25 mM Tris 192 mM Glycin 20% Methanol 0.01% SDS	**Tx Lysis buffer**	150 mM NaCl 0.05 % Triton X 100 10 mM Tris/HCl pH 8.0 1 x PIC 1 x PPI
Western Blot membrane stripping buffer	62.5 mM Tris/HCl pH 6.8 2% SDS 100 mM β-Mercaptoethanol		

5.2 Oligonucleotides

All oligonucleotides possessed a G/C content between 40% and 60% and were approximately 20-30 bp in length.

Restriction sites for specific enzymes were added to the cloning primers in 5'→3' orientation, allowing directed insertion into a specific target vector. Six thymidine residues were added to the 5' ends of the restriction sites in order to facilitate cleavage. The primers were designed to hybridize at temperatures of approximately 60°C.

Oligonucleotide name	Sequence 5'→ 3'
TBL1 shRNA	GCGAGGATATGGAACCTTAAT
TBLR1 shRNA	GGATGTCACGTCTCTAGATTG
Control shRNA	GATCTGATCGACACTGTAATG
TBLR1 qPCR for	AATGGTGCCCTGGTTCCA
TBLR1 qPCR rev	AGGTGCCATCCTCATTTATGCTA
TBLR1 qPCR probe	CCGCTGCACTCATCTCTATCATCCAGAAA
TBL1 qPCR for	ACGAGGTGAACTTTCTGGTATATCG
TBL1 qPCR rev	GGACTGGCTAATGTGACTTTCGA
TBL1 probe	ATCAGGTTTTTCCCACTCTGCCTTCACG

TBLR1 Exon5 qPCR for	TGCTGCCGCCACTAACCAGC
TBLR1 Exon5 qPCR rev	TGTGCTCCATTCTCCTCCCC
Flag-TBLR1 for	TTTTTGGTACCATGGATTACAAGGATGACGACGATAAG
Flag-TBLR1 rev	TTTTTTCTCGAGCTATTTCCGAAGGTCTAAGA
Flag-TBL1 for	TTTTTGGTACCATGGATTACAAGGATGACGACGATAAG
Flag-TBL1 rev	TTTTTTCTCGAGTTACTTTCGGAGATCTAAAACACAGACG
Genotyping TBLXR1-CRE 3552_31	CCAGTTCCCTTTTGGTATCC
Genotyping TBLXR1-CRE 3552_34	CTCACCATCAGAGCCTTGC
Genotyping TBLXR1 1260_1	GAGACTCTGGCTACTCATCC
Genotyping TBLXR1 1260_2	CCTTCAGCAAGAGCTGGGGAC
TBLR Southern Blot Probe 2 for	TCATTCTGCGTTTACCTTTGG
TBLR Southern Blot Probe 2 rev	CACACGCAGAGGAATAGTCTACA
ATGL promoter for	GACGGCTAGCACAGCAGAGGAGAAGAAAGA
ATGL promoter rev	GCGAAAGCTTCGGCGGAGGCGGAGACGCTGTGC
HSL promoter for	CCCCACGCGTGTCATTATGATCAGCCCA
HSL promoter rev	TTTTAGATCTCAAGCTGGCACAGCAGGTCTG

5.3 Antibodies

Primary Antibodies	Final Dilution	Isotype	Distributor, #
Abhd5 (CGI-58)	1:500	Mouse	Santa Cruz, # sc-100468
Actin	1:1000	Mouse	Santa Cruz, # A5441
AKT	1:1000	Rabbit	Cell Signalling, # 9272
acetyl-Histone H4	Only for IP	Rabbit	Millipore
ATGL	1:1000	Rabbit	Cell Signalling, # 4126
Beta 2 adrenergic receptor	1:200	Rabbit	Santa Cruz, # sc-570
Beta 3 adrenergic receptor	1:200	Rabbit	Santa Cruz, #sc-50436
CREB (128-262)	1:1000	Rabbit	Salk PBL 244
CREB phosphorylated (Ser133)	1:1000	Rabbit	Salk Montminy
FLAG M2	1:1000	Mouse	Sigma, #A 8592
GFP	Only for IP	Rabbit	Invitrogen, # A11122
GPS2	1:500	Mouse	Abcam, # ab53406
HDAC3	1:200	Mouse	Santa Cruz, # sc-17795
HSL	1:1000	Chicken	Chemicon, # AB3525
NCoR (C-20)	1:200	Goat	Santa Cruz, # sc-1609
p44/42 MAP Kinase (137F5)	1:500	Rabbit	Cell Signalling, # 4695
Perilipin	1:1000	Rabbit	Abcam, # ab3526
phospho-Akt (Ser473)	1:1000	Rabbit	Cell Signalling, # 9271
phospho-CREB (Ser133) clone 634-2	1:1000	Mouse	Upstate, # 05-807
phospho-HSL (Ser660)	1:1000	Rabbit	Cell Signalling, # 4126
phospho-HSL (Ser565)	1:1000	Rabbit	Cell Signalling
phospho-p44/42 MAP Kinase (Thr202/Tyr204)	1:1000	Rabbit	Cell Signalling, # 9101
phospho-PKA substrate (RRXS/T)	1:1000	Rabbit	Cell signalling, #9624
PKA regulatory SU	1:500	Rabbit	Abcam, #ab38222
PKA catalytic SU	1:500	Rabbit	Abcam, #ab71764
PPARγ	1:1000	Rabbit	Abcam, #ab27649
PPARγ (phospho S112)	1:1000	Rabbit	Abcam, #ab60953
RXR (C-20)	1:200	Rabbit	Santa Cruz, #sc-831

TBL1	1:1000	Rabbit	Abcam, #ab24548
TBLR1	1:1000	Rabbit	Novus, #NB600-270
TBLR1	1:1000	Mouse	Abnova
VCP	1:10000	Mouse	Abcam, #ab11433

Secondary Antibodies

Anti-mouse IgG-HRP	1:5000	Goat	BioRad, Munich
Anti-rabbit IgG-HRP	1:3000-1:5000	Goat	BioRad, Munich
Anti-chicken IgG-HRP	1:5000	Rabbit	Chemicon, #AP162P
Anti-goat IgG-HRP	1:5000	Donkey	Sigma, #sc-2020

5.4 Kits

Kit	Distributor
20x MOPS running buffer	Invitrogen, Karlsruhe
BLOCK-iT Adenoviral RNAi Expression System	Invitrogen, Karlsruhe
Cholesterol determination Kit	Randox, Crumlin, UK
Cyclic AMP EIA Kit	Cayman, Talinn
Enhanced Chemiluminescence (ECL) Kit	Amersham Biosciences, Freiburg
First Strand cDNA Synthesis Kit	Fermentas, St. Leon-Rot
Infinity ALT kit	Thermo Electron, Melbourne
NEFA – C Determination Kit	Wako, Neuss
NEON 10 µl transfection Kit	Invitrogen, Karlsruhe
Phusion Polymerase Kit	Finnzymes, Vantaa
PureLink HiPure Plasmid Filter Midiprep Kit	Invitrogen, Karlsruhe
PureLink HiPure Plasmid FP Maxiprep Kit	Invitrogen, Karlsruhe
Qiaprep Plasmid Miniprep Kit	Qiagen, Hilden
Qiaquick Gel Extraction Kit	Qiagen, Hilden
Qiaquick PCR Purification Kit	Qiagen, Hilden
Triglycerides Determination Kit	Sigma-Aldich Chemicals GmbH, Steinheim
Triglycerides Liquicolour	Human GmbH Wiesbaden

5.5 Software

Software	Distributor
BLAST	http://www.ncbi.nlm.nih.gov
Endnote	Thomson, Carlsbad, USA
Geneious	Auckland, New Zealand
GraphPad	GraphPad Software Inc., La Jolla, USA
Illustrator	Adobe, San Jose, USA
Microsoft Office	Microsoft, Unterschleißheim
MultAlin	bioinfo.genotoul.fr/multalin/multalin. html
Photoshop	Adobe, San Jose, USA
Pubmed	http://www.pubmedcentral.nih.gov
Quantity One	Bio-Rad, Munich
StepOne Plus System Software	Applied Biosystems, Darmstadt
Vector NTI Advance™ *Software*	Invitrogen, Karlsruhe

5.6 Consumables

Consumable	Distributor
6 well tissue culture dishes	Falcon, Gräfeling-Lochham
96 well MicroAmp plates	Applied Biosystems, Darmstadt
Cell scrapers (*Costar*)	Corning Inc., NY, USA
Centrifuge tubes (35 ml)	Beckmann, Munich
Cover slips	Carl Roth GmbH, Karlsruhe
Dialysis tubing	Carl Roth GmbH, Karlsruhe
Disposable scalpels	Feather, Cuome, JP
DNase / RNase free water	Invitrogen, Karlsruhe
Electroporation cuvettes	Steinbrenner, Wiesenbach
Filters (0.22 µm)	Millipore, Eschborn
Filters (0.45 µm)	Millipore, Eschborn
Gel staining boxes (Mini)	Carl Roth GmbH, Karlsruhe
Gloves (*Gentle Skin*)	Meditrade, Kiefersfelden
Gloves (*Safe Skin Purple Nitrile*)	Kimberly Clark, BE
Gradient gels 4-12% (NuPAGE)	Invitrogen, Karlsruhe
Hyperfilm ECL	Amersham, Freiburg
Immobilized streptavidin beads (UltraLink)	Pierce Biotech., Rockford, USA
Micro test tubes (1.5 ml, 2 ml)	Steinbrenner, Wiesenbach
Mouth protection	Meditrade, Kiefersfelden
Nitrocellulose membrane	Schleicher and Schüll, Dassel
Parafilm	Pechinery Inc., Wisconsin, USA
Pasteur pipettes	Brand, Wertheim
PCR tubes (200 µl)	Eppendorf, Hamburg
Petri dishes	Greiner, Kremsmünster, AU
Pipette tips (0.1 – 1000 µl)	Starlab, Helsinki, FI
Pipette tips (0.1 – 1000 µl) (Tip One Filter Tips)	Starlab, Helsinki, FI
Pipette tips (Electrophoresis / Protein)	BioRad, Munich
Rabbit IgG-agarose	Sigma, Munich
Safelock micro test tubes (1.5 ml and 2 ml)	Eppendorf, Hamburg
Saran cling film	Dow Chem. Co., Schwalbenbach
Serological pipettes (5 ml, 10 ml, 25 ml, 50 ml)	BD Biosciences, San Jose, USA
Syringes (10 ml Luer Lock)	Terumo, Leuven
Test tubes (15 ml and 50 ml)	Falcon, Gräfeling-Lochham
Tissue culture dishes (10 cm and 15 cm)	Falcon, Gräfeling-Lochham
Whatman paper	Whatman Int., UK

5.7 Chemicals and Reagents

Chemical	Distributor
(+)-Sodium L-ascorbate	Sigma, Munich
3-(N-morpholino)propanesulfonic acid (MOPS)	Carl Roth GmbH, Karlsruhe
Acetic acid (99%)	Sigma, Munich
Adenosine triphosphate (ATP)	Sigma, Munich
Agarose	Sigma, Munich
Antibiotics	Sigma, Munich
Aprotinin	Sigma, Munich
Boric acid	Sigma, Munich
Bovine serum albumin (BSA)	Sigma, Munich
Bromophenol blue	Sigma, Munich

Chloroform	DKFZ
Collagenase Type ll	Sigma, Munich
CL316243	Tocris Bioscience, Bristol
d-Biotin	Sigma, Munich
D-[^{14}C(U)]-Glucose	Perkin Elmer, Waltham
dCTP (alpha-32-P) 250microCi	Perkin Elmer, Waltham
Desoxynucleotides (dATP, dCTP, dGTP, dTTP)	Roche, Mannheim
Dexamethasone	Sigma, Munich
DMSO (Dimethyl sulfoxide)	Sigma, Munich
DOTAP Liposomal Transfection Reagent	Roche, Mannheim
D-Pantothenic acid hemicalcium salt	Sigma, Munich
DTT (Dithiothreitol)	Sigma, Munich
Dulbecco's modified Eagle's medium (DMEM)	Invitrogen, Karlsruhe
EDTA (Ethylenediaminetetraacetic acid)	Sigma, Munich
Ethanol (99%)	DKFZ
Ethidium bromide	Carl Roth GmbH, Karlsruhe
Fetal calf serum (FCS)	Invitrogen, Karlsruhe
Formaldehyde	DKFZ
Forskolin	Sigma, Munich
Gene Ruler 1kb DNA Ladder	Fermentas, St. Leon Rot
Glycerol	Baker, Deventer, NL
Hydrochloric acid (HCl) 37%	Acros Organics, New Jersey, USA
Hyperfilm ECL Western Blotting Detection Reagents	Amersham, Freiburg
IBMX	Sigma, Munich
Insulin human (recombinant yeast)	Sigma, Munich
Isopropanol	Sigma, Munich
Isoproterenol Hydrochloride	Calbiochem, Darmstadt
Lipofectamine2000 Reagent	Invitrogen, Karlsruhe
Lipopolysaccharides *E.coli*	Sigma, Munich
Loading dye solution (6x)	Fermentas, St. Leon Rot
Norepinephrine	Sigma, Munich
Magnesium chloride (MgCl$_2$)	Merck, Darmstadt
Magnesium sulfate (MgSO$_4$)	Sigma, Munich
Oil Red O	Sigma, Munich
optiMEM	Invitrogen, Karlsruhe
Orange G	Sigma, Munich
Page Ruler Prestained Protein Ladder	Fermentas, St. Leon Rot
Penicillin / Streptomycin (P/S)	Invitrogen, Karlsruhe
Phosphatase Inhibitor Cocktail	Sigma, Munich
Platinum qPCR SuperMix	Invitrogen, Karlsruhe
Potassium chloride (KCl)	Sigma, Munich
Poly-L-lysin	Sigma, Munich
Procaterol	Biozol, Heidelberg
Qiazol Lysis Reagent	Qiagen, Hilden
RiboLock Ribonuclease Inhibitor	Fermentas, St. Leon Rot
ROX Reference Dye	Invitrogen, Karlsruhe
Sodium chloride (NaCl)	Fluka, Munich
Sodium hydroxide (NaOH)	Sigma, Munich
Sodium orthovandate	Sigma, Munich
Trichloroacetic acid (TCA)	Sigma, Munich
Tripotassium phosphate (K$_3$PO$_4$)	Merck, Darmstadt
Tris base	Sigma, Munich

Triton X-100	Sigma, Munich
Trypsin-EDTA solution	Invitrogen, Karlsruhe
Tween-20	Sigma, Munich
β-Mercaptoethanol (98%)	Sigma, Munich

All other routinely used chemicals were purchased from Roth, Karlsruhe.

5.8 Instruments

Instrument	Distributor
Analytical scales	Satorius, Göttingen
Bacterial shaker	Infors AG, Böttmingen, CH
Camera (*Power Shot G6*)	Canon, Krefeld
Cell counter	Neolab, Heidelberg
Centrifuge (*2K15*)	Sigma, Munich
Centrifuge (*Biofuge fresco*)	Heraeus, Hanau
Centrifuge (*Biofuge pico*)	Heraeus, Hanau
Centrifuge (*Function Line*)	Heraeus, Hanau
Centrifuge (*Micro 22R*)	Hettich GmbH & Co, Tuttlingen
Centrifuge (*Super T21*)	Heraeus Sorvall, Langenselbold
ChemiDoc	BioRad, Munich
CO_2-incubator	Sanyo, Munich
CO_2-incubator (*Forma Scientific*)	Labotect, Göttingen
Electrophoresis chamber	Steinbrenner, Wiesenbach
Electrophoresis power supply (*Power Pack Basic*)	BioRad, Munich
Electrophoresis power supply (*Power Pack HC*)	BioRad, Munich
Electroporator (Gene PulserII)	BioRad, Munich
Film cassette	Amersham, Freiburg
Film developer	Amersham, Freiburg
Freezer, -20°C	Liebherr, Biberach
Freezer, -80°C (*Hera Freeze*)	Heraeus, Heilbronn
Fridge, 4°C	Liebherr, Biberach
Gas stove (GASI)	Schütt, Göttingen
Gel imager	Intas, Göttingen
Heat block	VWR, Darmstadt
Heat block (*Thermostat Plus*)	Eppendorf, Hamburg
Horizontal shaker (*Duomax 1030*)	Heidolph, Kehlheim
Hotplate / stirrer	VWR, Darmstadt
Incubator (*Function Line*)	Heraeus, Hanau
Luminex Magpix	Luminex, Austin, USA
Microscope (*Axiovert 40 CFL*)	Carl Zeiss, Jena
Microwave	Bosch, Stuttgart
Multistep pipette	Eppendorf, Hamburg
NEON transfection device	Invitrogen, Karlsruhe
Neubauer counting chamber	Carl Roth GmbH, Karlsruhe
Nitrogen tank	Thermo Electron corp., Erlangen
pH-meter	VWR, Darmstadt
Photometer (*NanoDrop ND-1000*)	Peqlab Biotechnology, Erlangen
Pipettes (2 µl, 10 µl, 20 µl, 100 µl, 200 µl, 1000 µl)	Gilson, Middleton, USA
Pipettes (20 µl, 200 µl, 1000 µl)	Eppendorf, Hamburg
Real time PCR System StepOne Plus	Applied Biosystems, Darmstadt

Rotating wheel	Neolab, Heidelberg
Scale	Kern und Sohn GmbH, Balingen
Scale (*BL 1500 S*)	Satorius, Göttingen
Scanner	Epson, Meerbusch
SDS electrophoresis chambers	BioRad, Munich
Sonicator Bioruptor^{TM}	Diagenode, Liège, Belgium
Stand	Carl Roth GmbH, Karlsruhe
Sterile benches (Class II type A/B3)	Sterilgard, Sanford, USA
Tabletop centrifuges (*Mini Spin Plus*)	Eppendorf, Hamburg
Thermocycler (*PTC-200*)	Biozym, Oldendorf
Tissue Lyser	Qiagen, Hilden
Ultracentrifuge *XL 70*	Beckmann, Munich
Vacuum pump	Neolab, Heidelberg
Vortex mixer (*REAX 2000*)	Heidolph, Kehlheim
Water bath	Neolab, Heidelberg
Water bath (*WBS*)	Fried Electric, Haifa, IL
Western Blot Chamber	BioRad, Munich

6 APPENDIX

6.1 Glossary

AC	Adenylate cyclase
Adrb	Beta-adrenergic receptor
AKT	Protein kinase B (PKB)
ANOVA	Analysis of variance
AP-1	Activating protein 1
ATGL	Adipocyte triglyceride lipase
ATKO	Adipocyte specific TBLR1 knockout
AU	Arbitrary units
AUC	Area under curve
BAT	Brown adipose tissue
BMI	Body mass index
bp	Base pairs
BSA	Bovine serum albumin
BW	Body weight
C/EBP	CCAAT/enhancer binding protein
cAMP	Cyclic adenosine monophosphate
cDNA	Complementary DNA
CGI-58	Comparative gene identification 58
CM	Conditioned macrophage medium
CMV	Cytomegalovirus
Ctrl	Control
DBD	DNA binding domain
Dex	Dexamethasone
DNA	Desoxyribonucleic acid
DTT	Dithiothreitol
ER	Estrogen receptor
FA	Fatty acid
FABP	Fatty acid binding protein
Fasn	Fatty acid synthase
FATP	Fatty acid transport protein
FCS	Fetal calf serum
FDR	False discovery rate
FFA	Free fatty acid
FSK	Forskolin
GC	Gastrocnemius muscle
GC	Gastrocnemius muscle
GFP	Green fluorescent protein
GPS2	G-protein pathway suppressor 2
GTT	Glucose tolerance test
HDAC	Histone deacetlyate
HDL	High density lipoprotein
HEK	Human embryonic kidney
HFD	High fat diet
HOMA	Homeostatic model assessment
HSL	Hormone sensitive lipase
IBMX	3-isobutyl-1-methylxanthine
ifu	Infectious units
IL6	Interleukin 6

IP	Immunoprecipitation
IR	Insulin receptor
IRS2	Insulin receptor substrate
ISI	Insulin sensitivity index
Iso	Isoproterenol
LBD	Ligand binding domain
LFD	Low fat diet
LKB1	AMPK activator liver kinase B
LPL	Lipoprotein lipase
LPS	Lipopolysaccharide
MCP1	Monocyte chemoattractant protein
MGL	Monoacylglycerol lipase
MOI	Multiplicity of infection
mRNA	Messenger RNA
NAA	Non-essential amino acid
NAFLD	Non-alcoholic fatty liver disease
NCoR	Nuclear co-repressor
NE	Norepinephrine
NEFA	Non esterified fatty acids
NLSD	Neural lipid storage disease
NZO/NZB	New Zealand Obese/ Black
OE	Over expression
p-	Phospho-
P/S	Penicillin / Streptomycin
PBS	Phosphate buffered saline
PCR	Polymerase chain reaction
PDE3B	Phosphodiesterase 3 B
PEPCK	Phosphoenolpyruvate carboxykinase
PGC1	PPAR gamma co-activator 1
PIC	Protease inhibitor cocktail
PKA	Protein kinase A
PP	Protein phosphatase
PPAR	Peroxisome proliferator activated receptor
PPI	Phosphatase inhibitor cocktail
PPRE	PPAR response element
qPCR	Quantitative polymerase chain reaction
RAR	Retinoic acid receptor
RNA	Ribonucleic acid
RXR	Retinoic x receptor
SEM	Standard error of the means
shRNA	Short hairpin RNA
siRNA	Small interfering RNA
SMRT	Silencing mediator of retinoic acid and thyroid hormone receptor
SUMO	Small ubiquitin-like modifier
SVF	Stromal vascular fraction
TBL1	Transducin beta like 1, x-linked
TBLR1	Transducin beta like 1 related 1
TBP	TATA binding protein
TG	Triglyceride
TNFα	Tumor necrosis factor alpha
TR	Thyroid hormone receptor
TZD	Thiazolidinediones
UCP1	Uncoupling protein 1

VCP	Valosin containing protein
VLDL	Very low density lipoproteins
WAT	White adipose tissue
WHO	World Health Association
β-AR	Beta adrenergic receptor

6.2 Figures and Tables

Tables   page

6.3 References

Alberti, K.G. and Zimmet, P.Z. (1998). Definition, diagnosis and classification of diabetes mellitus and its complications. Part 1: diagnosis and classification of diabetes mellitus provisional report of a WHO consultation. Diabet Med 15(7):539-53.

Alberti, K.G. et al. (2006). Metabolic syndrome–a new world-wide definition. A Consensus Statement from the International Diabetes Federation. Diabet Med 23:469–480.

Anbalagan, M. et al. (2011). Post-translational modifications of nuclear receptors and human disease. Nucl Recept Signal 10:e001

Anghel, S.I. et al. (2007). Adipose tissue integrity as a prerequisite for systemic energy balance: a critical role for peroxisome proliferator-activated receptor gamma. J Biol Chem 282(41):29946-57.

Arner, P. (1999). Catecholamine-induced lipolysis in obesity. Int J Obes Relat Metab Disord 23 Suppl 1:10-3.

Arner, P. et al. (2011). Dynamics of human adipose lipid turnover in health and metabolic disease. Nature Sep 25;478(7367):110-3.

Asensio, C. et al. (2005). The lack of beta-adrenoceptors results in enhanced insulin sensitivity in mice exhibiting increased adiposity and glucose intolerance. Diabetes 54(12):3490-5.

Avram, M.M. et al. (2007). Subcutaneous fat in normal and diseased states 3. Adipogenesis: from stem cell to fat cell. J Am Acad Dermatol 56:472-492.

Aye, T.T. et al. (2009). Selectivity in enrichment of cAMP-dependent protein kinase regulatory subunits type I and type II and their interactors using modified cAMP affinity resins. Mol Cell Proteomics 8(5):1016-28.

Barrett, L.W. et al. (2012). Regulation of eukaryotic gene expression by the untranslated gene regions and other non-coding elements. Cell Mol Life Sci 27.

Bhathena, S.J. (2006). Relationship between fatty acids and the endocrine and neuroendocrine system. Nutr Neurosci 9(1-2):1-10.

Buettner R., Scholmerich J. and Bollheimer L.C. (2007). High-fat diets: modeling the metabolic disorders of human obesity in rodents. Obesity (Silver Spring) 15: 798-808.

Burris, T.P. et al. (2012). Targeting orphan nuclear receptors for treatment of metabolic diseases and autoimmunity. Chem Biol 27;19(1):51-9.

Chawla, A. et al. (2001). Nuclear Receptors and Lipid Physiology: Opening the X-Files. Science 30: 1866-1870.

Chen, J.D., Evans, R.M. (1995). A transcriptional co-repressor that interacts with nuclear hormone receptors. Nature 377(6548):454-7.

Choi, H.K. et al. (2011). Reversible SUMOylation of TBL1-TBLR1 regulates β-catenin-mediated Wnt signaling. Mol Cell 22;43(2):203-16.

Christodoulides C., Vidal-Puig, A. (2010). PPARs and adipocyte function. Mol Cell Endocrinol 29;318(1-2):61-8.

Collins, S. et al. (2010). Positive and negative control of Ucp1 gene transcription and the role of β-adrenergic signaling networks. Int J Obes (Lond) 34 Suppl 1:S28-33.

Cornier, M.A. et al. (2008) The metabolic syndrome. Endocr Rev 29(7):777-822.

Costa, B. et al. (2012). Delaying progression to type 2 diabetes among high-risk Spanish individuals is feasible in real-life primary healthcare settings using intensive lifestyle intervention. Diabetologia 55(5):1319-28.

Dahlman, I. and Arner, P. (2010). Genetics of adipose tissue biology. Prog Mol Biol Transl Sci 94:39-74.

Draper, B.W. et al. (2001). Inhibition of zebrafish fgf8 pre-mRNA splicing with morpholino oligos: A quantifiable method for gene knock down. Genesis 30 (3): 154–6.

Eguchi, J. et al. (2011). Transcriptional Control of Adipose Lipid Handling by IRF4. Cell Metab 13(3):249-59.

Feldstein, A.E. et al. (2004). Free fatty acids promote hepatic lipotoxicity by stimulating TNF-alpha expression via a lysosomal pathway. Hepatology 40(1):185-94.

Festuccia, W.T. et al. (2006). PPARgamma agonism increases rat adipose tissue lipolysis, expression of glyceride lipases, and the response of lipolysis to hormonal control. Diabetologia 49(10):2427-36.

Fulop, T. et al. (2006). The metabolic syndrome. Pathol Biol (Paris), 54, 375-386.

Gaidhu, M.P. et al. (2010). Dysregulation of lipolysis and lipid metabolism in visceral and subcutaneous adipocytes by high-fat diet: role of ATGL, HSL, and AMPK. Am J Physiol Cell Physiol 298(4):C961-71.

Galgani, J.E. (2008). Metabolic flexibility and insulin resistance. Am J Physiol Endocrinol Metab 295(5):E1009-17.

Garcia-Barrado, M.J. et al. (2011). Differential sensitivity to adrenergic stimulation underlies the sexual dimorphism in the development of diabetes caused by Irs-2 deficiency. Biochem Pharmacol 81(2):279-88.

Glass, C.K. and Ogawa, S. (2006). Combinatorial roles of nuclear receptors in inflammation and immunity. Nat Rev Immunology 6, 44-55.

Granneman, J.G. and Moore, H.P. (2008). Location, location: protein trafficking and lipolysis in adipocytes. Trends Endocrinol Metab 19: 3–9.

Grundy, S.M. (2008). Metabolic syndrome pandemic. Arterioscler Thromb Vasc Biol, 28, 629-636.

Guenther, M.G., et al. (2000). A core SMRT corepressor complex containing HDAC3 and TBL1, a WD40-repeat protein linked to deafness. Genes Dev 14, 1048-57.

Guilherme, A. et al. (2008). Adipocyte dysfunctions linking obesity to insulin resistance and type 2 diabetes. Nat Rev Mol Cell Biol 9(5):367-77.

Haemmerle, G. et al. (2002a). Hormone-sensitive lipase deficiency in mice changes the plasma lipid profile by affecting the tissue-specific expression pattern of lipoprotein lipase in adipose tissue and muscle. J Biol Chem 277(15):12946-52.

Haemmerle, G. et al. (2002b). Hormone-sensitive lipase deficiency in mice causes diglyceride accumulation in adipose tissue, muscle, and testis. J Biol Chem 277(7):4806-15.

Haemmerle, G. et al. (2006). Defective lipolysis and altered energy metabolism in mice lacking adipose triglyceride lipase. Science 312(5774):734-7.

He, W. et al. (2003). Adipose-specific peroxisome proliferator-activated receptor gamma knockout causes insulin resistance in fat and liver but not in muscle. Proc Natl Acad Sci U S A. 100(26):15712-7.

Heasman, J. et al. (2000). Beta-catenin signaling activity dissected in the early Xenopus embryo: a novel antisense approach. Developmental Biology 222 (1): 124–34.

Henry, S.L. et al. (2012). White adipocytes: more than just fat depots. Int J Biochem Cell Biol 44(3):435-40.

Hom, G.J. et al. (2001). Beta(3)-adrenoceptor agonist-induced increases in lipolysis, metabolic rate, facial flushing, and reflex tachycardia in anesthetized rhesus monkeys. J Pharmacol Exp Ther 297(1):299-307.

Hotamisligil, G.S. (2006). Inflammation and metabolic disorders. *Nature* 444(7121):860-867.

Iyer, A., Brown, L. (2010). Lipid mediators and inflammation in glucose intolerance and insulin resistance. Drug Discovery Today: Disease Mechanisms, Vol 7, Issues 3–4, p. e191-e197.

Jimenez, M. et al. (2002). Beta(1)/beta(2)/beta(3)-adrenoceptor knockout mice are obese and cold-sensitive but have normal lipolytic responses to fasting. FEBS Lett 530(1-3):37-40.

Jo, J. et al. (2009). Hypertrophy and/or Hyperplasia: Dynamics of Adipose Tissue Growth. PLoS Comput Biol. Mar;5(3).

Jürgens H.S., et al. (2006). Hyperphagia, lower body temperature, and reduced running wheel activity precede development of morbid obesity in New Zealand obese mice. Physiol Genomics. Apr 13;25(2):234-41.

Kirkland, J. et al. (1990). Age, anatomic site, and the replication and differentiation of adipocyte precursors. Am J Physiol 258, C206–C210.

Kobayashi K., Forte T. M., et al. (2000). The db/db mouse, a model for diabetic dyslipidemia: molecular characterization and effects of Western diet feeding. Metabolism 49(1): 22-31.

Koda M. et al. (2004). Adenovirus vector-mediated in vivo gene transfer of brain-derived neurotrophic factor (BDNF) promotes rubrospinal axonal regeneration and functional recovery after complete transection of the adult rat spinal cord. J Neurotrauma. 2004 Mar;21(3):329-37.

Kopelman, P.G. (2000). Obesity as a medical problem. Nature, 404, 635-643.

Kralisch, S. et al. (2005). Isoproterenol, TNFalpha, and insulin downregulate adipose triglyceride lipase in 3T3-L1 adipocytes. Mol Cell Endocrinol 240(1-2):43-9.

Kulozik, P. et al. (2011). Hepatic deficiency in transcriptional cofactor TBL1 promotes liver steatosis and hypertriglyceridemia. Cell Metab 6;13(4):389-400.

Kylin, E. (1923) Studien über das Hypertonie-Hyperglyka "mie-Hyperurika" miesyndrom. Zentralbl Inn Med 44: 105-127.

Lampidonis, A.D. et al. (2011). The resurgence of Hormone-Sensitive Lipase (HSL) in mammalian lipolysis. Gene 477(1-2):1-11.

Langin, D. (2006). Adipose tissue lipolysis as a metabolic pathway to define pharmacological strategies against obesity and the metabolic syndrome. Pharmacol Res 53(6):482-91.

Lass, A. et al. (2006). Adipose triglyceride lipase-mediated lipolysis of cellular fat stores is activated by CGI-58 and defective in Chanarin-Dorfman Syndrome. Cell Metab. 3: 309–319.

Lass. A. et al. (2011). Lipolysis - a highly regulated multi-enzyme complex mediates the catabolism of cellular fat stores. Prog Lipid Res 50(1):14-27.

Lefebvre, P. et al. (2006). Sorting out the roles of PPAR alpha in energy metabolism and vascular homeostasis. J Clin Invest 116(3):571-80.

Li, J. and Wang, C.Y. (2008). TBL1-TBLR1 and beta-catenin recruit each other to Wnt target-gene promoter for transcription activation and oncogenesis. Nat Cell Biol 10, 160-9.

Li, J. et al. (2000). Both corepressor proteins SMRT and N-CoR exist in large protein complexes containing HDAC3. EMBO J 19, 4342-50.

Li, P. et al. (2011). Adipocyte NCoR knockout decreases PPARγ phosphorylation and enhances PPARγ activity and insulin sensitivity. Cell 147(4):815-26.

Liang, H. and Ward, W.F. (2006). PGC-1alpha: a key regulator of energy metabolism. Adv Physiol Educ 30(4):145-51.

Lindstrom P. (2007). The physiology of obese-hyperglycemic mice [ob/ob mice]. Scientific World Journal 7: 666-85.

Liu, X. et al. (2008). The structural basis of protein acetylation by the p300/CBP transcriptional coactivator. Nature 451 (7180): 846–50.

Lu, X. (2010). Differential control of ATGL-mediated lipid droplet degradation by CGI-58 and G0S2. Cell Cycle 9:2719–2725.

Maeda N. et al. (2008). Metabolic impact of adipose and hepatic glycerol channels aquaporin 7 and aquaporin 9. Nat Clin Pract Endocrinol Metab. 4(11):627-34.

Maisch, B. et al. (2011). Diabetic cardiomyopathy--fact or fiction? Herz 36(2):102-15.

Makowski, L. et al. (2001). Lack of macrophage fatty-acid-binding protein aP2 protects mice deficient in apolipoprotein E against atherosclerosis. Nat Med 7(6):699-705.

Matsuda M., DeFronzo R.A. (1999). Insulin sensitivity indices obtained from oral glucose tolerance testing: comparison with the euglycemic insulin clamp.Diabetes Care 22(9):1462-70.

Matthews D.R. et al. (1985). Homeostasis model assessment: insulin resistance and beta-cell function from fasting plasma glucose and insulin concentrations in man. Diabetologia 28 (7): 412–9.

McQuaid, S.E. et al. (2011). Downregulation of adipose tissue fatty acid trafficking in obesity: a driver for ectopic fat deposition? Diabetes 60(1):47-55.

Moorthy, B.S. et al. (2011). Phosphodiesterases catalyze hydrolysis of cAMP-bound to regulatory subunit of protein kinase A and mediate signal termination. Mol Cell Proteomics 10(2):M110.002295.

Morcos, P.A. et al. (2008). Vivo-Morpholinos: A non-peptide transporter delivers Morpholinos into a wide array of mouse tissues. BioTechniques. Dec;45(6):616-26.

Mottillo, E.P. and Granneman, J.G. (2011). Intracellular fatty acids suppress β-adrenergic induction of PKA-targeted gene expression in white adipocytes. Am J Physiol Endocrinol Metab 301(1):E122-31.

Nishimura, S. et al. (2009). Adipose tissue inflammation in obesity and metabolic syndrome. Discov Med. 8(41):55-60.

Osuga, J. et al. (2000) Targeted disruption of hormone-sensitive lipase results in male sterility and adipocyte hypertrophy, but not in obesity. Proc Natl Acad Sci U S A 97(2):787-92.

Parker, H. et al. (2008). The complex genomic profile of ETV6-RUNX1 positive acute lymphoblastic leukemia highlights a recurrent deletion of TBL1XR1. Genes Chromosomes Cancer 47(12):1118-25.

Pena-Penabad, C. et al. (2001). Dorfman-Chanarin syndrome (neutral lipid storage disease): new clinical features. Br J Dermatol 144(2):430-2.

Perissi, V. et al. (2004). A corepressor/coactivator exchange complex required for transcriptional activation by nuclear receptors and other regulated transcription factors. Cell 116, 511-26.

Perissi, V. et al. (2008). TBL1 and TBLR1 phosphorylation on regulated gene promoters overcomes dual CtBP and NCoR/SMRT transcriptional repression checkpoints. Mol Cell 29, 755-66.

Perissi, V. et al. (2010). Deconstructing repression: evolving models of co-repressor action. Nat Rev Genet 11(2):109-23.

Perreault, L. et al. (2012). Effect of regression from prediabetes to normal glucose regulation on long-term reduction in diabetes risk: results from the Diabetes Prevention Program Outcomes Study. Lancet. 16;379(9833):2243-51.

Popkin, B.M. et al. (2012). Global nutrition transition and the pandemic of obesity in developing countries. Nutr Rev. 70(1):3-21.

Ramadoss, S. et al. (2011). Transducin β-like protein 1 recruits nuclear factor κB to the target gene promoter for transcriptional activation. Mol Cell Biol 31(5):924-34.

Rasmussen, M. et al. (2003). Elevated β2-adrenoceptor protein concentration in adipose tissue from obese subjects is closely related to the body mass index and waist/hip ratio. Clin Sci 104, 93–102.

Rasouli, N., Kern, P.A. (2008). Adipocytokines and the Metabolic Complications of Obesity. Endocrinol Metab 93: S64–S73

Rodriguez-Cuenca, S. et al. (2012a). Peroxisome proliferator-activated receptor γ-dependent regulation of lipolytic nodes and metabolic flexibility. Mol Cell Biol 32(8):1555-65.

Rodriguez-Cuenca, S. et al. (2012b). Ablation of Pparγ2 impairs lipolysis and reveals murine strain differences in lipolytic responses. FASEB J 26(5):1835-44.

Rosenthal, N. and Brown, S. (2007). The mouse ascending: perspectives for human-disease models. Nat Cell Bio 9(9):993-9.

Rudofsky G. et al. (2011). Weight loss improves endothelial function independently of ADMA reduction in severe obesity. Horm Metab Res. 43(5):343-8.

Samocha-Bonet, D. et al. (2012). Insulin-sensitive obesity in humans - a 'favorable fat' phenotype? Trends Endocrinol Metab 23(3):116-24.

Sands, W.A. and, Palmer, T.M. (2008). Regulating gene transcription in response to cyclic AMP elevation. Cell Signal 20(3):460-6.

Schaffer, J.E. and Lodish, H.F. (1994). Expression cloning and characterization of a novel adipocyte long chain fatty acid transport protein. Cell, 79(3):427-36.

Scott, J.D. and Pawson, T. (2009) Cell signaling in space and time: where proteins come together and when they're apart. Science, 326, 1220-1224.

Spalding, K.L. et al. (2008). Dynamics of fat cell turnover in humans. Nature 453(7196):783-7.

Strawford, A. et al. (2004). Adipose tissue triglyceride turnover, de novo lipogenesis, and cell proliferation in humans measured with ^{2}H2O. Am J Physiol Endocrinol Metab 286:E577–E588.

Tanaka Y. et al. (1990). Experimental cancer cachexia induced by transplantable colon 26 adenocarcinoma in mice. Cancer Res 50(8):2290-5.

Tontonoz, P., Spiegelman, B.M. (2008) Fat and beyond: the diverse biology of PPARgamma. Annu Rev Biochem 77:289-312.

Trayhurn, P. (2007). Adipocyte biology. Obesity reviews 8, 41–44.

Wang, H. et al. (2009). Activation of hormone-sensitive lipase requires two steps, protein phosphorylation and binding to the PAT-1 domain of lipid droplet coat proteins. J. Biol. Chem. 284:32116–32125.

Wang, S.P. et al. (2001). The adipose tissue phenotype of hormone-sensitive lipase deficiency in mice. Obes Res 9(2):119-28.

Watson, P.J. et al. (2012) Nuclear hormone receptor co-repressors: Structure and function. Mol Cell Endocrinol 30; 348-135(2-3): 440–449.

Wellen, K.E., Hotamisligil, G.S. (2003). Obesity-induced inflammatory changes in adipose tissue. J Clin Invest 112:1785–1788.

WHO fact sheet No. 311, 2011. Global database on Body Mass Index, WHO, 2011.

Wolin, K.Y. et al. (2010). Obesity and cancer. Oncologist, 15, 556-565.

Wozniak, S.E. et al. (2009). Adipose Tissue: The New Endocrine Organ? A Review Article. Dig Dis Sci, 54:1847–1856.

Wu, J.W. et al. (2012). Fasting energy homeostasis in mice with adipose deficiency of desnutrin/adipose triglyceride lipase. Endocrinology 153(5):2198-207.

Yoon, H.G. et al. (2003). Purification and functional characterization of the human N-CoR complex: the roles of HDAC3, TBL1 and TBLR1. Embo J 22, 1336-46.

Yu, Y. H. and Ginsberg, H. N. (2005). Adipocyte signaling and lipid homeostasis: sequelae of insulin-resistant adipose tissue. Circ Res, 96, 1042-1052.

Zechner, R. et al. (2012). FAT SIGNALS - Lipases and Lipolysis in Lipid Metabolism and Signaling. Cell Metab. 15(3): 279–291.

Zechner, R. et al. (2009). Adipose triglyceride lipase and the lipolytic catabolism of cellular fat stores. J Lipid Res. 50(1):3-21.

Zhang, J. et al. (2002). The N-CoR-HDAC3 nuclear receptor corepressor complex inhibits the JNK pathway through the integral subunit GPS2. Mol Cell 9, 611-23.

Zhang, X.M. et al. (2006). TBLR1 regulates the expression of nuclear hormone receptor co-repressors. BMC Cell Biol 7;7:31.

Zhu G. et al. (1996). In vivo adenovirus-mediated gene transfer into normal and cystic rat kidneys. Gene Ther. Apr;3(4):298-304.

Zu, L. et al. (2009). Bacterial endotoxin stimulates adipose lipolysis via Toll-Like Receptor 4 and Extracellular Signal-regulated Kinase pathway, J Biol Chem. 284(9):5915-26.